



Instituto de Matemática Pura e Aplicada

# Mathematical Methods in Finance: Modeling and Numerical Analysis

Leonardo Erick Müller

July 31, 2009

Advisor: Jorge Zubeili  
Co-Advisor: Max O. Souza

## Abstract

This thesis concerns the study of strategies and the development of mathematical methods to deal with three specific problems in quantitative finance.

In the first problem, we address the use of Fourier methods for derivative pricing. We present a novel method to compute options prices, which extends the existing literature of Fourier methods in finance. The method makes it possible to price several payoffs not treated in the literature and also a portfolio of derivatives with different maturities.

We study the approximation of Fourier operators in different frameworks, having the financial application as a particular case. We also present a non-uniform fast Fourier transform (NUFFT) for the approximations used here and several numerical results.

The second problem concerns commodity pricing. We present a model for the liquefied natural gas (LNG) market based on a multidimensional stochastic process. Several derivatives over LNG are also presented with a numerical method to evaluate them.

In the third problem, we present a way of using interest rate derivatives to recover market expectation regarding future decisions by the monetary authority. This chapter describes a model that has monetary decisions as input and it proposes some regularization techniques in order to recover interest rate expectations from real data.

# Contents

<b>Introduction</b>	<b>4</b>
<b>1 Preliminaries and Notation</b>	<b>7</b>
1.1 Fourier Transform . . . . .	7
1.2 Probability and Stochastic Processes . . . . .	10
1.3 Mathematical Finance . . . . .	11
<b>2 Fourier Methods in Finance</b>	<b>16</b>
2.1 Review of FFT Methods in Finance . . . . .	17
2.1.1 Fourier Transformation with Attenuation Factor . . . . .	17
2.1.2 Generalized Fourier Transform . . . . .	18
2.2 The Fourier Transform for Tempered Distributions . . . . .	20
<b>3 Approximation of Fourier Operators</b>	<b>25</b>
3.1 Spectral Approximation of the Free-Space Heat Kernel . . . . .	27
3.2 Non-uniform Quadratures . . . . .	29
3.3 Heat Kernel . . . . .	36
<b>4 The Algorithm for Computing Non-uniform Quadratures</b>	<b>44</b>
4.1 FFT for Uniform Real Space Non-uniform Fourier Space . . . . .	45
4.2 NUFFT: the General Case . . . . .	46
4.3 Numerical Example . . . . .	48
<b>5 A Liquefied Natural Gas Pricing Model</b>	<b>56</b>
5.1 Spot Price Model . . . . .	58
5.2 LNG Derivatives . . . . .	60
5.2.1 Forward . . . . .	60
5.2.2 Cancellation Options . . . . .	61
5.3 Least-Squares Monte Carlo . . . . .	65
5.3.1 An Example . . . . .	66

<b>6</b>	<b>Interest Rates</b>	<b>70</b>
6.1	Model and Notation . . . . .	71
6.1.1	Future Contract . . . . .	72
6.1.2	Options on IDI . . . . .	74
6.2	Recovering Probabilities . . . . .	76
6.3	Numerical Results . . . . .	80
6.4	Conclusion . . . . .	83
<b>7</b>	<b>Final Considerations and Future Work</b>	<b>84</b>
	<b>Bibliography</b>	<b>87</b>

# Acknowledgments

First of all I would like to thank Jorge P. Zubelli for being a very supportive advisor. After four years working together, he became more than an advisor, a friend. Someone I could talk to about mathematics but also about life in general (as general as you can imagine and sometimes even more). His huge spectrum of interests is in part responsible for the diversity of this thesis, I am very grateful for that. He always gave me total liberty to work on the subjects I was interested on. Now I see that in a very subtle way he also made me work on the subject of his interest.

I would also like to thank Max O. Souza. Max was my advisor at PUC during my college years and have introduced me to mathematical economics. He is in part responsible for my decision of pursuing my M.Sc. in this area. During my PhD Max returned, now as my co-advisor, and I am very glad we could work together again. Max is the most optimistic person I know. If I publish half the papers he is sure I will, then certainly I will be a great researcher. With this kind of motivation, Max made me think “Yes I can” before the Obama fever, and is responsible for the energy necessary to overcome the moments I was certain I was not going to make it. While writing my thesis he was always very supportive, even when the dirty work had to be done. I am very thankful for his eight years of guidance and friendship.

I would like to thank Rana and all of my family for the support during the last years, and for the help they gave me to correct the spelling errors in this thesis. I am also thankful for the help Heloisa gave me in reviewing this text.

Finally I would like to thank Marco Avellaneda, Sebastian Jaimungal and Fernando Aiube for our inspiring conversations, and Rodrigo Targino for having helped me with part of the code used in this thesis.

# Introduction

The development of mathematical finance goes back to Bachelier, a student of Henri Poincaré, who in 1900 presented his PhD thesis [Bac00]. Bachelier developed (before Einstein) the first theory of Brownian motion and used it to model the price of a stock in time. He even managed to find prices for call and put options. Bachelier's work was neglected until Jimmie Savage and Paul Samuelson rediscovered it in the 1950s.

After the work of Bachelier, several others presented important works in the mathematical finance field, but the major breakthrough was achieved by Black-Scholes-Merton [BS73] [Mer73]. In 1973, they proved a pricing formula for call options, under accepted assumptions. This result had tremendous practical implications and eventually led the authors to be awarded the Nobel prize in 1997 (Black died in 1995).

At the time Scholes and Merton received the Nobel prize, they were already partners at the hedge fund Long-Term Capital Management (LTCM). The bailout of LTCM happened a year after Merton and Scholes received the Nobel prize. In September 21, 1998 the Business Week had the following headline:

*“**Misfire** Wall Street’s Rocket Scientists thought they had a sure-fire way to beat the markets. Boy, were they wrong!”* (Business-Week 09/21/1998)

After the bailout, LTCM kept operations. In 2000, when the fund was liquidated, the banks that financed LTCM had been paid back. The main problem with LTCM was the risk management. After the bailout of LTCM, risk management became a major issue in the financial industry. Until today, regulation for hedge funds is an important topic of debate.

Despite their unpleasant experience in the markets, the work of Black-Scholes-Merton had, and still has, a great influence among practitioners and scholars. After their seminal papers, several other works have followed and the mathematical finance field have received a large amount of attention. Since their work, which involves stochastic calculus and partial differential

equations, an increasing number of mathematical techniques have been applied to finance, ranging from asymptotic methods [FPS00], [SZ07], to controlled Markov Processes [FS06].

In the present thesis, we make a contribution to the mathematical finance field by presenting new models for some problems in quantitative finance and developing new mathematical techniques with applications in finance. To do so, we address three different problems in quantitative finance, always presenting solid solutions, from the mathematical model to the numerical methods.

Most of the mathematical techniques used in each problem of this thesis are similar and a brief review of it is given in Chapter 1. For the reader's convenience, we try to make each part self-contained.

The first problem this thesis addresses is the use of Fourier methods in derivative pricing. Fourier methods have been widely used in finance, see Chapter 2 for a review. Our work extends the literature by presenting a rigorous analysis of the discretization of Fourier operator that are related to mathematical finance.

In Chapter 2, we present a Fourier analytic solution of the pricing problem. This solution expresses derivative prices in terms of Fourier inversion. It uses explicit formulas for the characteristic functions of the underlying price, that are known for several models in the financial literature.

Numerical evaluations of the Fourier transform is a non-trivial computation due to the oscillatory nature of the integral. We present bounds for the numerical approximation of the Fourier transform for some different functions, including the Fourier transform of the principal value of a function. We pay special attention to the heat kernel case, where the estimate results in a spectral resolution for the heat kernel. The results for these numerical evaluations of the Fourier transform are presented in Chapter 3. The heat kernel case is addressed in Section 3.3.

The estimates for the computations of the Fourier transform of Chapter 3 are based on a non-uniform grid, so it is not possible to use FFT as a fast algorithm for the computations. To overcome this issue, we present a non-uniform fast Fourier transform (NUFFT) in Chapter 4. Another simple reason for the need of such techniques is the ubiquitous change of variable from prices to their logarithms.

Putting together the bounds of Chapter 3 and the NUFFT algorithm of Chapter 4, we construct a fast algorithm for the Fourier approximation, where less nodes are needed than in the uniform case. We present several numerical examples in Section 4.3. We also show some numerical results for the formulas of Chapter 2.

In Chapter 5, we address the study of a commodity model in the pres-

ence of an *arbitrageur*. We develop a multi-dimensional stochastic model that describes market prices when a specific seller has some price or logistic advantages over the majority of the market.

We use this model to explain the liquefied natural gas (LNG) market price, which has typically very little data. The model overcomes such lack of data by modeling LNG as a derivative of natural gas in several countries, which have plenty of data available. Using this model, we are able to study several derivatives over LNG.

Numerical methods for such multi-dimensional problems are time consuming. To overcome this difficulty, we employ Monte Carlo methods to compute derivative prices.

The third and final problem we study deals with interest rates modeling. We present a model that mixes two processes: one continuous and another with pure jumps. The continuous process represents the uncertainty of interest rates originated by small market fluctuations, while the pure jump process represents the monetary authority changes in the target rate.

The mathematical challenge imposed by this problem is the model's calibration to market data. We use regularization techniques to overcome this challenge. The model is presented in Chapter 6, where some numerical results are shown.

We believe the reader will find in this thesis that the development of quantitative models in finance goes hand in hand with the development of the appropriate mathematical techniques to solve them.



# Chapter 1

## Preliminaries and Notation

In this chapter, we give a brief overview of the mathematical techniques used in this work and present the notation used.

### 1.1 Fourier Transform

In this section, we recall the Fourier transform definition, both for notational reasons and for the reader's convenience.

The Fourier transform, for  $f \in \mathcal{S}(\mathbb{R}^m)$ , is denoted here as

$$\widehat{f}(\xi) := \mathcal{F}[f](\xi) := \int_{\mathbb{R}^m} e^{i\xi x} f(x) dx, \quad (1.1)$$

where  $\mathcal{S}(\mathbb{R}^m)$  is the Schwartz space of  $\mathcal{C}^\infty(\mathbb{R}^m)$  functions of rapid decrease, see [RS75]. This is not the usual definition found in the mathematical literature. However, it is standard in probability, see [Chu01] and in the finance literature, see [CT04].

The Fourier transform is a linear bijection from  $\mathcal{S}(\mathbb{R}^m)$  onto  $\mathcal{S}(\mathbb{R}^m)$ , whose inverse is given by the Fourier inversion formula

$$f(x) = \mathcal{F}^{-1}[\widehat{f}](x) = \frac{1}{(2\pi)^m} \int_{\mathbb{R}^m} e^{-i\xi x} \widehat{f}(\xi) d\xi. \quad (1.2)$$

We also recall the Fourier transform for  $f \in \mathcal{S}'(\mathbb{R}^m)$ , where  $\mathcal{S}'(\mathbb{R}^m)$  is the space of tempered distributions, which is the dual of  $\mathcal{S}(\mathbb{R}^m)$ , the Fourier transform can be defined as

$$(\mathcal{F}[f], \varphi) = (2\pi)^m (f, \mathcal{F}^{-1}[\varphi]) \quad \varphi \in \mathcal{S}(\mathbb{R}^m), \quad (1.3)$$

see [RR04]. This definition makes the Fourier transform in  $\mathcal{S}'(\mathbb{R}^m)$  an extension of the Fourier transform in  $\mathcal{S}(\mathbb{R}^m)$ . The Fourier transform for  $L^1(\mathbb{R}^m)$  and  $L^2(\mathbb{R}^m)$  are restrictions of the Fourier transform for  $\mathcal{S}'(\mathbb{R}^m)$ .

The Fourier transform has several useful properties. Some of them are reviewed below with the purpose of calling attention to the notation used here:

- $\mathcal{F}[f(x - a)](\xi) = e^{ia\xi} \widehat{f}(\xi)$
- $D^\alpha \widehat{f}(\xi) = \mathcal{F}[(ix)^\alpha f](\xi)$
- $(-i\xi)^\alpha \widehat{f}(\xi) = \mathcal{F}[D^\alpha f](\xi)$

Some specific distributions are often used in this thesis. To present the notation, we give a brief overview of them. First, consider the Cauchy principal value

$$\begin{aligned} 1/x : \mathcal{S}(\mathbb{R}) &\rightarrow \mathbb{R} \\ f &\rightarrow (1/x, f) := \int_{-\infty}^{\infty} \frac{f(x)}{x} dx, \end{aligned}$$

where

$$\int_{-\infty}^{\infty} \frac{f(x)}{x} dx := \lim_{\epsilon \downarrow 0} \left( \int_{\epsilon}^{\infty} \frac{f(x)}{x} dx + \int_{-\infty}^{-\epsilon} \frac{f(x)}{x} dx \right).$$

This defines a distribution in  $\mathcal{S}'(\mathbb{R})$ .

Another important distribution is the Heaviside function

$$H(x) := \begin{cases} 1 & \text{if } x > 0 \\ 0 & \text{if } x \leq 0 \end{cases}.$$

In this work, we use the notation

$$\mathcal{X}_{x_0}(x) := \begin{cases} 1 & \text{if } x > x_0 \\ 0 & \text{if } x \leq x_0 \end{cases} \quad \text{and} \quad \mathcal{X}_A(x) := \begin{cases} 1 & \text{if } x \in A \\ 0 & \text{if } x \notin A \end{cases}. \quad (1.4)$$

Hence  $H(x) = \mathcal{X}_0(x)$ . The Fourier transform of the Heaviside function is given by

$$\widehat{H}(\xi) = \left( -\frac{1}{i\xi} + \pi\delta_0 \right), \quad (1.5)$$

where  $1/i\xi$  is interpreted as a principal value and  $\delta$  is the delta function at the origin given by  $\delta(f) := f(0)$ , for  $f \in \mathcal{S}(\mathbb{R})$ .

Another concept we recall is the convolution, which is defined for  $f, g \in \mathcal{S}(\mathbb{R})$  as

$$(f * g)(y) = \int_{\mathbb{R}} f(y - x)g(x)dx.$$

The convolution can be defined for  $f \in \mathcal{S}(\mathbb{R})$  and  $T \in \mathcal{S}'(\mathbb{R})$  as

$$(T * f)(\psi) = T(\tilde{f} * \psi) \quad \forall \quad \psi \in \mathcal{S}(\mathbb{R}) ,$$

where  $\tilde{f}(x) := f(-x)$ . It is possible to define the Fourier transform in this case as

$$\mathcal{F}[T * f] = \mathcal{F}[f]\mathcal{F}[T] ,$$

see [RS75].

For functions defined on compact spaces, the Fourier transform has a special form: the Fourier series. We briefly review the notation we use. Let  $f \in L^1[-\pi L, \pi L]$ , then we can define

$$c_k = \int_{-\pi L}^{\pi L} f(x) e^{\frac{ikx}{L}} dx , \quad (1.6)$$

and the Fourier series of  $f$  is given by

$$\frac{1}{2\pi L} \sum c_k e^{-\frac{ikx}{L}} . \quad (1.7)$$

Several results on the convergence of the Fourier series to the function  $f$  are known. For example, if  $f \in L^2[-\pi L, \pi L]$ , then the Fourier series converges in  $L^2$  to  $f$ , which is a consequence of the fact that  $\phi_k(x) = \exp(ikx/L)$ ,  $k \in \mathbb{Z}$  forms a maximal orthogonal set in  $L^2(-\pi L, \pi L)$ .

We are most interested in the discrete Fourier transform (DFT), which is the discrete version of the Fourier transform. For  $X \in \mathbb{R}^N$  the DFT of  $X$  is given by

$$\widehat{X}_j = \sum_n X_n e^{\frac{2\pi ikn}{N}} \quad (1.8)$$

and the inverse of the DFT is given by

$$X_n = \frac{1}{N} \sum_j \widehat{X}_j e^{-\frac{2\pi ikn}{N}} . \quad (1.9)$$

DFT arises in several applications, in this thesis, it appears as an approximation of the Fourier transform by finite sums and also as the truncation of the Fourier series.

The naive computation of the DFT demands  $N^2$  operations. A fast algorithm, known as fast Fourier transform (FFT), reduces the computation of the DFT to  $\mathcal{O}(N \log N)$  operations. The FFT became popular after the work of [CT65], but a fast algorithm for the computations of DFT goes back to Gauss around 1805, see [HJB85]. The main idea of FFT is to find a clever factorization of the DFT matrix  $F_N \in \mathbb{R}^{N \times N}$ , given by  $F_N(k, n) = \exp(-2\pi ikn/N)$ , see [Van92] for the computational aspects.

## 1.2 Probability and Stochastic Processes

In this section, we present a brief overview of the topics on probability and stochastic processes used herein. References on the subject are [CW90] and [Sat99].

In this thesis, the triple  $(\Omega, \mathcal{F}, \mathbb{P})$  denotes a complete probability space, where  $\Omega$  is a set of points  $\omega$ ,  $\mathcal{F}$  is a  $\sigma$ -algebra containing all  $\mathbb{P}$ -null sets, and  $\mathbb{P}$  is a probability measure. When we say that  $X$  is a random variable on the probability space  $(\Omega, \mathcal{F}, \mathbb{P})$ , we mean that  $X$  is real-valued function on  $\Omega$ , measurable with respect to  $\mathcal{F}$ .

The characteristic function of a random variable is defined as

$$\varphi(z) = \mathbb{E} [e^{izX}] . \quad (1.10)$$

For properties of the characteristic function and a review of probability theory we refer to [CW90].

The filtered complete probability space is denoted by  $(\Omega, \mathcal{F}, \mathbb{F}, \mathbb{P})$ , where, as in [Pro04], we write  $\mathbb{F}$  for the filtration  $(\mathcal{F}_t)_{0 \leq t \leq \infty}$  and we assume that  $\mathcal{F}_0$  contains all the  $\mathbb{P}$ -null sets. We use  $\xrightarrow{\mathbb{P}}$  to denote convergence in probability, see [CW90] and the French acronyms *càdlàg* (*continu à droite, limité à gauche*) is used to define the right continuous, left limited process, see [Pro04].

The main class of stochastic processes we are interested in this work are the Levy processes, see [Sat99] for a comprehensive treatment of the subject. We briefly review the definition of a Levy process

**Definition:** A Levy process is a càdlàg stochastic process,  $(X_t)_{t \geq 0}$ , on  $(\Omega, \mathcal{F}, \mathbb{F}, \mathbb{P})$  taking values in  $\mathbb{R}$  and with the following properties:

- *Independent increments.* That is, given  $t_0 \leq \dots \leq t_N$ , and defined  $Y_n := X_{t_n} - X_{t_{n-1}}$  we have  $\{Y_n\}_{n=1}^N$  independent;
- *Stationary increments.* That is, the distribution of  $X_{t+s} - X_t$  does not depend on  $t$ ;
- *Stochastic continuity.* That is,

$$X_{t+h} \xrightarrow[h \downarrow 0]{\mathbb{P}} X_t .$$

An important stochastic process is the Brownian motion.

**Definition:** A Brownian motion is a adapted continuous stochastic process  $(W_t)_{t \geq 0}$ , on  $(\Omega, \mathcal{F}, \mathbb{F}, \mathbb{P})$  taking values in  $\mathbb{R}$  and with the following properties:

- $W_0 = 0$ .
- *Independent increments.* That is, given  $t_0 \leq \dots \leq t_N$ , and defined  $Y_n := W_{t_n} - W_{t_{n-1}}$  we have  $\{Y_n\}_{n=1}^N$  independent;
- The distribution of  $Y_n$  is normal with mean zero and variance  $t_n - t_{n-1}$ .

A very important result is that Levy processes can be characterized, in the Fourier domain, by the Levy-Khinchin theorem, see [Fel66].

**Theorem 1.2.1 (Levy-Khinchin)** *Let the adapted process  $(X_t)_{t \geq 0}$  be a Levy process, then*

$$\begin{aligned} \mathbb{E} [e^{izX_t}] &= e^{t\psi(z)} \\ \psi(z) &= -\frac{1}{2}\sigma z^2 + i\gamma z + \int_{-\infty}^{\infty} (e^{izx} - 1 - izx\mathcal{X}_{|x| \leq 1}) d\nu, \end{aligned} \quad (1.11)$$

where  $\nu$  is called the Levy measure and it is a positive Radon measure on  $\mathbb{R} \setminus \{0\}$  such that

$$\int_{-1}^1 x^2 d\nu \leq \infty \text{ and } \int_{|x| \geq 1} d\nu \leq \infty.$$

The reciprocal of Theorem 1.2.1 is also proved in [Fel66].

## 1.3 Mathematical Finance

Several concepts of stochastic processes, stochastic calculus, partial differential equations, among other mathematical topics, have been used to model financial markets. The use of such advanced mathematical concepts to model financial markets became known as mathematical finance.

A standard introduction to stochastic calculus is [Oks05], see [Pro04] for a more advanced treatment. For an introduction to stochastic calculus applied to finance there are [CT04] or [Shr04]. In this section, we present a short overview on the topic.

The ground work for mathematical finance is the work of Black-Scholes-Merton [BS73], [Mer73]. They assumed that the stock prices satisfy the following linear stochastic differential equation (SDE)

$$\frac{dS_t}{S_t} = \mu dt + \sigma dW_t, \quad (1.12)$$

where  $W_t$  is a Brownian motion defined on the filtered complete probability space  $(\Omega, \mathcal{F}, \mathbb{F}, \mathbb{P})$ . The SDE (1.12) has an unique solution given by

$$S_t = S_0 \exp \left( \left( \mu - \frac{\sigma^2}{2} \right) t + \sigma W_t \right) . \quad (1.13)$$

$S_t$  given by (1.13) is known as geometrical Brownian motion (GBM).

One of the most important problems addressed by mathematical finance is the pricing of a *contingent claim*. In this thesis, we are only interested in *European contingent claim*. An European contingent claim with maturity time  $T$  is a  $L^2(\Omega, d\mathbb{P})$ ,  $\mathcal{F}_T$ -measurable random variable. Several authors make no distinction between *contingent claim* and *derivative contract*. Here, an European derivative contract on the underlying asset  $S$  and maturity time  $T$  is a  $L^2(\Omega, d\mathbb{P})$ ,  $\sigma(S_T)$ -measurable random variable, so it can be written as  $g(S_T)$ , where  $g$  is called the *payoff* of the derivative. In this work, we omit the word European.

The most important financial derivatives are the *call* and *put* options. A call option, with maturity time  $T$  and strike  $K$ , is a contract that gives the owner the right at the delivery time  $T$  to buy stock for the strike price  $K$ . Considering that, the price at  $T$  is given by  $S_T$  and the payoff can be expressed as  $(S_T - K)^+$ , where  $(x)^+ := \max(x, 0)$ . Similarly, the put option gives the owner the right to sell the asset and its payoff is given by  $(K - S_T)^+$ . The call and put payoff are shown in Figure 1.1.

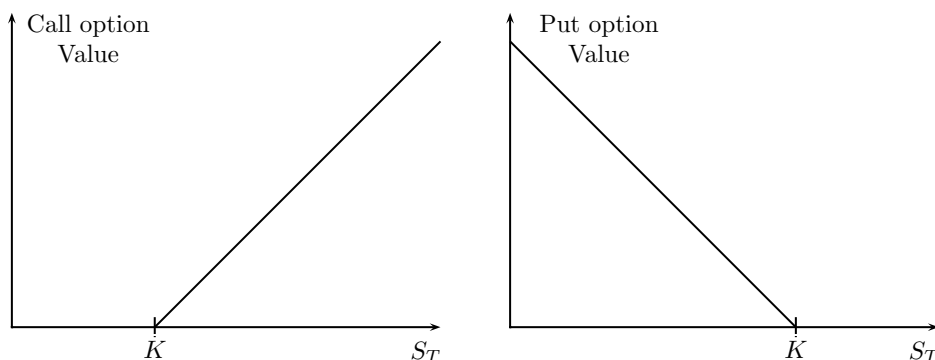


Figure 1.1: Payoff for the call option, with strike  $K$ , is shown on the left, and payoff for the put option, with strike  $K$ , is shown on the right.

Consider a market with  $d$  assets whose prices are given by a càdlàg process  $S_t \in \mathbb{R}^d$ , on a filtered complete probability space  $(\Omega, \mathcal{F}, \mathbb{F}, \mathbb{P})$ , for notational

convenience consider that one of the assets is a risk-free investment, paying interest rates  $r$ . A simple trading strategy can be defined by a simple predictable d-dimensional process

$$\varphi_t := \varphi_0 \mathcal{X}_0(t) + \sum_{j=0}^n \varphi_j \mathcal{X}_{(T_j, T_{j+1}]}(t), \quad (1.14)$$

where  $T_0 = 0 < T_1 < \dots < T_{n+1} = T$  are non-anticipating random times and  $\varphi_j$  is a bounded random variable that is  $\mathcal{F}_{T_j}$ -measurable, see [Pro04]. In its general form, a trading strategy is a process that can be approximated, in the uniform convergence in  $(t, \omega)$ , by simple predictabel processes, see [Pro04].

Given a strategy, we can define the strategy value for a given time  $t$  as

$$V^\varphi(t) = \varphi(0)S(0) + \int_0^t \varphi(s)dS(s). \quad (1.15)$$

A strategy is called self-financing if

$$dV^\varphi(t) = \varphi(t)dS(t). \quad (1.16)$$

We say that a market is arbitrage free if there is no self-financing strategy,  $\varphi$ , with

$$\mathbb{P}(V^\varphi(T) \geq e^{rT}V^\varphi(0)) = 1 \text{ and } \mathbb{P}(V^\varphi(T) > e^{rT}V^\varphi(0)) > 0, \quad (1.17)$$

where  $r$  is the risk-free rate.

In the seminal work [BS73], Black and Scholes built a self-financing strategy,  $\varphi$ , using the stock price, modeled by a GBM (1.13), and the risk-free investment. The strategy is built to have the same payoff as the call option at time  $T$ . Such strategy is called *replicating strategy*. Considering that  $\varphi$  is a self-financing strategy and that the value of  $V^\varphi(T)$  and the payoff at time  $T$  are the same, the price of the call option at  $t = 0$  must be  $V^\varphi(0)$ . That is known as the *rule of one price* and is a consequence of the non-arbitrage hypothesis. Black and Scholes found the following formula for the price of a call option with maturity T, and strike K

$$C(S_0, K, T) = S_0 N(d_+) - Ke^{rT} N(d_-) \\ d_+ = \frac{\log\left(\frac{S_0}{K}\right) + \left(r + \frac{\sigma^2}{2}\right)T}{\sigma\sqrt{T}} \quad d_- = d_+ - \sigma\sqrt{T}. \quad (1.18)$$

The price is independent of the drift coefficient  $\mu$  in (1.13). This is a central result in mathematical finance.

Following Black and Scholes, several authors developed the idea of risk neutral pricing. This idea is based in the notion of an *equivalent martingale measure*, which is an equivalent measure such that the discounted prices,  $e^{-rt}S_t$ , are martingales, see [CT04]. The following theorem is a central result in mathematical finance.

**Theorem 1.3.1 (Fundamental theorem of asset pricing [CT04])** *A market model defined by  $(\Omega, \mathcal{F}, \mathbb{F}, \mathbb{P})$  and asset prices  $(S_t)_{t \in [0, T]}$  is arbitrage-free if and only if there exists an equivalent martingale measure  $\mathbb{Q}$ .*

A proper mathematical statement of the fundamental theorem of asset pricing is beyond the scope of this brief review. References on Theorem 1.3.1 for discrete time are [HP81] and [MR05]. The continuous version can be found in [DS94], [DS98], and [Yan98]. In these work the notion of non arbitrage and admissible strategies are rigorously studied.

A consequence of the Theorem 1.3.1 is that for a given contingent claim  $H$ , let  $V(t, H)$  denote its price. Then

$$V(t, H) = \mathbb{E}^{\mathbb{Q}} [e^{-r(T-t)} H | \mathcal{F}_t] , \quad (1.19)$$

this formula is known as *risk neutral pricing formula*. A simple example of change of measure can be given in the geometrical Brownian case. Under the martingale equivalent measure (1.13) becomes

$$S_t = S_0 e^{rt - \frac{\sigma^2}{2}t + \sigma \widetilde{W}_t} , \quad (1.20)$$

where  $\widetilde{W}_t$  is a Brownian motion under  $\mathbb{Q}$ , the existence of such measure is a consequence of the Girsanov theorem, see [Oks05].

Formula 1.19 reduces the pricing problem to computing an integral. However, in general, the density of the process does not have a closed form representation. To overcome this difficulty, we use the characteristic function.

In (1.13),  $\log S_t$  has normal distribution with mean  $\mu - \frac{\sigma^2}{2}$  and variance  $\sigma^2$ . The characteristic function of a random variable with distribution  $N(b, \sigma^2)$  is given by

$$\varphi(z) = e^{t(ibz - \frac{\sigma^2 z^2}{2})} . \quad (1.21)$$

Letting  $b = \mu - \frac{\sigma^2}{2}$  in Equation (1.21), we have the characteristic for log prices in the Black and Scholes model.

Following Black-Scholes-Merton, several other authors presented different models for stock prices. For example, Merton [Mer75] introduced normally distributed jumps in the log price. A different approach to jumps was given



[BS73]	$\ln(\varphi(z)) = ibz - \frac{\sigma^2}{2}z^2$
[Mer75]	$\ln(\varphi(z)) = izb - \frac{\sigma^2}{2}z^2 + \lambda \left( e^{i\mu z - \frac{1}{2}z^2\delta^2} - 1 \right)$
[Kou02]	$\ln(\varphi(z)) = izb - \frac{\sigma^2}{2}z^2 + iz\lambda \left( \frac{p}{\lambda_+ - iz} + \frac{1-p}{\lambda_- + iz} \right)$

Table 1.1: The log of the characteristic functions of some processes used in finance, with  $t=1$ .

by [Kou02] who introduced an asymmetric exponential density for the jumps. Characteristic functions for these models can be seen in Table 1.1. For many other models in which the characteristic function is available see [CT04].

A popular class of models used in finance are the *stochastic volatility model* and among them the most popular is the Heston model [Hes93]. The SDE for Heston model is given by

$$\begin{aligned} dS_t &= S_t\mu dt + \sqrt{v_t}S_t dW_t^1, \\ dv_t &= -\lambda(v_t - \bar{v}) dt + \nu\sqrt{v_t}dW_t^2, \end{aligned} \quad (1.22)$$

where  $W_t^1$  and  $W_t^2$  are Brownian motions with correlation  $\rho$ . The characteristic function for the Heston model is given by

$$\varphi_t(z) = e^{C(z,t)\bar{v} + D(z,t)v}, \quad (1.23)$$

where

$$\begin{aligned} \beta(z) &= \lambda - i\rho\nu z \\ d(z) &= \sqrt{\beta(z)^2 - 2(-z^2/2 - iz/2)\nu^2} \\ r_+(z) &= (\beta(z) + d(z))/\nu^2 \\ r_-(z) &= (\beta(z) - d(z))/\nu^2 \\ g(z) &= r_-(z)/r_+(z) \\ D(z,t) &= r_-(z) \frac{1 - e^{-d(z)t}}{1 - g(z)e^{-d(z)t}} \\ C(z,t) &= \lambda \left( r_-(z)t - \frac{2}{\nu^2} \ln \left( \frac{1 - ge^{-d(z)t}}{1 - g(z)} \right) \right). \end{aligned}$$

In [Hes93], Heston presented a closed form solution for options pricing, which is one of the main reasons for the popularity of this model. For a review on the Heston model see [Gat06].

## Chapter 2

# Fourier Methods in Finance

Fourier methods in finance are used in a variety of situations. Several authors used Fourier methods to find analytical formula for the price of derivatives. Heston [Hes93] used Fourier analysis to find an explicit solution of a parabolic partial differential equation with mixed differentiation terms, that models the price of a call option. To do so, Heston explicitly derived the formula for the characteristic function of a stochastic volatility model.

The characteristic function of several processes used in finance are known in closed form. We have for example the Levy-Khinchin representation given in Theorem 1.2.1. Duffie, Pan and Singleton [DPS00] found the characteristic function for general jump-diffusion model and also the derivative price for a special class of payoff functions.

In a different direction, Carr-Madan[CM99] and Lewis [Lew00] used the Fourier transform to find the price of an European call option in the Fourier space and then used FFT to find the price in real space. The main idea of the method is that European derivatives are convolutions in real space of the payoff and the density of the asset on the maturity date. In order to compute option prices, Carr-Madan [CM99] had to set a damping constant and Lewis [Lew00] had to set a translation in the complex plane to invert the generalized Fourier transform.

Lee [Lee04] has shown that the accuracy of the method presented by Carr-Madan is sensitive to the choice of the damping constant. Lee presented a strategy to choose the damping parameter. He also extended the method to several others payoff functions, and presented some bounds for the FFT approximation.

The FFT approach was also used by [JJSB] and [JSB], to price American options by the Fourier time stepping. In a different direction [LFBO07] used Richardson extrapolation to the prices of Bermudian options in order to price American options.

As opposed to [CM99] and [Lew00], this thesis deals with the Fourier transform for generalized functions. Therefore, no dumping parameter is needed, and the characteristic function is only used in real space.

This chapter is organized as following. In Section 2.1, we briefly review the two ground works on the application of FFT to finance. In Subsection 2.1.1, we review the work of Carr-Madan and in Subsection 2.1.2, we review the work of Lewis. In Section 2.2, we present a new approach based on the Fourier transform for tempered distributions. Our method applies to several derivatives not treated by [CM99], [Lew00], [Lee04], and [DPS00].

## 2.1 Review of FFT Methods in Finance

In this section, we give a brief overview on the work of Carr-Madan and Lewis. See [CM99], [Lew00], [Lee04] or [CT04] for a complete review.

### 2.1.1 Fourier Transformation with Attenuation Factor

In [CM99], the authors developed a method to numerically calculate the price of call options for several strikes. The pricing formula for a given strike,  $e^k$ , is

$$C_T(k) = \int_k^{+\infty} e^{-rT} (e^s - e^k) \rho_T(s) ds ,$$

for some risk-neutral density,  $\rho_T$  for the log-prices, as in Equation 1.19. The attenuated price is defined as

$$C_T^\alpha(k) := e^{\alpha k} C_T(k) . \tag{2.1}$$

In general,  $C_T(k)$  is not integrable, but  $C_T^\alpha$  is. The Fourier transform of the attenuated price is

$$\begin{aligned} \widehat{C}_T^\alpha(\xi) &= \int_{-\infty}^{+\infty} e^{i\xi k} C_T^\alpha(k) dk \\ &= e^{rT} \frac{\varphi(\xi - (\alpha + 1)i)}{\alpha^2 + \alpha + \xi^2 + i(2\alpha + 1)\xi} , \end{aligned} \tag{2.2}$$

where  $\varphi$  is the characteristic function of the distributions  $\rho$ . The attenuation factor makes it necessary to use the characteristic function defined in the complex plane. The price can be obtained by Fourier inversion

$$C_T(k) = e^{-\alpha k} \mathcal{F}^{-1} \left[ \widehat{C}_T^\alpha \right] (k) \tag{2.3}$$

The Fourier transform in 2.3 can be approximated by FFT. In [CT04] a different approach was used. More precisely, let

$$C_T^1(k) = C_T(k) - (1 - e^{k-rT})^+, \quad (2.4)$$

so,

$$\begin{aligned} \widehat{C}_T^1(\xi) &= \int_{-\infty}^{+\infty} e^{i\xi k} C_T^1(k) dk \\ &= e^{i\xi rT} \frac{\varphi(\xi - i) - 1}{i\xi(1 + i\xi)}. \end{aligned} \quad (2.5)$$

The problem with (2.5) is the slow decay of  $\widehat{C}_T^1(\xi)$  for large  $\xi$ , to improve that they used

$$C_T^2(k) = C_T(k) - C_{BS}^\sigma(k), \quad (2.6)$$

where  $C_{BS}^\sigma(k)$  is the Black and Scholes price for an option with volatility  $\sigma$ , strike  $e^k$  and maturity  $T$ . So

$$\begin{aligned} \widehat{C}_T^2(\xi) &= \int_{-\infty}^{+\infty} e^{i\xi k} C_T^2(k) dk \\ &= e^{i\xi rT} \frac{\varphi(\xi - i) - \varphi^{BS}(\xi)}{i\xi(1 + i\xi)}, \end{aligned} \quad (2.7)$$

where  $\varphi^{BS}(\xi) = \exp\left(-\frac{\sigma^2 T}{2}(\xi^2 + i\xi)\right)$ . The decay in (2.7) is exponential for most of applications to finance, while the decay of (2.5), is polynomial. The problem with (2.7) is that we need to find a good  $\sigma$  to improve the method and we need to compute  $C_{BS}$  for every strike.

## 2.1.2 Generalized Fourier Transform

In a different direction from Carr-Madan [CM99], Lewis [Lew00] works with the analytic continuation of the Fourier transform. For a given asset  $S_t$  and payoff  $f$  at  $T$ , the value of the contract at  $t = 0$ , for observed prices  $s = \log S_0$  is

$$C(s) = e^{-rT} \int_{-\infty}^{\infty} f(e^{s+x+rT}) \rho_T(x) dx, \quad (2.8)$$

which follows from Equation (1.19). To use the Fourier transform in (2.8) some assumptions are needed:

- $\rho$  is Fourier integrable in a strip  $\mathcal{S}_1$ . That is, there are  $a, b \in \mathbb{R}$  such that

$$\int_{-\infty}^{\infty} e^{-ax} |\rho(x)| dx \leq \infty \quad \int_{-\infty}^{\infty} e^{-bx} |\rho(x)| dx \leq \infty .$$

This holds for several processes used in finance. For example, log-normal jump diffusion has  $\mathcal{S}_1 = \mathbb{C}$ .

- $g(x) = f(e^{x+rT})$  is Fourier integrable in a strip  $\mathcal{S}_2$  with  $\mathcal{S} = \mathcal{S}_1 \cap \mathcal{S}_2 \neq \emptyset$ . Again this hypothesis is valid for several payoffs used in finance. For example, consider the call option, then  $\mathcal{S}_2 = \{z \in \mathbb{C} \mid \text{Im}(z) > 1\}$ .

Given  $z \in \mathcal{S}$ ,

$$\begin{aligned} \int_{-\infty}^{\infty} e^{izs} C(s) ds &= e^{-rT} \int_{-\infty}^{\infty} \rho_T(x) \int_{-\infty}^{\infty} e^{izs} g(x+s) ds dx \\ &= e^{-rT} \int_{-\infty}^{\infty} e^{-izx} \rho_T(x) \int_{-\infty}^{\infty} e^{izy} g(y) dy dx. \end{aligned} \quad (2.9)$$

Hence,

$$\mathcal{F}[C](z) = e^{-rT} \varphi(-z) \mathcal{F}[g](z), \quad (2.10)$$

where  $\varphi$  is the characteristic function  $\varphi(z) = \mathcal{F}[\rho_T](z)$ . The transform of the call options, for  $\text{Im}(z) > 1$ , is given by

$$\begin{aligned} \mathcal{F}\left[(e^{x+rT} - K)^+\right] &= \int e^{ixz} (e^{x+rT} - K)^+ dx \\ &= \frac{e^{k(iz+1)-izrT}}{iz - z^2}. \end{aligned} \quad (2.11)$$

The price of the call options is then given by

$$\begin{aligned} C(S) &= \frac{e^{-rT}}{2\pi} \int_{i\omega-\infty}^{i\omega+\infty} e^{-izs} \mathcal{F}[C](z) dz \\ &= \frac{e^{-rT}}{2\pi} \int_{i\omega-\infty}^{i\omega+\infty} e^{-izs} \varphi(-z) \frac{e^{k(iz+1)-izrT}}{iz - z^2} dz, \end{aligned} \quad (2.12)$$

for some  $\omega$  in  $(1, 1 + \alpha)$ , where  $\alpha$  depends on the characteristic function, see [Lew00].

## 2.2 The Fourier Transform for Tempered Distributions

In this section, we present a method to obtain derivative prices from characteristic functions. This method is related to [Lew00], see Subsection 2.1.2, but different from Lewis, we use the Fourier transform only in the real space. We consider payoffs in  $\mathcal{S}'(\mathbb{R})$  and densities in  $\mathcal{S}(\mathbb{R})$ , see Chapter 1. For a special class of payoffs, that contains several important derivatives in financial markets, we explicitly present the formula for the value of the derivative.

In our first result, we express the pricing formula as a convolution. In the following theorem, we establish a simple assumption for the validity of the pricing formula, under fairly general conditions. In Theorem 2.2.2, we use the former result to prove a pricing formula for more general payoffs.

**Theorem 2.2.1** *Let  $f$  be the payoff at time  $T$  of an European derivative, such that*

$$g(s) := f(e^{s+rT}) \in \mathcal{S}'(\mathbb{R}).$$

*Suppose  $\rho_T \in \mathcal{S}(\mathbb{R})$ , then the price is given by*

$$C^g(s) = e^{-rT} \mathcal{F}^{-1} \left[ \mathcal{F}[g] \widetilde{\mathcal{F}[\rho]} \right] (s),$$

*where  $\widetilde{f}(x) := f(-x)$ .*

**Proof:** The risk-neutral pricing (1.19) can be written as

$$G^g(s) = e^{-rT} \int_{-\infty}^{\infty} f(e^{s+x+rT}) \rho_T(x) dx, \quad (2.13)$$

so, by definition of  $g$ , it follows that

$$\begin{aligned} G^g(s) &= e^{-rT} \int_{-\infty}^{\infty} g(x+s) \rho_T(x) dx \\ &= e^{-rT} (g * \widetilde{\rho})(s). \end{aligned} \quad (2.14)$$

The result then follows from the definition of the Fourier transform for convolutions. ■

Using Theorem 2.2.1, we can obtain an explicit formula for several payoffs used in finance, not necessarily in  $\mathcal{S}'(\mathbb{R})$ . The pricing formula is given in the next theorem.

**Theorem 2.2.2** Consider a payoff of the form

$$g(x) = \sum_{j=1}^n (c_j^+ + d_j^+ e^x) \mathcal{X}_{v_j}(x) + \sum_{k=1}^m (c_k^- + d_k^- e^x) \mathcal{X}_{v_k}(-x), \quad (2.15)$$

over an asset  $S_T$  with density  $\rho_T \in \mathcal{S}(\mathbb{R})$ . Then the price of the contract is given by

$$\begin{aligned} G^f(s) &= \frac{e^{-rT}}{2\pi} \int e^{-irT\xi} \frac{\mathcal{F}[\rho](-\xi)}{i\xi} \left( \sum_{k=1}^m c_k^- e^{-iv_k\xi} - \sum_{j=1}^n c_j^+ e^{i\xi v_j} \right) e^{-i\xi s} d\xi \\ &\quad + \frac{e^{-rT}}{2\pi} \int e^{-irT\xi} \frac{\mathcal{F}[\rho](-\xi)}{1+i\xi} \left( \sum_{k=1}^m +d_k^- e^{-iv_k\xi} - \sum_{j=1}^n d_j^+ e^{i\xi v_j} \right) e^{-i\xi s} d\xi \\ &\quad + \frac{e^{-rT}}{2} \left( \sum_{k=1}^m c_k^- - \sum_{j=1}^n c_j^+ \right) + e^{s+rT} \sum_{k=1}^m d_k^+. \end{aligned} \quad (2.16)$$

**Proof:** Notice that

$$\begin{aligned} g^l(x) &:= g(x) - e^x \sum_{k=1}^m d_k^+ \\ &= \sum_{j=1}^n c_j^+ \mathcal{X}_{v_j}(x) - d_j^+ e^x \mathcal{X}_{-v_j}(-x) + \sum_{k=1}^m (c_k^- + d_k^- e^x) \mathcal{X}_{v_k}(-x), \end{aligned} \quad (2.17)$$

so  $g^l \in \mathcal{S}'(\mathbb{R})$ . The Fourier transform of  $g^l$  is given by

$$\begin{aligned} \mathcal{F}[g^l](\xi) &= \sum_{j=1}^n c_j^+ e^{i\xi v_j} \mathcal{F}[H] + d_j^+ \frac{e^{i\xi v_j}}{1+i\xi} \\ &\quad + \sum_{k=1}^m c_k^- e^{-iv_k\xi} \mathcal{F}[H](-\xi) + d_k^- \frac{e^{-iv_k\xi}}{1+i\xi} \\ &= \left( \frac{1}{i\xi} + \pi\delta \right) \left( \sum_{k=1}^m c_k^- e^{-iv_k\xi} - \sum_{j=1}^n c_j^+ e^{i\xi v_j} \right) \\ &\quad + \frac{1}{1+i\xi} \left( \sum_{j=1}^n d_j^+ e^{i\xi v_j} + \sum_{k=1}^m +d_k^- e^{-iv_k\xi} \right). \end{aligned} \quad (2.18)$$

Using the risk-neutral pricing formula (1.19), we obtain

$$\begin{aligned}
G^g(s) &= e^{-rT} \int_{-\infty}^{\infty} g(x + s + rT) \rho_T(x) dx \\
&= e^{-rT} \left( \int_{-\infty}^{\infty} g^l(x + s + rT) \rho_T(x) dx + \int_{-\infty}^{\infty} e^{x+s+rT} \rho_T(x) dx \sum_{k=1}^m d_k^+ \right) \\
&= e^{-rT} \int_{-\infty}^{\infty} g^l(x + s + rT) \rho_T(x) dx + e^{s+rT} \sum_{k=1}^m d_k^+ .
\end{aligned} \tag{2.19}$$

In the last equation, we used the martingale property of discounted prices. So, according to Theorem 2.2.1, we have

$$\begin{aligned}
G^g(s) &= \frac{e^{-rT}}{2\pi} \int e^{-irT\xi} \frac{\mathcal{F}[\rho](-\xi)}{i\xi} \left( \sum_{k=1}^m c_k^- e^{-iv_k\xi} - \sum_{j=1}^n c_j^+ e^{i\xi v_j} \right) e^{-i\xi s} d\xi \\
&\quad + \frac{e^{-rT}}{2\pi} \int e^{-irT\xi} \frac{\mathcal{F}[\rho](-\xi)}{1+i\xi} \left( \sum_{k=1}^m +d_k^- e^{-iv_k\xi} - \sum_{j=1}^n d_j^+ e^{i\xi v_j} \right) e^{-i\xi s} d\xi \\
&\quad + \frac{e^{-rT}}{2} \left( \sum_{k=1}^m c_k^- - \sum_{j=1}^n c_j^+ \right) + e^{s+rT} \sum_{k=1}^m d_k^+ . \quad \blacksquare
\end{aligned} \tag{2.20}$$

The payoff function given by Equation (2.15) used in Theorem 2.2.2 is very general. We now give a brief overview of some payoffs to which Theorem 2.2.2 applies. For an introduction to payoffs used in financial markets see [Hul08].

- Call

$$g^C(x) = \mathcal{X}_k(x) (e^x - e^k)$$

This option gives the owner the right to buy at time  $T$  the asset for the strike price  $e^k$ .

- Digital

$$g^D(x) = \mathcal{X}_k(x)$$

This option gives the owner one unit of money if the stock is above some strike  $e^k$  at maturity  $T$ .



- Bull Spread

$$g^{\text{Bull}}(x) = \mathcal{X}_{k_1}(x) (e^x - e^{k_1}) - \mathcal{X}_{k_2}(x) (e^x - e^{k_2})$$

This payoff is made of buying a call with strike  $e^{k_1}$  and selling a call with strike  $e^{k_2}$ , all the calls with the same maturity and  $k_2 > k_1$ .

- Butterfly

$$g^{\text{B}}(x) = \mathcal{X}_{k_1}(x) (e^x - e^{k_1}) - 2\mathcal{X}_{k_2}(x) (e^x - e^{k_2}) + \mathcal{X}_{k_3}(x) (e^x - e^{k_3})$$

This payoff is made of buying a call with strikes  $e^{k_1}$  and  $e^{k_3}$  and selling two calls with strike  $e^{k_2}$ , all the calls with the same maturity,  $k_3 > k_1$  and  $k_2 = \log((e^{k_1} + e^{k_3})/2)$ .

- Straddle

$$g^{\text{S}}(x) = \mathcal{X}_k(x) (e^x - e^k) + \mathcal{X}_{-k}(-x) (e^k - e^x)$$

This payoff is made of buying a call option, and buying a put option with the same strike,  $e^k$  and the same maturity  $T$ .

The payoffs of the Digital, Butterfly, Bull Spread and Straddle are shown in Figure 2.1, the payoffs of the call and put options are shown in Figure 1.1.

The pricing method presented in this section has one main advantage over the method presented by Carr-Madan, Subsection 2.1.1 and Lewis, Subsection 2.1.2. In Theorem 2.2.2 no extra parameter was needed, while in Lewis and Carr-Madan, the definition of an extra parameter is needed. The generalized payoff formula of Theorem 2.2.2 makes it possible to obtain a closed form pricing formula for a portfolio of derivatives, which is often the case in the markets.

All Fourier transforms found in this section involve either  $h(\xi)/\xi$  or  $h(\xi)/(1+i\xi)$ . Numerical inversion for this kind of function will be treated in Chapter 3.

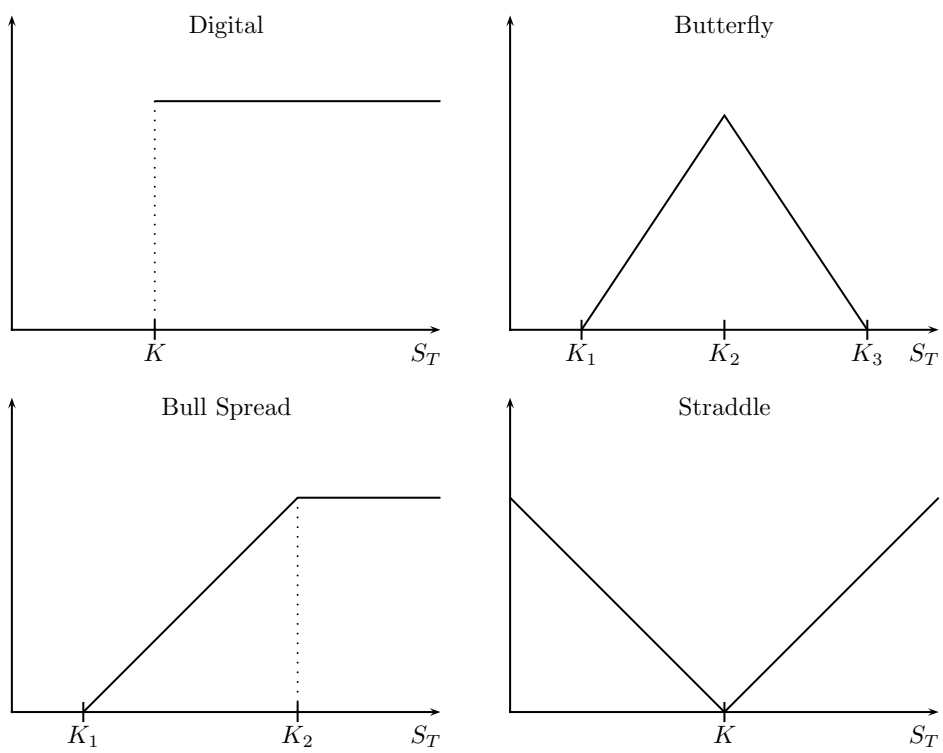


Figure 2.1: Payoffs

# Chapter 3

## Approximation of Fourier Operators

Fourier methods have been used for several problems, ranging from physics and electromagnetism to mathematical finance.

From the physics and engineering point of view, this chapter presents a fast method for the evaluation of the heat potentials. Here we follow the lines given by the work of Greengard and Lin [GL00], who developed an approximation method based on non-uniform quadrature. This kind of method was used in [LG07] to solve inhomogeneous heat equation in free space.

In this chapter, we improve the approximation method developed by Greengard and Lin [GL00] by obtaining a sharper bound, which is valid for a class of functions having the heat kernel as a particular case. In another direction, we present bounds for other types of Fourier transforms arising from the lack of differentiability of the transformed function.

We start with a simple example as motivation. Consider the heat equation problem for a finite rod,

$$\begin{aligned} u_t &= u_{xx} & t > 0, |x| \leq L\pi \\ u(-L\pi, t) &= u(L\pi, t) = 0 \\ u(x, 0) &= f(x) & |x| \leq L\pi . \end{aligned}$$

The solution is given by

$$u(x, t) = K_L(x, t) * f(x) , \tag{3.1}$$

where  $K_L(x, t)$  is the heat kernel

$$K_L(x, t) := \frac{1}{2\pi L} \sum_{k=-\infty}^{\infty} e^{-t(\frac{k}{L})^2} e^{i\frac{k}{L}x} . \tag{3.2}$$

The following lemma shows the error we make when we approximate  $K_L(x, t)$  by a finite sum.

**Lemma 3.0.3**

$$E^p(t) := \left| \frac{1}{2\pi L} \sum_{|k|>p} e^{-t(\frac{k}{L})^2} e^{i\frac{k}{L}x} \right| \leq \frac{1}{2\sqrt{\pi t}} e^{-t(\frac{p}{L})^2}. \quad (3.3)$$

**Proof:**

$$\begin{aligned} E^p(t) &\leq \frac{1}{2\pi L} \sum_{|k|>p} e^{-t(\frac{k}{L})^2} \leq \frac{e^{-t(\frac{p}{L})^2}}{\pi L} \sum_{s=1}^{\infty} e^{-t(\frac{s}{L})^2} \\ &\leq \frac{1}{\pi L} e^{-t(\frac{p}{L})^2} \int_0^{\infty} e^{-t(\frac{s}{L})^2} ds = \frac{1}{2\sqrt{\pi t}} e^{-t(\frac{p}{L})^2} \quad \blacksquare \end{aligned}$$

For the infinite rod case, we have the following kernel

$$G(x, t) = \frac{e^{-\frac{x^2}{4t}}}{2\sqrt{\pi t}} = \frac{1}{2\pi} \int_{-\infty}^{+\infty} e^{-s^2 t} e^{isx} ds. \quad (3.4)$$

The heat kernel (3.2) can be seen as the equispaced approximation of Green's function (3.4). Thus, the uniform approximation of the integral in (3.4) by uniform mesh of size  $L^{-1}$  is related to the approximation of the infinite rod problem by the finite one in the interval  $[-\pi L, \pi L]$ . Thus, if we let  $L \rightarrow \infty$  in (3.2), we obtain (3.4). A consequence of Lemma 3.3 is that, for fixed  $L$ , we get a better approximation of (3.4) by increasing the number of Fourier modes.

Consider now the truncation of the infinite interval. The next lemma gives a bound for the error.

**Lemma 3.0.4**

$$\left| \int_{-\infty}^{\infty} e^{-s^2 t} e^{isx} ds - \int_{-p}^p e^{-s^2 t} e^{isx} ds \right| \leq \min \left( \frac{1}{pt}, \sqrt{\frac{\pi}{t}} \right) e^{-p^2 t} \quad (3.5)$$

**Proof:** First notice that

$$\begin{aligned} E(t, x) &:= \left| \int_{-\infty}^{\infty} e^{-s^2 t} e^{isx} ds - \int_{-p}^p e^{-s^2 t} e^{isx} ds \right| \\ &\leq 2 \int_p^{\infty} e^{-s^2 t} ds. \end{aligned} \quad (3.6)$$

Then, a simple integration by parts results in

$$\begin{aligned} E(t, x) &\leq 2 \int_p^\infty D_s \left( e^{-s^2 t} \right) \frac{-1}{2st} ds \\ &\leq \frac{-e^{-s^2 t}}{st} \Big|_p^\infty - \int_p^\infty e^{-s^2 t} \frac{1}{s^2 t} ds \leq \frac{e^{-p^2 t}}{pt}. \end{aligned} \quad (3.7)$$

For the other inequality observe that

$$\begin{aligned} E(t, x) &\leq 2 \int_p^\infty e^{-s^2 t} ds \leq 2 \int_0^\infty e^{-(y+p)^2 t} dy \\ &\leq 2e^{-p^2 t} \int_0^\infty e^{-y^2 t} dy = \sqrt{\frac{\pi}{t}} e^{-p^2 t}. \quad \blacksquare \end{aligned} \quad (3.8)$$

Lemma 3.0.4 shows that for large values of  $t$  we need lower  $p$  to obtain the same accuracy. In the opposite direction, consider the error for the uniform quadrature

$$E_n^Q = \left| \int_{-p}^p e^{-s^2 t} e^{isx} ds - \sum_{k=1}^N e^{-s_k^2 t} e^{is_k x} \right|, \quad (3.9)$$

where  $s_k = -p + \frac{2p}{N}(k-1)$ .  $E_n^Q$  increases with  $t$ . In order to observe this, notice that  $\left| D_s \left( e^{-s^2 t} e^{isx} \right) \right| = e^{-s^2 t} \sqrt{x^2 + 4s^2 t^2}$ , which for  $x = 0$  has a maximum of  $\sqrt{t} (\sqrt{2e})^{-1}$ .

An example of the approximation of the Fourier transform by uniform quadrature is given in Figure 3.1. In order to use FFT we must have  $\Delta_x \Delta_s = 2\pi/N$ , so we have to define  $x_j = x_{\min} + j\Delta_x$ ,  $j = 0, \dots, N-1$ , where  $x_{\min} = -(N/2)\Delta_x$ .

The problem shown by Figure 3.1 is that for large values of  $t$  we must have a dense sampling on a small support, while for small  $t$  we have to enlarge the support of the sampling. In this thesis, we focus on non-uniform approximations to overcome this limitation of uniform approximations.

### 3.1 Spectral Approximation of the Free-Space Heat Kernel

In this section, we give a brief overview of the work of Greengard and Lin [GL00], which was the starting point of this chapter. In their work, they addressed the following question:

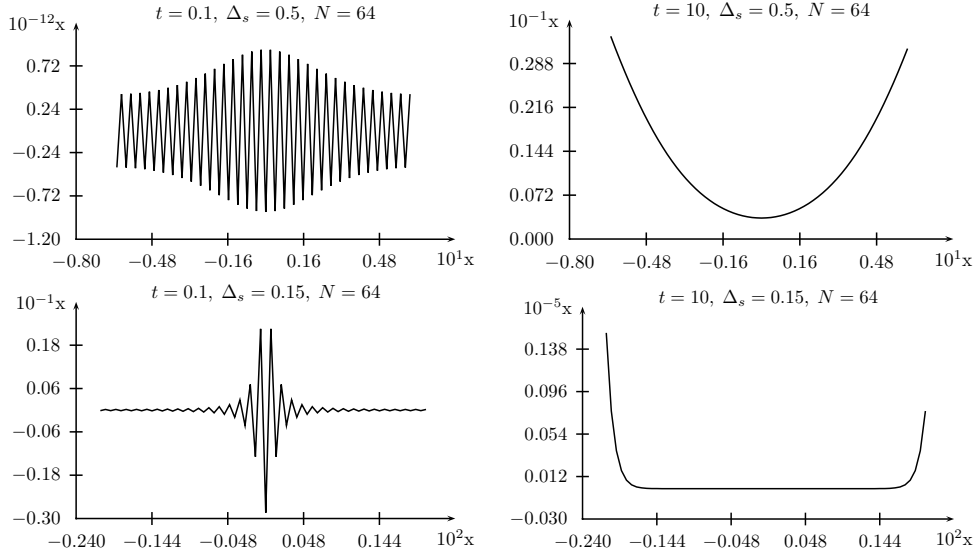


Figure 3.1: The error of the uniform approximation to the Fourier transform, as in (3.9) is shown for different values of  $\Delta_s$  and  $t$ .

*“How many quadrature points are required on an interval  $[a, b]$  in the Fourier domains in order to resolve the spectrum to within some specified precision  $\epsilon$ ?”(Greengard and Lin [GL00])*

To answer this question they presented a discretization of the heat kernel based in the Gauss-Legendre quadrature, as seen in Theorem 3.1.1. In this thesis, as in [GL00], we work with Gauss-Legendre quadrature. To simplify notation consider the following definition.

**Definition:** From here on, we always use  $\mathcal{S}_{[a,b]}^n := (s_1, \dots, s_n)$  and  $\mathcal{W}_{[a,b]}^n := (w_1, \dots, w_n)$  to denote the nodes and weights for the  $n$ -point Gauss-Legendre quadrature on the interval  $[a, b]$ .

With this definition we can present the following theorem.

**Theorem 3.1.1 ([GL00])** *Given  $n$ , and  $\epsilon$ , let  $\mathcal{S}_{[a,b]}^n$  and  $\mathcal{W}_{[a,b]}^n$  be the nodes and weights for the Gauss-Legendre quadrature, where  $[a, b] = [2^j, 2^{j+1}]$  then for  $t > t_0$ , we have*

$$\left| \int_a^b e^{-ts^2} e^{ixs} ds - \sum_{j=1}^n w_j e^{-ts_j^2} e^{ixs_j} \right| \leq \epsilon(b-a) + \frac{\sqrt{2\pi}(b-a)}{\sqrt{n}} \left( \frac{(b-a)|x|}{2n} + \frac{\sqrt{-\log(\epsilon)}}{\sqrt{n}} \right)^{2n} \quad (3.10)$$

$$\left| \int_a^b e^{-ts^2} e^{ixs} ds - \sum_{j=1}^n w_j e^{-ts_j^2} e^{ixs_j} \right| \leq \frac{\epsilon(b-a)}{p} + \frac{\sqrt{2\pi}(b-a)}{\sqrt{n}} \left( \frac{(b-a)|x|}{2n} + \frac{\sqrt{-\log(\epsilon t_0)}}{\sqrt{n}} \right)^{2n} \quad (3.11)$$

where  $\exp(-p^2 t_0)/\sqrt{7\pi t_0} = \epsilon$ .

A different version of this theorem will be shown in Theorem 3.3.3, which is based in Theorem 3.2.3. We will also present results for the estimation of the Fourier transform of  $h(s)/s$  and  $h(s)/(1+is)$  (Theorems 3.2.4, 3.2.6, 3.3.4, and 3.3.7).

## 3.2 Non-uniform Quadratures

In the previous section, we have shown the problem with the uniform quadrature to approximate the continuous Fourier transform. Historically, non-uniform quadratures have been used as an improvement over the uniform case. In this section, we present some bounds for the sampling error for non-uniform approximations of the Fourier transform for a special class of functions.

The first result of this section is a simple application of Stirling's approximation,

$$\sqrt{2\pi n} \frac{2n+1}{2} e^{-n} < n! < 2\sqrt{\pi n} \frac{2n+1}{2} e^{-n}, \quad (3.12)$$

see [AS65]. The result of the following lemma will be used in the sequel.

### Lemma 3.2.1

$$\frac{n!^4}{(2n)!^3} \leq 2\sqrt{n\pi} \left( \frac{1}{\alpha_1 n} \right)^{2n} \quad \text{and} \quad \frac{n!^4}{(2n)!^2} \leq 4n\pi \left( \frac{1}{2} \right)^{4n}, \quad (3.13)$$

where  $\alpha_1 := 8/e$ .

**Proof:** These results follow from Stirling's approximation (3.12). For the first inequality, notice that

$$\begin{aligned} \frac{n!^4}{(2n)!^3} &\leq \frac{\left( 2\sqrt{\pi n} \frac{2n+1}{2} e^{-n} \right)^4}{\left( \sqrt{2\pi} (2n) \frac{4n+1}{2} e^{-2n} \right)^3} \\ &\leq 2\sqrt{n\pi} \left( \frac{e}{2^3 n} \right)^{2n} = 2\sqrt{n\pi} \left( \frac{1}{\alpha_1 n} \right)^{2n}. \end{aligned}$$

For the second inequality, we have

$$\begin{aligned} \frac{n!^4}{(2n)!^2} &\leq \frac{\left(2\sqrt{\pi}n^{\frac{2n+1}{2}}e^{-n}\right)^4}{\left(\sqrt{2\pi}(2n)^{\frac{4n+1}{2}}e^{-2n}\right)^2} \\ &= 4n\pi \left(\frac{1}{2}\right)^{4n} . \quad \blacksquare \end{aligned}$$

The second result used in this chapter is the standard estimate for  $n$ -point Gauss-Legendre quadrature (see [DR75]).

**Theorem 3.2.2** *Let  $\mathcal{S}_{[a,b]}^n$  and  $\mathcal{W}_{[a,b]}^n$  be the nodes and weights for the  $n$ -point Gauss-Legendre quadrature on the interval  $[a, b]$ . Then, if  $h \in \mathcal{C}^{2n}[a, b]$ ,*

$$\begin{aligned} E_n^Q(h) &:= \left| \int_a^b h(s)ds - \sum_{j=1}^n w_j h(s_j) \right| \\ &\leq \frac{(b-a)^{2n+1}(n!)^4}{(2n+1)(2n)!^3} \sup_{s \in (a,b)} |D^{2n}(h(s))| . \end{aligned}$$

The approximations of Fourier transform in this section concern a specific class of functions.

**Definition:** We say that  $h(s; \beta) \in \mathcal{D}_{[a,b]}^n(f)$  if  $h(s; \beta) \in \mathcal{C}^{2n}[a, b]$ , and if derivatives of  $h(s; \beta)$  in  $s$  is bounded by

$$|D_s^j h(s; \beta)| \leq \beta^{\frac{j}{2}} (2n)^{\frac{j}{2}} f(s) ,$$

for some bounded  $f$ . A short definition of  $\mathcal{D}_{[a,b]}^n(f)$  is given by

$$\mathcal{D}_{[a,b]}^n(f) := \left\{ h(s; \beta) \in \mathcal{C}^{2n}[a, b]; |D_s^j h(s; \beta)| \leq \beta^{\frac{j}{2}} (2n)^{\frac{j}{2}} f(s) \quad j = 1, \dots, 2n \right\} .$$

When clear from the context, we denote  $\mathcal{D}_{[a,b]}^n(f)$  by  $\mathcal{D}$  and  $h(s; \beta)$  by  $h(s)$ . We are particularly interested in the Heat kernel, Lemma 3.3.1 proves that

$$h(s; t) = e^{-ts^2} \in \mathcal{D}_{[a,b]}^n \left( (4n\pi)^{1/4} e^{-ts^2/2} \right) .$$

The result of the next theorem will be later shown as an extension and improvement to [GL00]. Theorem 3.2.3, when applied to the heat kernel, can be used, for example, to solve the inhomogeneous heat equation in free space, see [LG07].

Using Lemma 3.2.1 and Theorem 3.2.2, we can prove our first approximation of the Fourier transform.



**Theorem 3.2.3** Given  $n$ , let  $\mathcal{S}_{[a,b]}^n$  and  $\mathcal{W}_{[a,b]}^n$  be the nodes and weights for the Gauss-Legendre quadrature. Then, if  $h \in \mathcal{D}_{[a,b]}^n(f)$  it follows that

$$\begin{aligned} & \left| \int_a^b h(s)e^{ixs} ds - \sum_{j=1}^n w_j h(s_j)e^{ixs_j} \right| \\ & \leq \frac{\sqrt{\pi}(b-a)}{\sqrt{n}} f^* \left( \frac{(b-a)|x|}{\alpha_1 n} + \frac{(b-a)\sqrt{2\beta}}{\alpha_1 \sqrt{n}} \right)^{2n}, \end{aligned} \quad (3.14)$$

where  $f^* = \max_{s \in [a,b]} f(s)$  and  $\alpha_1 = 8/e$ .

**Proof:** From  $h \in \mathcal{D}_{[a,b]}^n(f)$  we have

$$\begin{aligned} |D^{2n}(h(s)e^{isx})| & \leq \sum_{j=0}^{2n} \binom{2n}{j} |D^j h(s)| |D^{2n-j}(e^{isx})| \\ & \leq \sum_{j=0}^{2n} \binom{2n}{j} \beta^{\frac{j}{2}} (2n)^{\frac{j}{2}} f(s) |x|^{2n-j} \\ & \leq f(s) \sum_{j=0}^{2n} \binom{2n}{j} (\sqrt{2\beta n})^j |x|^{2n-j} \\ & \leq f(s) (|x| + \sqrt{2\beta n})^{2n}. \end{aligned} \quad (3.15)$$

Using (3.15), it follows from Theorem 3.2.2 that

$$\begin{aligned} E_n^Q & := \left| \int_a^b h(s)e^{ixs} ds - \sum_{j=1}^n w_j h(s_j)e^{ixs_j} \right| \\ & \leq \frac{(b-a)^{2n+1} (n!)^4}{(2n+1)(2n)!^3} f^* (|x| + \sqrt{2\beta n})^{2n} \\ & \leq \frac{(b-a)^{2n+1}}{(2n+1)} \left( 2\sqrt{n\pi} \left( \frac{e}{2^{3n}} \right)^{2n} \right) f^* (|x| + \sqrt{2\beta n})^{2n}, \end{aligned}$$

where we used Lemma 3.2.1 in the last inequality. The final step is given by

$$\begin{aligned} E_n^Q & \leq \frac{(b-a)8\sqrt{n\pi}}{(2n+1)} f^* \left( \frac{(b-a)|x|}{\alpha_1 n} + \frac{(b-a)\sqrt{2\beta}}{\alpha_1 \sqrt{n}} \right)^{2n} \\ & \leq \frac{(b-a)\sqrt{\pi}}{\sqrt{n}} f^* \left( \frac{(b-a)|x|}{\alpha_1 n} + \frac{(b-a)\sqrt{2\beta}}{\alpha_1 \sqrt{n}} \right)^{2n}. \quad \blacksquare \end{aligned}$$

The next approximation concerns the principal value of some Fourier transform. This kind of transformation is often seen in several different situations. As an example, we have the Fourier transform of

$$v(x) = \int_{-\infty}^x g(s) ds, \quad (3.16)$$

which is given by

$$\mathcal{F}[v](\xi) = \mathcal{F}[g](\xi) \left( \pi\delta - \frac{1}{i\xi} \right).$$

Such transformation is very often found in mathematical finance, see Section 2.2, and probability, in which it is used to compute cumulative probability.

**Theorem 3.2.4** *Given  $n$ , let  $\mathcal{S}_{[a,b]}^n$  and  $\mathcal{W}_{[a,b]}^n$  be the nodes and weights for the Gauss-Legendre quadrature. Then, if  $h \in \mathcal{D}_{[a,b]}^n(f)$  with  $0 \notin [a,b]$ , it follows that*

$$\left| \int_a^b \frac{h(s)}{is} e^{isx} ds - \sum_{j=1}^n w_j \frac{h(s_j)}{is_j} e^{ixs_j} \right| \leq f^* \left( \frac{b-a}{4s_m} \right)^{2n+1} \frac{8\pi e^{s_m \sqrt{2\beta n}}}{n} \quad (3.17)$$

$$+ \frac{\sqrt{\pi}(b-a)}{\sqrt{n}} f^* |x| \left( \frac{(b-a)|x|}{n\alpha_1} + \frac{(b-a)\sqrt{2\beta}}{\alpha_1\sqrt{n}} \right)^{2n},$$

where  $\alpha_1 = 8/e$ ,  $\bar{s} = \max(|a|, |b|)$ ,  $\underline{s} = \min(|a|, |b|)$ ,  $f^* = \max_{s \in [a,b]} f(s)$ , and  $s_m = \arg \max_{s \in [a,b]} \exp(|s|\sqrt{2\beta n})|s|^{-2n-1}$ .

**Proof:** We bound the derivative

$$\begin{aligned} \left| D_s^j \left( \frac{e^{isx}}{is} \right) \right| &= \left| -ie^{isx} \sum_{k=0}^j \binom{j}{k} (ix)^k \frac{(j-k)!(-1)^{j-k}}{s^{j-k+1}} \right| \\ &= \left| -\frac{i(-1)^j e^{isx} j!}{s^{j+1}} \sum_{k=0}^j \frac{(-isx)^k}{k!} \right| \\ &\leq \frac{j!}{|s|^{j+1}} \left| \sum_{k=0}^j \frac{(-isx)^k}{k!} \right|. \end{aligned} \quad (3.18)$$

By Taylor's theorem for some  $\tilde{s}$  with  $|\tilde{s}| < |s|$ , we then have

$$\begin{aligned} \left| D_s^j \left( \frac{e^{isx}}{is} \right) \right| &\leq \frac{j!}{|s|^{j+1}} \left| e^{-isx} - \frac{(-ix\tilde{s})^{j+1}}{(j+1)!} \right| \\ &\leq \frac{j!}{|s|^{j+1}} \left( 1 + \frac{(|x|s)^{j+1}}{(j+1)!} \right). \end{aligned} \quad (3.19)$$

Using the bound (3.19), we are ready to compute

$$\begin{aligned}
\left| D^{2n} \left( \frac{h(s)e^{isx}}{is} \right) \right| &\leq \sum_{j=0}^{2n} \binom{2n}{j} |D^{2n-j}h(s)| \left| D^j \left( \frac{e^{isx}}{is} \right) \right| \\
&\leq \sum_{j=0}^{2n} \binom{2n}{j} (\beta 2n)^{\frac{2n-j}{2}} f(s) \frac{j!}{|s|^{j+1}} \left( 1 + \frac{(|x|s)^{j+1}}{(j+1)!} \right) \\
&\leq f(s) \sum_{j=0}^{2n} \left( \frac{(2n)!}{|s|^{2n+1}} \frac{|s\sqrt{2\beta n}|^{2n-j}}{(2n-j)!} + \binom{2n}{j} \sqrt{2\beta n}^{2n-j} |x|^j \frac{|x|s}{|s|(j+1)} \right) \\
&\leq f(s) \left( \frac{(2n)!e^{|s|\sqrt{2\beta n}}}{|s|^{2n+1}} + \frac{|x|s}{|s|} \left( \sqrt{2\beta n} + |x| \right)^{2n} \right), \tag{3.20}
\end{aligned}$$

where the second line is a consequence of  $h \in \mathcal{D}$  and (3.19). Using Lemma 3.2.1 and Theorem 3.2.2, it follows from (3.20) that

$$\begin{aligned}
E &:= \left| \int_a^b \frac{h(s)e^{ixs}}{is} ds - \sum_{j=1}^n w_j \frac{h(s_j)e^{ixs_j}}{is_j} \right| \\
&\leq \frac{(b-a)^{2n+1}}{(2n+1)} f^* \left( \left( \frac{4\pi}{2^{4n}} \right) \frac{e^{s_m\sqrt{2\beta n}}}{s_m^{2n+1}} + 2\sqrt{n\pi} \left( \frac{e}{n8} \right)^{2n} |x| \left( \sqrt{2\beta n} + |x| \right)^{2n} \right) \\
&\leq f^* \left( \left( \frac{b-a}{4s_m} \right)^{2n+1} \frac{16\pi e^{s_m\sqrt{2\beta n}}}{2n+1} + \frac{2\sqrt{n\pi}(b-a)}{2n+1} x \left( \frac{(b-a)\sqrt{2\beta}}{\alpha_1\sqrt{n}} + \frac{(b-a)|x|}{n\alpha_1} \right)^{2n} \right) \\
&\leq f^* \left( \left( \frac{b-a}{4s_m} \right)^{2n+1} \frac{8\pi e^{s_m\sqrt{2\beta n}}}{n} + \frac{\sqrt{\pi}(b-a)|x|}{\sqrt{n}} \left( \frac{(b-a)\sqrt{2\beta}}{\alpha_1\sqrt{n}} + \frac{(b-a)|x|}{n\alpha_1} \right)^{2n} \right).
\end{aligned}$$

■

It is interesting to observe that the minimum for  $\exp(|s|\sqrt{2\beta n})|s|^{-2n-1}$  is achieved at  $s = \frac{2n+1}{\sqrt{2\beta n}}$  with value  $(\sqrt{2\beta n}/(2n+1))^{2n+1}$ .

Theorem 3.2.4 is related to Theorem 3.2.3. To see this, first notice that Theorem 3.2.4 has the extra term  $f^* \left( \frac{(b-a)}{(4s_m)} \right)^{2n+1} 8\pi \exp(s_m\sqrt{2\beta n})/n$ , besides that, the second line of (3.17) is the the bound obtained in Theorem 3.2.3 times  $|x|$ .

Theorem 3.2.4 is not valid when  $0 \in [a, b]$ . Thus a different approach is needed in this case. To treat it, we find an approximation of

$$I_1(x) := \int_{|s| \leq \delta} \frac{h(s)}{is} e^{isx} ds. \tag{3.21}$$

To approximate  $I_1$  we assume that the derivatives of  $h$  at 0 are available. The following lemma gives the desired approximation.

**Lemma 3.2.5** *For a given  $\delta$  and  $h \in \mathcal{C}^{n+1}[-\delta, \delta]$ , we then have*

$$\begin{aligned} E^{I_1}(n, \delta) &:= \left| \int_{|s|<\delta} \frac{e^{ixs} h(s)}{is} ds - \sum_{j=1}^n h^{(j)}(0) \frac{f_{j-1}^\delta(x)}{j!i} - h(0) \int_{|s|\leq\delta} \frac{\sin(sx)}{s} ds \right| \\ &\leq \sup_{|s|<\delta} |D^{n+1}h(s)| \frac{2\delta^{n+1}}{(n+1)(n+1)!}, \end{aligned} \quad (3.22)$$

where

$$f_n^\delta(x) := \sum_{j=0}^n \frac{n!}{(n-j)!} \frac{\delta^{n-j}}{(-ix)^{j+1}} ((-1)^{n-j} e^{-ix\delta} - e^{ix\delta}).$$

**Proof:** First notice that

$$\begin{aligned} I_1(x) &= \int_{|s|\leq\delta} \frac{h(s)}{is} e^{isx} ds \\ &= \int_{|s|\leq\delta} \frac{e^{isx}}{is} \left( \sum_{j=0}^n \frac{h^{(j)}(0) s^j}{j!} + \frac{h^{(n+1)}(z(s)) s^{n+1}}{(n+1)!} \right) ds \\ &= -i \int_{|s|\leq\delta} e^{isx} \left( \sum_{j=1}^n \frac{h^{(j)}(0) s^{j-1}}{j!} + \frac{h^{(n+1)}(z(s)) s^{n+1}}{(n+1)!} \right) ds + h(0) \int_{|s|\leq\delta} \frac{e^{isx}}{is} ds, \end{aligned} \quad (3.23)$$

where  $z(s) \in [-s, s] \subset [-\delta, \delta]$  that is given by the Taylor's theorem. The result follows from the fact that

$$f_n(x) = \int_{|s|\leq\delta} s^n e^{ixs} ds. \quad \blacksquare$$

Our next approximation concerns  $h(s)/(c + is)$ . One example of the appearance of such transform is

$$u(x) = e^{cx} \int_x^\infty g(s) e^{-cs} ds.$$

The Fourier transform of  $u$  is given by

$$\mathcal{F}[u](\xi) = \frac{\mathcal{F}[g](\xi)}{c + i\xi}. \quad (3.24)$$

Such functions are seen in several applications, for example, [CM99] used a similar transform to find option prices. In Section 2.2, Fourier transforms similar to (3.24) were also seen. The following theorem presents a bound for the Fourier transform for this type of functions.

**Theorem 3.2.6** *Given  $n$ , let  $\mathcal{S}_{[a,b]}^n$  and  $\mathcal{W}_{[a,b]}^n$  be the nodes and weights for the Gauss-Legendre quadrature. Then, if  $h \in \mathcal{D}_{[a,b]}^n(f)$  it follows that*

$$\left| \int_a^b \frac{h(s)}{c + is} e^{ixs} ds - \sum_{j=1}^n w_j \frac{h(s_j)}{c + is_j} e^{ixs_j} \right| \leq f^* \left( \frac{b-a}{4|c + \underline{s}|} \right)^{2n+1} \frac{8\pi e^{\sqrt{2\beta n(c^2 + \bar{s}^2)}}}{n} e^{xc} \\ + \frac{\sqrt{\pi}(b-a)}{\sqrt{n}} f^* |x| \left( \frac{(b-a)|x|}{\alpha_1 n} + \frac{(b-a)\sqrt{2\beta}}{\alpha_1 \sqrt{n}} \right)^{2n},$$

where  $\alpha_1 = 8/e$ ,  $\bar{s} = \max(|a|, |b|)$ ,  $\underline{s} = \min(|a|, |b|)$ , and  $f^* = \max_{s \in [a,b]} f(s)$ .

**Proof:** To calculate a bound for the derivative consider

$$\begin{aligned} \left| D^j \left( \frac{e^{isx}}{c + is} \right) \right| &= \left| e^{isx} \sum_{k=0}^j \binom{j}{k} (ix)^k \frac{(j-k)! (-i)^{j-k}}{(c + is)^{j-k}} \right| \\ &= \left| \frac{e^{isx} j!}{(c + is)^{j+1}} \sum_{k=0}^j \frac{(ix)^k (-i)^k (c + is)^k}{k!} \right| \\ &\leq \frac{j!}{|c + is|^{j+1}} \left| \sum_{k=0}^j \frac{(xc + ix s)^k}{k!} \right|. \end{aligned} \quad (3.25)$$

Using Taylor's theorem for some  $d \in \mathbb{C}$  with  $|d| < |x|\sqrt{c^2 + s^2}$ , we have

$$\begin{aligned} \left| D^j \left( \frac{e^{isx}}{c + is} \right) \right| &\leq \frac{j!}{|c + is|^{j+1}} \left| e^{xc} e^{isx} - \frac{d^{j+1}}{(j+1)!} \right| \\ &\leq \frac{j!}{|c + is|^{j+1}} \left( e^{xc} + \frac{(|x|\sqrt{c^2 + s^2})^{j+1}}{(j+1)!} \right). \end{aligned} \quad (3.26)$$

Using the fact that  $h \in \mathcal{D}$  and (3.26), we are ready to estimate

$$\begin{aligned}
\left| D^{2n} \left( \frac{h(s)e^{isx}}{c+is} \right) \right| &\leq \sum_{j=0}^{2n} \binom{2n}{j} |D^{2n-j}h(s)| \left| D^j \left( \frac{e^{isx}}{c+is} \right) \right| \\
&\leq \sum_{j=0}^{2n} \binom{2n}{j} (2\beta n)^{\frac{2n-j}{2}} f(s) \frac{j!}{|c+is|^{j+1}} \left( e^{xa} + \frac{(|x|\sqrt{c^2+s^2})^{j+1}}{(j+1)!} \right) \\
&\leq f(s)e^{xc} \sum_{j=0}^{2n} \frac{(2n)!}{|c+is|^{2n+1}} \frac{\left( \sqrt{2\beta n(c^2+s^2)} \right)^{2n-j}}{(2n-j)!} + \\
&\quad + f(s) \sum_{j=0}^{2n} \binom{2n}{j} \sqrt{2\beta n}^{2n-j} |x|^j \frac{|x|}{(j+1)} \\
&\leq f(s) \left( \frac{(2n)!e^{xc}e^{\sqrt{2\beta n(c^2+s^2)}}}{|c+is|^{2n+1}} + |x| \left( \sqrt{2\beta n} + |x| \right)^{2n} \right). \tag{3.27}
\end{aligned}$$

We used (3.27), Lemma 3.2.1, and Theorem 3.2.2 to obtain the following estimate

$$\begin{aligned}
E(n) &:= \left| \int_a^b \frac{h(s)}{c+is} e^{ixs} ds - \sum_{j=1}^n w_j \frac{h(s_j)}{c+is_j} e^{ixs_j} \right| \\
&\leq \frac{(b-a)^{2n+1}(n!)^4}{(2n+1)(2n)!^2} f^* \frac{e^{xc}e^{\sqrt{2\beta n(c^2+s^2)}}}{|c+i\underline{s}|^{2n+1}} \\
&\quad + \frac{(b-a)^{2n+1}(n!)^4}{(2n+1)(2n)!^3} f^* |x| \left( \sqrt{2\beta n} + |x| \right)^{2n} \\
&\leq 8\pi \left( \frac{b-a}{4|c+i\underline{s}|} \right)^{2n+1} \frac{f^* e^{xc}e^{\sqrt{2\beta n(c^2+s^2)}}}{n} \\
&\quad + \frac{\sqrt{\pi}(b-a)}{\sqrt{n}} f^* |x| \left( \frac{(b-a)\sqrt{2\beta}}{\alpha_1\sqrt{n}} + \frac{|x|(b-a)}{\alpha_1 n} \right)^{2n}. \quad \blacksquare
\end{aligned}$$

It is interesting to notice that Theorem 3.2.4 and 3.2.6 are essentially the same if we let  $c \rightarrow 0$ .

### 3.3 Heat Kernel

In this section, we focus on the heat kernel,  $h(s) = e^{-ts^2}$ . This particular case of Section 3.2 was studied by [GL00], as seen in Section 3.1. Here, we extend

their results to different transform and improve the bound they obtained.

We prove versions of Theorems 3.2.3, 3.2.4, and 3.2.6 for the heat kernel. With these results, we are able to, given a precision  $\epsilon$ , find for any  $t > t_0$  for a given  $t_0$ , the required quadrature points in the Fourier domain to achieve this precision.

First, we prove that, given  $[a, b]$  and  $n$ , we have  $h(s) = e^{-ts^2} \in \mathcal{D}_{[a,b]}^n(f)$ , for some  $f$ .

**Lemma 3.3.1** *If  $h(s) = e^{-ts^2}$ , then we have*

$$|D^j h(s)| \leq \beta^{\frac{j}{2}} n^{\frac{j}{2}} f(s) \quad j = 1, \dots, n \quad (3.28)$$

for  $\beta = \frac{2t}{e}$  and  $f(s) = (4n\pi)^{\frac{1}{4}} e^{-\frac{ts^2}{2}}$ .

**Proof:** From [Sza51], we have the following estimate for Hermite functions

$$\frac{1}{n!} |h_n(x)| \leq \frac{\sqrt{2}^n}{\sqrt{n!}} e^{-\frac{x^2}{2}}, \quad (3.29)$$

so, when  $h(s) = e^{-ts^2}$ ,

$$\begin{aligned} D^j \left( e^{-ts^2} \right) &= t^{\frac{j}{2}} D_x^j \left( e^{-x^2} \right) \Big|_{x=s\sqrt{t}} \\ &= t^{\frac{j}{2}} h_j \left( s\sqrt{t} \right). \end{aligned} \quad (3.30)$$

Using (3.29) and (3.30), we have the following bound for the derivative

$$\left| D^j \left( e^{-ts^2} \right) \right| \leq (2t)^{\frac{j}{2}} \sqrt{j!} e^{-\frac{ts^2}{2}}. \quad (3.31)$$

Now using (3.12), we have

$$\begin{aligned} \left| D^j \left( e^{-ts^2} \right) \right| &\leq (2t)^{\frac{j}{2}} \sqrt{2\sqrt{\pi} j^{j+\frac{1}{2}} e^{-j}} e^{-\frac{ts^2}{2}} \\ &\leq \left( \frac{2t}{e} \right)^{\frac{j}{2}} n^{\frac{j}{2}} (4n\pi)^{\frac{1}{4}} e^{-\frac{ts^2}{2}}. \quad \blacksquare \end{aligned}$$

All theorems in the previous section deal with integrals over finite intervals. We now present some bounds for the truncation of the infinite integral.

**Lemma 3.3.2**

$$\begin{aligned} \left| \int_{-\infty}^{\infty} \frac{e^{-s^2 t}}{s} e^{isx} ds - \int_{-p}^p \frac{e^{-s^2 t}}{s} e^{isx} ds \right| &\leq \min \left( \frac{1}{pt}, \sqrt{\frac{\pi}{t}} \right) \frac{e^{-p^2 t}}{p} \\ \left| \int_{-\infty}^{\infty} \frac{e^{-s^2 t}}{a + is} e^{isx} ds - \int_{-p}^p \frac{e^{-s^2 t}}{a + is} e^{isx} ds \right| &\leq \min \left( \frac{1}{pt}, \sqrt{\frac{\pi}{t}} \right) \frac{e^{-p^2 t}}{\sqrt{a^2 + p^2}} \end{aligned} \quad (3.32)$$

**Proof:** First notice that

$$E_1(t, x) := \left| \int_{-\infty}^{\infty} \frac{e^{-s^2 t}}{s} e^{isx} ds - \int_{-p}^p \frac{e^{-s^2 t}}{s} e^{isx} ds \right| \leq 2 \int_p^{\infty} \frac{e^{-s^2 t}}{s} ds .$$

Using integration by parts, we have

$$\begin{aligned} E_1(t, x) &\leq 2 \int_p^{\infty} D_s \left( e^{-s^2 t} \right) \frac{-1}{2s^2 t} ds = \frac{e^{-s^2 t}}{s^2 t} \Big|_p^{\infty} - \int_p^{\infty} e^{-s^2 t} \frac{2}{s^2 t} ds \\ &\leq \frac{e^{-p^2 t}}{p^2 t} , \end{aligned}$$

so we have one of the bounds. Now consider

$$\begin{aligned} E_1(t, x) &\leq 2 \int_p^{\infty} \frac{e^{-s^2 t}}{s} ds = 2 \int_0^{\infty} \frac{e^{-(y+p)^2 t}}{y+p} dy \\ &\leq 2 \frac{e^{-p^2 t}}{p} \int_0^{\infty} e^{-y^2 t} dy = \sqrt{\frac{\pi}{t}} \frac{e^{-p^2 t}}{p} . \end{aligned} \tag{3.33}$$

For the second integral, notice that

$$E_2(t, x) := \left| \int_{-\infty}^{\infty} \frac{e^{-s^2 t}}{a+is} e^{isx} ds - \int_{-p}^p \frac{e^{-s^2 t}}{a+is} e^{isx} ds \right| \leq 2 \int_p^{\infty} \frac{e^{-s^2 t}}{\sqrt{a^2 + s^2}} ds .$$

It follows from integration by parts that

$$\begin{aligned} E_2(t, x) &\leq 2 \int_p^{\infty} \frac{D_s \left( e^{-s^2 t} \right)}{-2st\sqrt{a^2 + s^2}} ds \\ &= \frac{e^{-s^2 t}}{st\sqrt{a^2 + s^2}} \Big|_p^{\infty} - \int_p^{\infty} \frac{e^{-s^2 t}}{\sqrt{a^2 + s^2}} \left( \frac{1}{s^2} + \frac{1}{a^2 + s^2} \right) ds \\ &\leq \frac{e^{-p^2 t}}{pt\sqrt{a^2 + p^2}} . \end{aligned}$$

Finally consider

$$\begin{aligned} E_2(t, x) &\leq 2 \int_p^{\infty} \frac{e^{-s^2 t}}{\sqrt{a^2 + s^2}} ds = 2 \int_0^{\infty} \frac{e^{-(y+p)^2 t}}{\sqrt{a^2 + (y+p)^2}} dy \\ &\leq 2 \frac{e^{-p^2 t}}{\sqrt{a^2 + p^2}} \int_0^{\infty} e^{-y^2 t} dy = \frac{\sqrt{\pi} e^{-p^2 t}}{\sqrt{t(a^2 + p^2)}} \blacksquare \end{aligned}$$



We now present the version of Theorem 3.2.3 for the heat kernel. This result follows the line of [GL00], which proved Theorem 3.1.1. Theorem 3.3.3 has some improvements over Theorem 3.1.1, as we show next.

**Theorem 3.3.3** *Given  $n$ , and  $\epsilon$ , let  $\mathcal{S}_{[a,b]}^n$  and  $\mathcal{W}_{[a,b]}^n$  be the nodes and weights for the Gauss-Legendre quadrature, where  $[a, b] = [2^j, 2^{j+1}]$  then for  $t > t_0$ , we have*

$$\left| \int_a^b e^{-ts^2} e^{ixs} ds - \sum_{j=1}^n w_j e^{-ts_j^2} e^{ixs_j} \right| \leq \epsilon(b-a) + \frac{2(b-a)\pi^{\frac{3}{4}}}{n^{\frac{1}{4}}} e^{-\frac{t_0 \underline{s}^2}{2}} \left( \frac{(b-a)x}{\alpha_1 n} + \frac{\sqrt{-\log(\epsilon)}}{\alpha_2 \sqrt{n}} \right)^{2n} \quad (3.34)$$

$$\left| \int_a^b e^{-ts^2} e^{ixs} ds - \sum_{j=1}^n w_j e^{-ts_j^2} e^{ixs_j} \right| \leq \epsilon \frac{(b-a)}{p} + \frac{2(b-a)\pi^{\frac{3}{4}}}{n^{\frac{1}{4}}} e^{-\frac{t_0 \underline{s}^2}{2}} \left( \frac{(b-a)x}{\alpha_1 n} + \frac{\sqrt{-\log((\epsilon\sqrt{t_0}))}}{\alpha_2 \sqrt{n}} \right)^{2n}, \quad (3.35)$$

where  $p = \sqrt{-\log(\epsilon\sqrt{t_0})}/t_0$ ,  $\underline{s} = \min(|a|, |b|)$ ,  $\alpha_1 = 8/e$ , and  $\alpha_2 = 4\sqrt{2/e}$ .

**Proof:** For  $(b-a)\sqrt{t} < \sqrt{-\log(\epsilon)}$  and  $(b-a)\sqrt{t} < \sqrt{-\log(\epsilon\sqrt{t_0})}$  the theorem is a consequence of Theorem 3.2.3 and Lemma 3.3.1. For  $a\sqrt{t} = (b-a)\sqrt{t} > \sqrt{-\log(\epsilon)}$ , we have

$$\left| \int_a^b e^{-ts^2} e^{isx} ds \right| \leq e^{-ta^2} \int_a^b ds \leq \epsilon(b-a). \quad (3.36)$$

For  $a\sqrt{t} = (b-a)\sqrt{t} > \sqrt{-\log(\epsilon\sqrt{t_0})}$ , it follows that

$$\left| \int_a^b e^{-ts^2} e^{isx} ds \right| \leq e^{-ta^2} \int_0^{b-a} e^{-tx^2} dx \leq \epsilon\sqrt{t_0} \int_0^{b-a} e^{-\left(\frac{\log(\epsilon\sqrt{t_0})}{(b-a)^2}\right)x^2} dx$$

so defining  $y = \frac{\sqrt{-\log(\epsilon\sqrt{t_0})}}{b-a}x$ , we have

$$\begin{aligned} \left| \int_a^b e^{-ts^2} e^{isx} ds \right| &\leq \epsilon \frac{\sqrt{t_0}(b-a)}{\sqrt{-\log(\epsilon\sqrt{t_0})}} \int_0^{\sqrt{-\log(\epsilon\sqrt{t_0})}} e^{-y^2} dy \\ &\leq \epsilon \frac{\sqrt{t_0}(b-a)}{\sqrt{-\log(\epsilon\sqrt{t_0})}} \frac{\sqrt{\pi}}{2}. \end{aligned}$$

Now let  $p = \frac{\sqrt{-\log(\epsilon\sqrt{t_0})}}{\sqrt{t_0}}$  then

$$\left| \int_a^b e^{-ts^2} e^{isx} ds \right| \leq \epsilon \frac{b-a}{p} \quad \blacksquare \quad (3.37)$$

The above result improves [GL00] for large values of  $s$ , due to the fast decay of the function  $e^{-t_0s^2/2}$  presented in Theorem 3.3.3 that is not present in [GL00]. Another difference is that while we use  $\alpha_1 \approx 2.94$ , [GL00] uses 2. The result of [GL00] has the advantage of using  $\sqrt{n}$ , where in our result we have  $n^{1/4}$ . See Figure 3.2 for a comparison of the results.

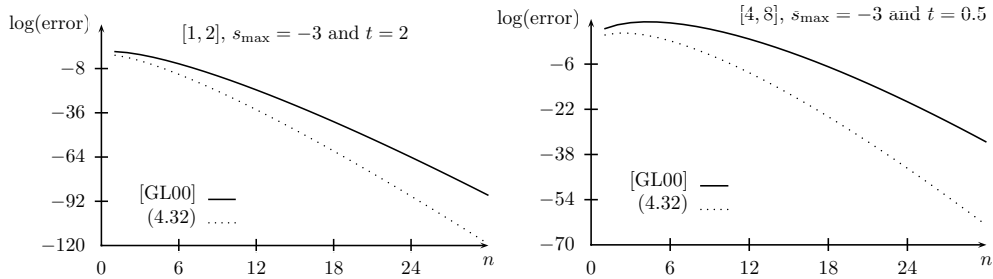


Figure 3.2: Comparison of the accuracy for a given  $n$  and  $t$  of the estimates in Equation (3.34) and [GL00].

We also study a version of Theorem 3.2.4 for the heat kernel case.

**Theorem 3.3.4** *Given  $n$ , and  $\epsilon$ , let  $\mathcal{S}_{[a,b]}^n$  and  $\mathcal{W}_{[a,b]}^n$  be the nodes and weights for the Gauss-Legendre quadrature, where  $[a, b] = [2^j, 2^{j+1}]$ , then for  $t > t_0$ ,*

we have

$$\begin{aligned} \left| \int_a^b \frac{h(s)}{is} e^{isx} ds - \sum_{j=1}^n w_j \frac{h(s_j)}{is_j} e^{ixs_j} \right| &\leq 2^{7/2} \pi^{5/4} \left( \frac{b-a}{4s_m} \right)^{2n+1} \frac{e^{\kappa(s_m)}}{n^{3/4}} \\ &+ (b-a) e^{-t_0 a^2} \frac{(4\pi^3)^{1/4}}{n^{1/4}} \left( \frac{\sqrt{-\log(\epsilon)}}{\alpha_2 \sqrt{n}} + \frac{(b-a)x}{n\alpha_1} \right)^{2n} + \epsilon \log \left( \frac{b}{a} \right), \end{aligned} \quad (3.38)$$

where  $\alpha_1 = 8/e$ ,  $\alpha_2 = 4\sqrt{2/e}$ ,  $s_m = \arg \max_{s \in [a,b]} e^{|s|\sqrt{2\beta n}} |s|^{-2n}$ , and  $\kappa(s) = \min \left( n/e, -t_0 s_m^2 + s_m \sqrt{-4 \log(\epsilon) n / \sqrt{(b-a)e}} \right)$ .

**Proof:** For  $(b-a)\sqrt{t} > \sqrt{-\log(\epsilon)}$ , we have

$$\begin{aligned} \left| \int_a^b \frac{e^{-t\xi^2}}{i\xi} e^{is\xi} d\xi \right| &\leq e^{-ta^2} \int_a^b \frac{1}{\xi} d\xi \leq e^{-t(b-a)^2} \int_a^b \frac{1}{\xi} d\xi \\ &\leq \epsilon \int_a^b \frac{1}{\xi} d\xi \leq \epsilon (\log(b) - \log(a)). \end{aligned} \quad (3.39)$$

For  $(b-a)\sqrt{t} \leq \sqrt{-\log(\epsilon)}$ , observe that

$$\max_{t>0} \left( -ts^2 + s\sqrt{\frac{4tn}{e}} \right) = \frac{n}{e}, \quad (3.40)$$

and

$$-ts_m^2 + s_m \sqrt{\frac{4tn}{e}} \leq -t_0 s_m^2 + s_m \sqrt{-\frac{4 \log(\epsilon) n}{(b-a)e}}. \quad (3.41)$$

The result then follows from Lemma 3.0.4 and Theorem 3.2.3.  $\blacksquare$

The bound in Theorem 3.3.4 is valid for every interval of the form  $[2^j, 2^{j+1}]$ . For practical applications, we cannot make  $j \rightarrow -\infty$ , so we need another approximation for an interval of the type  $[-\delta, \delta]$ . For this purpose, we present a version of Lemma 3.2.5 for the heat kernel case.

**Lemma 3.3.5**

$$\begin{aligned} E^{I_1}(n, \delta) &:= \left| \int_{|s|<\delta} \frac{e^{ixs} e^{-ts^2}}{is} ds - \sum_{j=1}^n h^{(j)}(0) \frac{f_{j-1}^\delta(x)}{j!} - h(0) \int_{|s|\leq\delta} \frac{e^{ixs}}{is} ds \right| \\ &\leq \frac{2}{\pi^{1/4}} \left( \frac{2e}{n+1} \right)^{\frac{n+1}{2}} t^{\frac{n+1}{2}} \frac{\delta^{n+1}}{n^{3/4}}, \end{aligned}$$

(3.42)

where  $f_n^\delta(x)$  is as in Lemma 3.2.5 and

$$h^{(j)}(0) = \begin{cases} 0 & \text{If } j = 2n + 1 \\ \frac{(2n)!}{n!} (-t)^n & \text{If } j = 2n \end{cases}.$$

**Proof:** Using Lemma 3.2.5 and (3.12), we then have

$$\begin{aligned} E^{I_1}(n, \delta) &\leq \sup_{|y| < \delta} |D^{n+1}h(y)| \frac{2\delta^{n+1}}{(n+1)(n+1)!} \\ &\leq \frac{2(4\pi)^{\frac{1}{4}} n^{\frac{1}{4}} \left(\frac{2t}{e}\right)^{\frac{n+1}{2}} (n+1)^{\frac{n+1}{2}} \delta^{n+1}}{(n+1)(n+1)!} \\ &\leq \frac{2}{\pi^{\frac{1}{4}}} \left(\frac{2e}{n+1}\right)^{\frac{n+1}{2}} t^{\frac{n+1}{2}} \frac{\delta^{n+1}}{n^{\frac{3}{4}}}. \quad \blacksquare \end{aligned} \quad (3.43)$$

The bound in Lemma 3.3.5 grows with  $t$ . It is possible to find an uniform bound version of the previous lemma.

**Lemma 3.3.6** *Given  $\kappa > 0$  and  $t > \bar{t}$ , we have*

$$\begin{aligned} E^{I_1}(n, \delta) &:= \left| \int_{|s| < \delta} \frac{e^{ixs} e^{-ts^2}}{is} ds - \sum_{j=1}^n h^{(j)}(0) \frac{f_{j-1}^{\sqrt{\bar{t}\delta}}(x/\sqrt{t})}{j!} - h(0) \int_{|s| \leq \delta} \frac{e^{ixs}}{is} ds \right| \\ &\leq \frac{2}{\pi^{\frac{1}{4}}} \left(\frac{2e}{n+1}\right)^{\frac{n+1}{2}} \bar{t}^{\frac{n+1}{2}} \frac{\delta^{n+1}}{n^{\frac{3}{4}}} + \kappa, \end{aligned} \quad (3.44)$$

where  $f_n(x)$  as in 3.2.5,  $h^{(j)}(0)$  as in Lemma 3.3.5, and

$$\kappa = \sqrt{\pi} \frac{e^{-\bar{t}\delta^2}}{\sqrt{\bar{t}\delta^2}}.$$

**Proof:** A simple change of variables shows that

$$\int_{|s| < \delta} \frac{e^{ixs} e^{-ts^2}}{is} ds = \int_{-\sqrt{\bar{t}\delta}}^{\sqrt{\bar{t}\delta}} \frac{e^{i\frac{x}{\sqrt{\bar{t}}}y} e^{-y^2}}{iy} dy.$$

Then, for  $t > \bar{t}$ , we have

$$\left| \int_{|s| < \delta} \frac{e^{ixs} e^{-ts^2}}{is} ds \right| = \left| \int_{-\sqrt{\bar{t}\delta}}^{\sqrt{\bar{t}\delta}} \frac{e^{i\frac{x}{\sqrt{\bar{t}}}y} e^{-y^2}}{iy} dy \right| + \left| 2 \int_{\sqrt{\bar{t}\delta}}^{\infty} \frac{e^{i\frac{x}{\sqrt{\bar{t}}}y} e^{-y^2}}{iy} dy \right|.$$

The result follows from Lemma 3.3.2 and Lemma 3.3.5.  $\blacksquare$

Our final bound is a version of Theorem 3.2.6 for the heat kernel.

**Theorem 3.3.7** *For a given  $\epsilon$ , let  $\mathcal{S}_{[a,b]}^n$  and  $\mathcal{W}_{[a,b]}^n$  be the nodes and weights for the Gauss-Legendre quadrature, then for  $t > t_0$ , we have*

$$\left| \int_a^b \frac{h(s)}{c+is} e^{ixs} ds - \sum_{j=1}^n w_j \frac{h(s_j)}{c+is_j} e^{ixs_j} \right| \leq 2^{7/2} \pi^{5/4} \left( \frac{b-a}{4|c+ia|} \right)^{2n+1} \frac{e^{xc} e^{\frac{n}{e} \left(1 + \frac{c^2}{a^2}\right)}}{n^{3/4}} \\ + \frac{(4\pi^3)^{1/4} a}{n^{1/4}} e^{-t_0 a^2} |x| \left( \frac{\sqrt{-\log(\epsilon)}}{\alpha_2 \sqrt{n}} + \frac{|x|}{\alpha_1 n} \right)^{2n} + \epsilon \left( \sinh^{-1} \left( \frac{b}{c} \right) - \sinh^{-1} \left( \frac{a}{c} \right) \right),$$

where  $\alpha_1 = 8/e$  and  $\alpha_2 = 4\sqrt{2/e}$ .

**Proof:** For  $(b-a)\sqrt{t} > \sqrt{-\log(\epsilon)}$ , we have

$$\left| \int_a^b \frac{e^{-ts^2}}{c+is} e^{ixs} ds \right| \leq e^{-ta^2} \int_a^b \frac{1}{\sqrt{c^2+s^2}} ds \\ \leq \epsilon \left( \sinh^{-1} \left( \frac{b}{c} \right) - \sinh^{-1} \left( \frac{a}{c} \right) \right). \quad (3.45)$$

For  $(b-a)\sqrt{t} \geq \sqrt{-\log(\epsilon)}$ , notice that

$$\max_{t \geq 0} \left( -ts^2 + \sqrt{c^2+s^2} \sqrt{\frac{4nt}{e}} \right) = \frac{n}{e} \left( 1 + \frac{c^2}{s^2} \right). \quad \blacksquare \quad (3.46)$$

In Section 3.2, we made some comments about the relation between Theorems 3.2.4 and 3.2.6. Considering that Theorems 3.3.4 and 3.3.7 are applications of Theorems 3.2.4 and 3.2.6 for the heat kernel, some relation between these results are natural. The relation follows from the fact that, given  $[a, b] = [2^j, 2^{j+1}]$ , we have

$$\lim_{c \rightarrow 0} \left( \sinh^{-1} \left( \frac{b}{c} \right) - \sinh^{-1} \left( \frac{a}{c} \right) \right) = \log \left( \frac{b}{a} \right),$$

so, the bounds in Theorem 3.2.6 converges to the bounds in Theorem 3.2.4.

# Chapter 4

## The Algorithm for Computing Non-uniform Quadratures

In this chapter, we introduce the non-uniform fast Fourier transform (NUFFT). This algorithm will be used to present a fast algorithm for the bounds developed in Chapter 3.

The fast Fourier transform is used in many applications where uniformly-spaced samples arise. But for several applications, such as iterative magnetic resonance image (MRI) reconstruction or geology, no uniform samples are available. To make use of the computational advantage of the FFT for non-uniform grids, NUFFT algorithm was developed. In this chapter, we give a brief review of the fast Fourier transform for non-uniform sampling.

To introduce the problem, consider  $\Pi := [-\frac{1}{2}, \frac{1}{2})$  and

$$I_N := \left\{ k \in \mathbb{Z} \mid -\frac{N}{2} \leq k < \frac{N}{2} \right\}.$$

The discrete Fourier transform for non-equispaced grid is given by

$$f(v_j) = \sum_{k \in I_N} f_k e^{-2\pi i x_k v_j} \quad (j \in I_M), \quad (4.1)$$

where  $x_k \in \Pi$  and  $v_n \in N\Pi$ . The Fourier transform in its form (4.1) is non-uniform in both real and Fourier space. The NUFFT algorithm to address this problem is called type 3 NUFFT. Special algorithms are available when the grid is uniform in real or Fourier space. The problem

$$f(v_j) = \sum_{k \in I_N} f_k e^{-2\pi i k v_j} \quad (j \in I_M), \quad (4.2)$$

is called type 1 NUFFT. And the type 2 NUFFT is given by

$$f(j) = \sum_{k \in I_N} f_k e^{-2\pi i x_k j / N} \quad (j \in I_M) . \quad (4.3)$$

For  $x_k = k\Delta_x$  and  $v_j = j\Delta_v$ , with  $\Delta_x \Delta_v = N^{-1}$  we have the usual fast Fourier transform.

The computation of the NUFFT has been addressed by several authors, see for example [Ste98], [PST98], [AD96], [DR95] and [DR93]. The NUFFT algorithm we present here follows closely [Ste98] and [PST98].

This chapter is organized as following. In Section 4.1, we give a brief overview for the algorithm for type 1 NUFFT (4.2). The algorithm for type 3 NUFFT (4.1) is addressed in Section 4.2. In Section 4.3 we present some numerical examples concerning the accuracy of NUFFT computation, the bounds of Chapter 3 and some results for pricing financial derivatives using the formulas of Chapter 2.

## 4.1 FFT for Uniform Real Space Non-uniform Fourier Space

First, we present the algorithm for non-uniformity in Fourier space, that is type 1 NUFFT (4.2). To compute this transform, it is necessary to define an oversampling factor  $\alpha > 1$  and set  $n := \lceil \alpha_1 N \rceil$ , where  $\lceil \cdot \rceil$  is the notation for the ceiling functions [GKP89]. Let  $\varphi$  be a function with period 1 that has uniformly convergent Fourier series. We approximate  $f(v)$  by

$$f(v) = s_1(v) := \sum_{j \in I_n} g_j \varphi \left( v - \frac{j}{n} \right) . \quad (4.4)$$

Replacing  $\varphi$  in (4.4) by its Fourier series, we get

$$\begin{aligned} s_1(v) &= \sum_{k \in \mathbb{Z}} \hat{g}_k c_k e^{-2\pi i k v} \\ &= \sum_{r \in \mathbb{Z}} \sum_{n \in I_n} \hat{g}_{k+nr} c_{k+nr} e^{-2\pi i (k+nr)v} , \end{aligned} \quad (4.5)$$

where

$$\begin{aligned} \hat{g}_k &:= \sum_{j \in I_n} g_j e^{2\pi i \frac{kj}{n}} , \\ \hat{c}_k &:= \int_{\Pi} \varphi(v) e^{2\pi i k v} dv . \end{aligned} \quad (4.6)$$

Using the fact that  $|c_k| \rightarrow 0$  as  $|k| \rightarrow \infty$ , we can assume that  $\varphi$  and  $n$  are so that the summation in (4.5) can be approximated by 0 for  $r \neq 0$ . Comparing (4.2) to (4.5), it is natural to define

$$\widehat{g}_k := \begin{cases} f_k/c_k & \text{If } k \in I_N \\ 0 & \text{If } k \notin I_N \end{cases}. \quad (4.7)$$

Using (4.7), we can calculate  $g$  by the Fourier inversion

$$g_j = \frac{1}{n} \sum_{k \in I_N} \widehat{g}_k e^{-2\pi i \frac{kj}{n}}. \quad (4.8)$$

The final step towards the approximation of (4.2) is to find a function  $\psi_1$  with  $\text{supp } \psi_i \subset [-m/n, m/n]$ , with  $m \ll n$  that approximates  $\varphi$ . This approximation makes the summation in (4.4) attractive. Finally we have the approximation given by

$$f(v_j) \approx \sum_{j \in I_{n,m}(v_j)} g_j \psi \left( v_j - \frac{j}{n} \right), \quad (4.9)$$

where  $I_{n,m}(v) = \{j \in I_n \mid -\frac{m}{n} \leq v - \frac{j}{n} \leq \frac{m}{n}\}$ . Notice that for  $j \notin I_{n,m}$ , the value of  $\psi(v_j - j/n)$  is zero, because  $v_j - j/n$  is outside the support of  $\psi_1$ . So the type 1 NUFFT makes  $\mathcal{O}(\alpha_1 N \log(\alpha_1 N))$  arithmetical operations.

As in [Ste98] and [PST98], we chose  $\varphi$  as the dilated periodized Gaussian bell

$$\varphi^G(x) := \frac{1}{\sqrt{\pi b}} \sum_{r \in \mathbb{Z}} e^{-n^2 \frac{(x+r)^2}{b}}, \quad (4.10)$$

with  $b = \frac{2\alpha m}{(2\alpha-1)\pi}$ . The Fourier transform of  $\varphi$  is given by

$$\widehat{\varphi^G}(k) = \frac{1}{n} e^{-\left(\frac{\pi k}{n}\right)^2 b}. \quad (4.11)$$

The truncated version of  $\varphi^G$  is given by

$$\psi^G(x) := \frac{1}{\sqrt{\pi b}} \sum_{r \in \mathbb{Z}} e^{-n^2 \frac{(x+r)^2}{b}} \mathcal{X}_{[-m,m]}(n(x+r)). \quad (4.12)$$



## 4.2 NUFFT: the General Case

To find an approximation for (4.1), let  $\varphi_1 \in L^2(\mathbb{R})$  and define

$$G(x) = \sum_{k \in I_N} f_k \varphi_1(x - x_k). \quad (4.13)$$

Let  $0 < m \ll 1$ ,  $a = 1 + 2m$  and  $\alpha_1 > 1$  be given. Define  $n_1 := \lceil \alpha_1 N \rceil$  and  $n_2 := an_1$ . We can compute the Fourier transform of  $G$  by

$$\widehat{G}(v) = \sum_{k \in I_N} f_k e^{-2\pi i x_k v} \widehat{\varphi}_1(v). \quad (4.14)$$

Comparing (4.14) and (4.1), we see that if we know  $\widehat{G}(v)$ , we can compute  $f(v)$  by

$$f(v_j) = \frac{\widehat{G}(v_j)}{\widehat{\varphi}_1(v_j)}. \quad (4.15)$$

For this, we need to compute  $\widehat{G}(v)$ . To do so, first note that

$$\begin{aligned} \widehat{G}(v) &= \frac{1}{n_1} \sum_{k \in I_N} f_k \int_{\mathbb{R}} e^{-2\pi i x v} \varphi_1(x - x_k) dx \\ &= \sum_{k \in I_N} f_k \sum_{r \in \mathbb{Z}} \int_{a\Pi} e^{-2\pi i(x+ra)v} \varphi_1(x + ra - x_k) dx. \end{aligned} \quad (4.16)$$

Discretizing the integral in (4.16) by a rectangular rule with size  $n_1^{-1}$ , we get

$$\widehat{G}(v) \approx \sum_{k \in I_N} f_k \sum_{r \in \mathbb{Z}} \sum_{j \in I_{n_2}} e^{-2\pi i \left(\frac{j}{n_1} + ra\right)v} \varphi_1\left(\frac{j}{n_1} + ra - x_k\right). \quad (4.17)$$

The approximation (4.17) is more time consuming than the original problem. To solve this problem, we approximate  $\varphi_1$  by  $\psi_1$  with  $\text{supp} \psi_1 \subset m\Pi$ . Note that  $(-\frac{a}{2}, \frac{a}{2}) + \Pi \subset (-1 - m, 1 + m)$ , so replacing  $\varphi_1$  in (4.17) by  $\psi_1$  the sum is zero for  $r \neq 0$ . Then, by changing the sum order in (4.17) we have

$$\widehat{G}(v) \approx S(v) := \sum_{j \in I_{n_2}} \left( \sum_{k \in I_N} f_k \psi_1\left(\frac{j}{n_1} - x_k\right) \right) e^{-2\pi i \left(\frac{j}{n_1}\right)v}, \quad (4.18)$$

with this, we can compute

$$F_j = \sum_{k \in I_N} f_k \psi_1\left(\frac{j}{n_1} - x_k\right) \quad (j \in I_{n_2}). \quad (4.19)$$

This calculation takes only  $mn_2$  multiplications and not  $n_2N$  which would make (4.19) useless. With this formulation we reduce the problem (4.1) to

$$S(v) = \frac{1}{n_1} \sum_{j \in I_{n_2}} F_j e^{-2\pi i (\frac{j}{n_1})v} . \quad (4.20)$$

Equation (4.20) is still non-uniform in  $v$ , but it is uniform in  $j$ . So problem (4.20) is now a type 1 NUFFT that was already treated in Section 4.1.

Following [PST98], we choose for  $\varphi_1$  the dilated periodized Gaussian bell

$$\varphi_a^G(x) := \frac{1}{\sqrt{\pi b}} \sum_{r \in \mathbb{Z}} e^{-n^2 \frac{(x+ar)^2}{b}} . \quad (4.21)$$

with  $b = \frac{2\alpha m}{(2\alpha-1)\pi}$ . The Fourier transform of  $\varphi_a^G$  is given by

$$\widehat{\varphi_a^G}(k) = \frac{1}{n} e^{-\left(\frac{\pi k}{n}\right)^2 b} . \quad (4.22)$$

The truncated version of  $\varphi_a^G$  is given by

$$\psi_a^G(x) := \frac{1}{\sqrt{\pi b}} \sum_{r \in \mathbb{Z}} e^{-n^2 \frac{(x+r)^2}{b}} \mathcal{X}_{[-m,m]}(n(x+r)) . \quad (4.23)$$

### 4.3 Numerical Example

In this section, we show some results based on the bounds we presented in Chapter 3 and the NUFFT algorithm we presented in this chapter. We developed an algorithm that uses the bounds in Chapter 3 to construct a grid of a given precision and then uses NUFFT to compute the value for a non-uniform grid in  $s$ .

We are mainly interested in testing the bounds of Chapter 3, to do so several types of error are addressed in this section.

- Total error;

$$E^T = \left| \int_{-\infty}^{\infty} h(s) e^{isx} ds - \text{NUFFT}(\omega_n h(s_n), s_n, x_n) \right| .$$

- Truncation error

$$E^p = \left| \int_{-\infty}^{\infty} h(s) e^{isx} ds - \int_{-p}^p h(s) e^{isx} ds \right| .$$

- Quadrature error

$$E^Q = \left| \int_{-p}^p h(s)e^{isx} ds - \sum_{n=1}^N \omega_n h(s_n)e^{is_n x} \right|.$$

- NUFFT error

$$E^{NU} = \left| \sum_{n=1}^N \omega_n h(s_n)e^{is_n x} - \text{NUFFT}(\omega_n h(s_n), s_n, x) \right|.$$

First, consider the discretization of the heat kernel given by Equation (3.4). Using Theorem 3.2.3 (or Theorem 3.3.3), which controls  $E^Q$  and Lemma 3.0.4, which controls  $E^p$ , ignoring the error due to the NUFFT approximation,  $E^{NU}$ , it is possible to, given  $\epsilon$ , find the non-uniform mesh to achieve the desired accuracy, that is find a mesh such that  $E^p + E^Q < \epsilon$ .

As a first example, we construct a quadrature to achieve an accuracy of  $\epsilon_1 = 10^{-5}$  and  $\epsilon_2 = 10^{-10}$ . The numerical result of this quadrature is compared with the true value given in (3.4). The results are shown in Figure 4.1.

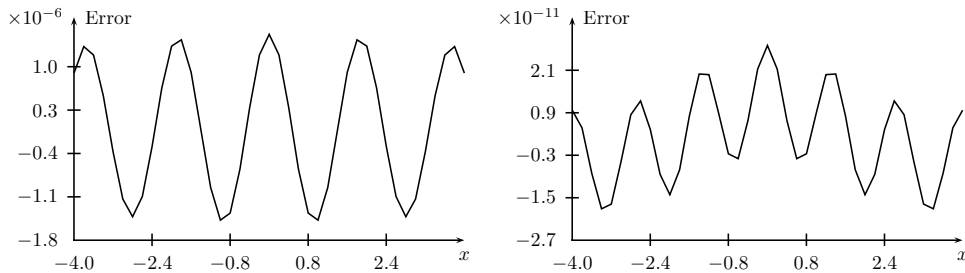


Figure 4.1: The error of the NUFFT approximation for (3.4), with mesh given by Theorem 3.2.3 and Lemma 3.0.4. In both graphics we have  $t = 1$ . The graphic on the left is for  $\epsilon_1 = 10^{-5}$  and uses 69 points to discretize (3.4). The graphic on the right is for  $\epsilon_2 = 10^{-10}$  and uses 122 points.

The good result shown in Figure 4.1 depends on the right choice of the parameters of the NUFFT approximation. In the algorithm, we only built estimates for the errors  $E^p$  and  $E^Q$ . Thus, large values of  $E^{NU}$  can make the algorithm fail to achieve the desired precision. This problem is shown in Figure 4.2, where we compare the approximation results given precision  $\epsilon = 10^{-10}$  for different values of  $m$ , which defines the support of  $\psi$ , see Section 4.2.

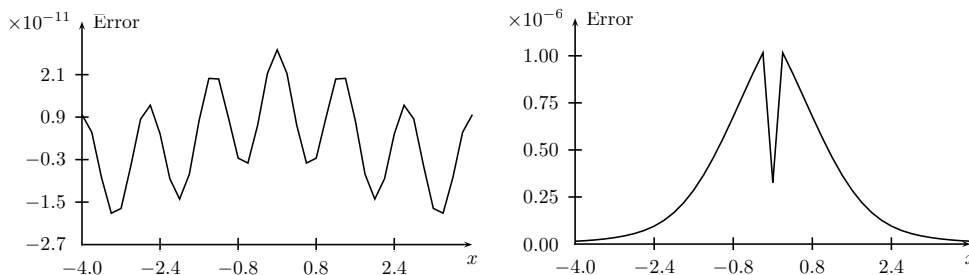


Figure 4.2: The error of the NUFFT approximation for (3.4), with mesh given by Theorem 3.2.3 and Lemma 3.0.4. In both graphics we have  $t = 1$  and precision  $10^{-10}$ . The graphic on the left has  $m = 25$  and the graphic on the right has  $m = 5$ .

$m$	error ( $E^{NU}$ )
5	$6.38e - 06$
10	$2.91e - 11$
15	$9.02e - 14$
25	$8.03e - 14$

Table 4.1: The error for different parameters  $m$  using random grid in the real and the Fourier space, with  $N = 128$ . The results is the maximum absolute value of the results, when compared to the results obtained by DFT.

To test the influence of the parameter  $m$ , we choose a random grid in the real and the Fourier space with 128 points and measure the accuracy of the NUFFT by comparing the results with the DFT. The results are shown in Table 4.1. From now on, we assume  $m = 25$ .

Consider the quadrature error,  $E^Q$ , bounds for these errors are given by Theorem 3.2.3 and Theorem 3.3.3. In Figure 4.3, we compare the bound obtained by Theorem 3.2.3 with the numerical error (notice that our bound improves the one in [GL00], as seen in Figure 3.2). The numerical error is obtained by Gauss-Kronrod quadrature, see [Sha08]. This quadrature is chosen because it supports singularities.

In Figure 3.1, we compared the accuracy of the uniform grid for different values of  $t$ . It is interesting to compare the accuracy of the non-uniform approximation using NUFFT with the uniform one using FFT, in order to check the improvements of the non-uniform quadrature over the uniform one.

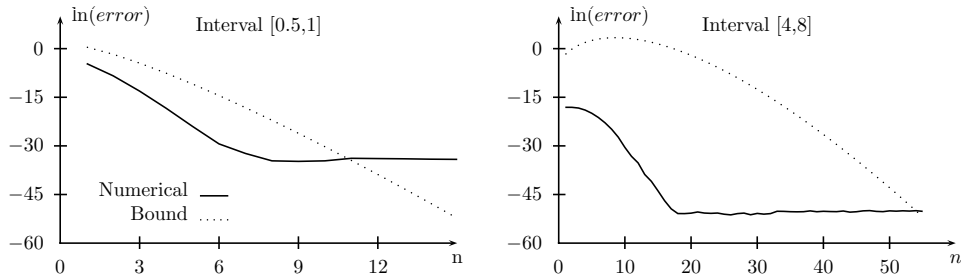


Figure 4.3: Comparison of the quadrature error,  $E^Q$ , with the bound given by Theorem 3.2.3. The solid line is the error obtained comparing the result computed by our quadrature with the Gauss-Kronrod quadrature. The dotted line is the bound from Theorem 3.2.3. The results are presented for two different integration intervals.

To do so, we set a precision ( $\epsilon = 10^{-4}$ ) and establish a non-uniform grid to achieve the desired accuracy for  $t \in [1, 10]$ , using the results of Chapter 3. For the uniform approximation we use the same grid size and range as the non-uniform one. The results are shown in Figure 4.4.

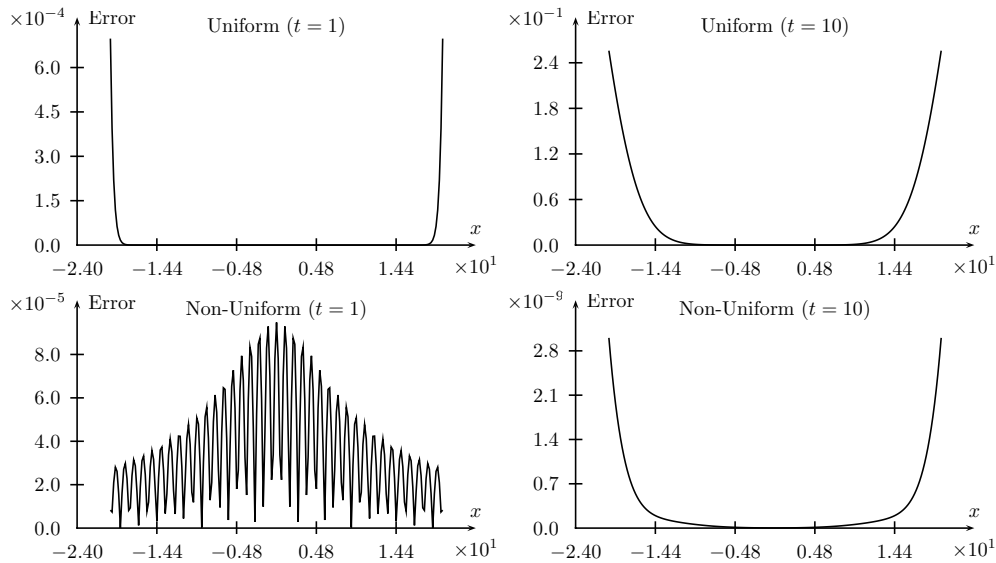


Figure 4.4: Comparison of the accuracy of the non-uniform approximation with the uniform one. For the non-uniform approximation, the grid is chosen based in Theorem 3.2.3 and for the uniform approximation, the same grid size and range as the non-uniform case is used.

		$\delta$ , as in Lemma 3.3.5					
		$2^{-1}$		$2^{-3}$		$2^{-5}$	
n		value	relative	value	relative	value	relative
0		$1.85e-01$	$7.84e-02$	$3.83e-03$	$5.19e-03$	$6.10e-05$	$3.25e-04$
2		$1.34e-02$	$5.79e-03$	$1.79e-05$	$2.43e-05$	$1.79e-08$	$9.53e-08$
4		$7.82e-04$	$3.43e-04$	$6.67e-08$	$9.04e-08$	$4.15e-12$	$2.22e-11$
6		$3.76e-05$	$1.66e-05$	$2.02e-10$	$2.75e-10$	$3.21e-13$	$2.48e-14$
8		$1.53e-06$	$6.78e-07$	$7.70e-12$	$1.04e-11$	$2.42e-12$	$3.53e-13$

Table 4.2: Error of the principal value approximation,  $E^{I_1}(n, \delta)$ , on the interval  $[-\delta, \delta]$ , as in Lemma 3.3.5. We consider the grid  $x_k = -3 + 0.2k$   $k = 0, \dots, 29$ . Table shows the maximum error *value* in  $k$ , and maximum *relative* error in  $k$ .

In Figure 4.4 the main advantage of non-uniform approach can be seen. For small values of  $x$  the error is small in both uniform and non-uniform approximation, and for large values of  $x$ , where the integral is more oscillatory, the non-uniform approach obtained better results. For large value of  $t$  the function takes very small values of large  $s$ , making most points of the uniform quadrature of little use, and so the quadrature did non acheive a good acuracy. In an oposite direction the non-uniform grid is more dense for small values of  $s$ .

Now we will focus our attention in the principal value quadrature for the heat kernel case. In our first numerical example, we studied the numerical error of the approximation given by Lemma 3.3.5. To measure the accuracy of the approximation, we again compared our result with the adaptive Gauss-Kronrod quadrature. We compute the result for a mesh  $x_k = -3 + 0.2k$   $k = 0, \dots, 29$ . Table 4.3 presents the worst result in  $k$  for several different values of  $\delta$ , which defines the integration interval, as in Lemma 3.3.5.

We also measure the error of the quadrature for the principal value, using Theorem 3.3.4 and Lemma 3.3.5. Lemma 3.3.5 is used with  $n = 8$ . Table 4.3 shows the error of our approximation for several desired accuracies ( $\epsilon$ ) and ranges of approximation of Lemma 3.3.5 ( $\delta$ ). Again, we use the adaptive Gauss-Kronrod quadrature to estimate the error of the results.

It is worth noticing that, the error in Table 4.3, for  $\epsilon = 10^{-8}$  and  $\delta = 2^{-1}$ , is higher than the desired accuracy, this happens because we fix  $n = 8$ , so the error of the approximation in  $[-\delta, \delta]$  is higher than  $\epsilon$ , as Table 4.3 shows.

To study the bounds obtained in Theorem 3.2.4, we compared the result obtained by the non-uniform quadrature using NUFFT with the result ob-

$\delta$ , as in Lemma 3.3.5						
$2^{-1}$				$2^{-5}$		
$\epsilon$	$\#\xi$	$E^Q$	$E^T$	$\#\xi$	$E^Q$	$E^T$
$1e-2$	20	$1.61e-06$	$7.92e-03$	48	$1.91e-09$	$7.93e-03$
$1e-5$	46	$1.53e-06$	$9.59e-06$	90	$2.47e-12$	$8.69e-06$
$1e-8$	70	$1.53e-06$	$1.53e-06$	132	$2.47e-12$	$9.41e-09$

Table 4.3: Numerical results for the approximation of the principal value Fourier transform using Theorem 3.3.4 and Lemma 3.3.5. For some desired precision ( $\epsilon$ ), the table shows the number of grid points ( $\xi$ ), the quadrature error ( $E^Q$ ), and the total error ( $E^T$ ).

tained by the Gauss-Kronrod quadrature, the results are shown in Figure 4.5.

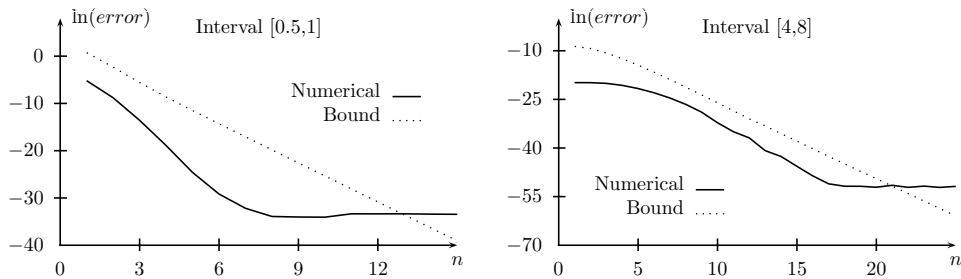


Figure 4.5: Comparison of the quadrature error,  $E^Q$ , with the bound given by Theorem 3.2.4. The solid line is the error obtained comparing the result computed by our quadrature with the Gauss-Kronrod quadrature. The dotted line is the bound from Theorem 3.2.4. The results are presented for two different integration intervals.

Now consider the third quadrature, for  $h(s)/(c+is)$ , given by Theorem 3.2.6. Lemma 3.3.2 finds estimates for the truncation of the infinite integral, so we can find a finite integration interval  $[-p, p]$  that approximates the finite one. In Theorem 3.3.3, we used dyadic intervals to find a partition  $[-p, p]$ . The choice of the smaller interval,  $[-2^{-j}, 2^{-j}]$ , proves to have a significant impact on the number of nodes, as seen in Table 4.3.

To study the bounds obtained in Theorem 3.2.6, we compared the result obtained by the non-uniform quadrature using NUFFT with the result obtained by the Gauss-Kronrod quadrature. The results are shown in Figure 4.6.

Minimum interval $[-2^{-j}, 2^{-j}]$						
$j = 1$				$j = 3$		
$\epsilon$	$\#\xi$	$E^Q$	$E^T$	$\#\xi$	$E^Q$	$E^T$
$1e - 1$	21	$3.90e - 05$	$5.83e - 02$	45	$7.63e - 07$	$5.83e - 02$
$1e - 3$	43	$1.36e - 07$	$7.84e - 04$	74	$5.58e - 09$	$7.84e - 04$
$1e - 5$	61	$4.33e - 10$	$8.67e - 06$	103	$6.73e - 13$	$8.67e - 06$

Table 4.4: Numerical accuracy of Theorem 3.2.6. For some desired precision ( $\epsilon$ ), table shows the number of grid points ( $\#\xi$ ), the quadrature error ( $E^Q$ ), and the total error ( $E^T$ ).

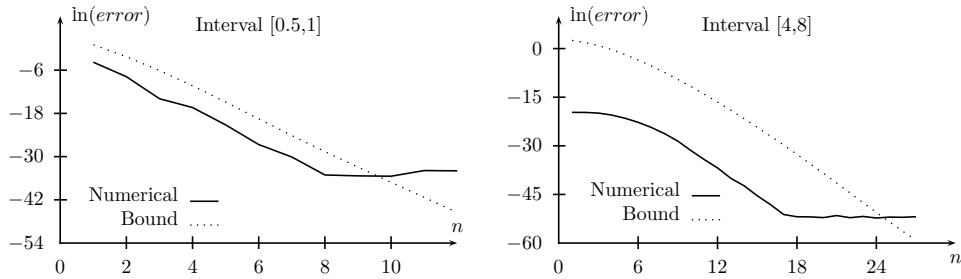


Figure 4.6: Comparison of the quadrature error,  $E^Q$ , with the bound given by Theorem 3.2.6. The solid line is the error obtained comparing the result obtained by our quadrature with the Gauss-Kronrod quadrature. The dotted line is the bound from Theorem 3.2.6. The results are presented for two different integration intervals.

To our final result, we study the error obtained by the quadrature when computing the value of a call option, as studied in Chapter 2. The results are shown for the Black and Scholes case, for which the bounds of Theorem 3.2.4 and Theorem 3.2.6 apply directly. We used the Black and Scholes framework, so the answer has a closed form solution given by Equation (1.18). This makes it possible to validate the method and measure its accuracy. For the example, we use  $\sigma = 0.3$ ,  $r = 0$  and  $K = 10$ . The result is shown in Figure 4.3. In Chapter 7, numerical results for the Heston and Merton models will be shown.



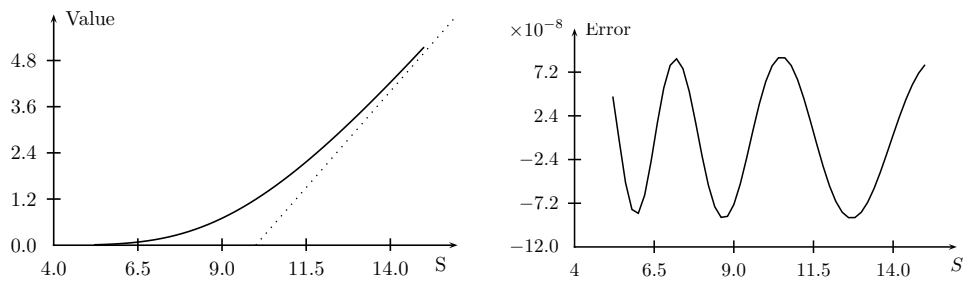


Figure 4.7: The error for computing the price of a call option. We use 196 points to evaluate the principal value transform, and 313 points for the second transform. We choose  $K = 10$ ,  $\sigma = 0.3$ ,  $r = 0$  and the desired precision was  $\epsilon = 10^{-6}$ .

## Chapter 5

# A Liquefied Natural Gas Pricing Model

Energy commodities form an important part of most markets. Several mercantile exchanges around the world trade energy commodities in different forms. Oftentimes, the broad literature in mathematical finance is not directly applied to commodities due to their special nature.

One of the main differences between commodities and financial derivatives is the presence of the *cost of carry*, which consists of the cost of holding a position in a commodity. To enter in a long position in a commodity, which means buying a commodity like rice, soy or oil, there is the cost of storage, the cost of financing the position and the cash flow for owning the asset. The important implication of the cost of carry is that we do not have a non-arbitrage price for future prices of commodities. What we do have is a non-arbitrage interval.

Another interesting characteristic of commodity prices is its mean reverting nature [Sch97]. This makes commodities related to interest rate derivatives, to establish a parallel with the financial literature.

The differences between financial derivatives and commodities resulted in two subjects each one of them with a specific literature. See for example [Bla76], [Sch97], [DL92].

An instance of a commodity is natural gas. It is an important source of generation of electricity, as fuel for vehicles, and in households for heating and cooking. The global demand for natural gas has been increasing steadily in the last years. Because of its nature, transportation is a crucial issue for the natural gas market. There are two ways of transporting natural gas: pipelines and *liquefied natural gas* (LNG). If there is a pipeline available, then it is the cheapest transportation option. LNG is the alternative when no pipeline is available since it takes up to 1/600th the volume of natural gas

and then can be transported by special ships, known as LNG carriers.

LNG has received a lot of attention in recent years. Several studies have been made about natural gas and LNG, like [VJ06],[Jen03],[SLNv05] just to mention some of them. Even for political reasons LNG has attracted attention:

*“Given notable cost reductions for both liquefaction and transportation of LNG, significant global trade is developing, (...) And high natural gas prices projected by distant futures prices have made imported gas a more attractive option for us.”*(Alan Greenspan, 2004)

LNG “*per se*” is not directly considered a commodity, because it is not traded in any mercantile exchange. LNG trades are over-the-counter (OTC) and in general between two countries. LNG does not constitute a local market, we cannot try to find a proxy for the price in any specific market, the reason being that the owner of the cargo is trying to find arbitrage opportunities among different markets. In the Asian-Pacific market, LNG prices are indexed to crude oil prices. In Europe, there are different indices, such as crude oil (note that crude oil prices are different in Asia and Europe), or a basket of indexes (like oil products, coal, inflation, among others). In the USA, LNG is usually indexed by the Henry Hub gas prices.

In this chapter, we present a model for the spot price of LNG, although most results apply to other commodities. Our model reflects most of the stylized facts on natural gas markets. The intuition brought up by the model helps to explain the international correlation of natural gas prices in the world [SLNv05], which is a consequence of the LNG seller as an *arbitrageur* of international gas market. The LNG producer sells to the market with higher prices and this causes a decrease in local prices.

One of the main advantages of our model is that no data for LNG is used, in the sense that we find the spot price for LNG based on the prices of natural gas for each of the local markets. This makes it possible to calibrate the model using the huge amount of data for natural gas.

Once the spot price is modeled, we are able to treat derivatives and introduce some contracts for LNG. The two contracts that we study are futures for LNG and cancellation options. This second contract is uncommon in the literature <sup>1</sup>. It is a contract that gives the owner the right to buy LNG

---

<sup>1</sup>Flexibility in LNG contracts has been growing significantly in recent years. See for example the cancellation contract (<http://www.eia.doe.gov/oiaf/analysispaper/global/lngmarket.html>). It exemplifies several new contracts for short-term markets that have been used.

in a given date and the right to cancel the contract by paying some fee on certain dates. Some uses and motivation of this contract are shown in Section 5.2.

## 5.1 Spot Price Model

The first step towards modeling LNG is finding its spot price. As it turns out, LNG has several idiosyncrasies, such as trades over-the-counter (OTC), generally between two countries and LNG is a global market. Furthermore, we do not have any database regarding LNG trades. Those are some of the aspects we considered while constructing the model.

Natural gas is a commodity in most countries. Several mercantile exchanges have derivatives over natural gas prices. Just to give an example, let us consider the the USA. The most used reference pricing point in the USA is the Henry Hub. It is the pricing point for natural gas contracts traded on the New York Mercantile Exchange (NYMEX). The NYMEX trades future contracts for natural gas (called Henry Hub Futures), they also have options over Henry Hub futures. Natural gas prices are very well modeled in each market. We use the fact that there is a model for natural gas in every country to model LNG as a derivative using all the different prices around the globe as primary asset for this derivative.

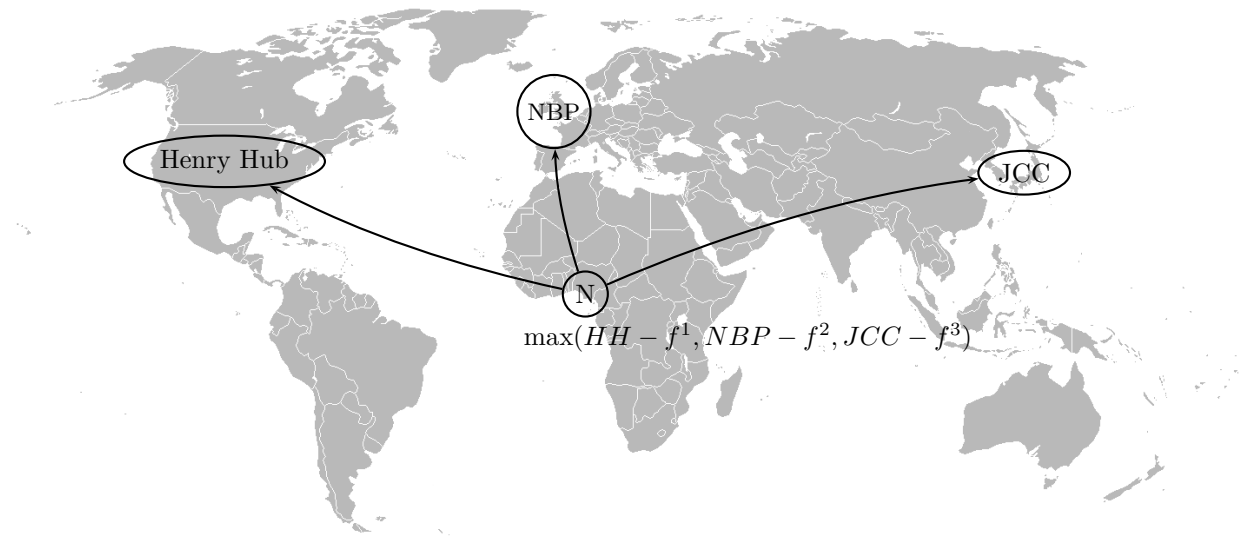


Figure 5.1: The LNG seller has access to several markets, and maximizes the profit in all of them.

In order to model the market, let us consider a specific producer like Nigeria, for example. Nigeria can sell LNG to any country, see Figure 5.1. For instance, if it sells in the USA, Nigeria will receive the spot price for natural gas in the USA, which in general is related to NYMEX Henry Hub prices. In order to sell in the USA, the producer pays the netback costs (transport, liquefaction, re-gasification...). The profit of selling to the USA is then the Henry Hub price subtracted by the netback cost. The price will be given by a profit maximization by this seller. Some basic market hypotheses will be needed:

- The seller has access to  $K$  markets, and pays  $f^k \in \mathbb{R}$  of netback cost in order to sell to market  $k$ .
- The prices of natural gas are given by  $S_t \in \mathbb{R}_+^K$ , a  $K$ -dimensional stochastic process defined on the filtered, probability space  $(\Omega, \mathcal{F}, \mathbb{F}, \mathbb{Q})$ . In the  $k$ th market, natural gas is a commodity and the price will be given by the stochastic process  $S_t^k$ . We assume that  $\mathbb{Q}$  is a martingale equivalent measure for a given market price of risk, see [MR05].

If the producer sells to market  $k$ , he receives a profit of  $S_t^k - f^k$ . The maximum profit is given by

$$G(S_t) = \max_{k=1, \dots, K} (S_t^k - f^k) \quad (5.1)$$

In this model, we consider that the amount of natural gas traded by LNG is small, so it does not affect local market prices. This is clearly a simplification.

To buy a cargo from a specific producer, the buyer has to pay no less than  $G(S_t)$ , assuming that he pays the netback costs. Doing so the seller is indifferent to selling the cargo or maximizing the profit arbitrating in global markets.

This price rule implies that buying LNG is no better than buying in the local market. Once LNG is re-gasified and is inside a specific market, it becomes natural gas and so has the price given by the local market.

This model reflects several aspects of the LNG market in which every seller and buyer has different netback costs. It is common for a country to concentrate the demand for LNG, which occurs when a market has a spike in prices for natural gas. In this case, this same country is the natural destiny for every free cargo.

Notice that by defining the spot value as in equation (5.1) makes the spot price itself a derivative of natural gas price.

The model presented here will be used in the next section, where we introduce some derivatives for LNG. We will also introduce some applications of the derivative markets as hedge for energy markets.

## 5.2 LNG Derivatives

Natural gas is a very important component in the world energy matrix. As a consequence, hedging with this strategic resource is crucial. Changes in the prices of local markets are important. For this kind of hedging, derivatives over natural gas at local markets are the best choice. Those derivatives are traded at mercantile exchanges.

Based on the LNG model presented above, it is natural to ask why should someone hedge using LNG, when the cheapest choice is hedging in local markets.

We now will try to explain the reasons for such hedging. There are some countries where natural gas prices cannot be hedged in local markets. Not every country has mercantile exchanges trading natural gas. In those cases, LNG contracts are an interesting way of hedging.

We add that the market has its micro-structure. For instance, it is always better for the seller, due to logistic reasons, to sell in advance. This logistic risk is not in the model itself and may give a discount over the theoretical price, making LNG interesting for the buyer.

Several countries, and even some firms, are worried about changes in demand, which is essential to hedge against. Other reasons for hedging might be problems in pipelines, problems in local production, excess of demand based on bigger than expected growth. To hedge against such events, the option to buy more gas is needed. In this context, LNG is a highly competitive alternative.

### 5.2.1 Forward

Forward prices of LNG are straightforward once we have the spot price model. The price is given by

$$F^G(t, T, S_t) = \mathbb{E}[G(S_T) | \mathcal{F}_t] , \quad (5.2)$$

considering that interest rates are independent with natural gas prices. It is interesting to notice that  $G(S_T)$  is not traded, but risk-neutral pricing applies because the hedging strategy can be done trading  $S$ . This is the most basic contract possible and it is an useful hedge alternative when there

is certainty about the future demand, so the owner of the contract is buying in advance.

## 5.2.2 Cancellation Options

Future contracts are not flexible enough to cover all the hedge possibilities needed. In this section we present a contract that is an attempt to deal with wider hedging possibilities.

It is natural to have a contract that gives the owner the right, but not the obligation to buy. This makes it possible to hedge against uncertainty in a future time.

We can generalize this flexibility. During the validity of the contract, the owner may receive some information that allows him to know beforehand that the cargo will not be needed. In this case, he may want to cancel the cargo in advance.

We now define a contract that has these properties.

**Definition:** The cancellation option is a contract that gives the holder the following rights:

- At times  $t_1, \dots, t_N \leq T$  the holder has the right to cancel the contract paying fees  $c_1, \dots, c_N$ , respectively.
- If the holder does not cancel the contract, then at time  $T$ , then he will buy the LNG cargo paying  $A \cdot S_T^1 + B$ , where  $A$  is a proportion of some benchmark market, and  $B$  is a fixed cost.

The value of a cancellation option at time  $t$ , for market price  $S_t$  is denoted by  $V(t, S_t)$ .

To value this contract, first note that at delivery the value of the contract is

$$V(T, S_T) = G_T(S_T) - (AS_T^1 + B). \quad (5.3)$$

Or if we can cancel at deliver  $t_N = T$

$$V(T, S_T) = \max(G_T(S_T) - (AS_T^1 + B), -c_N). \quad (5.4)$$

To help fix the notation, consider the example of the cancellation option for which it is possible to cancel for  $t = T$  as in equation (5.4). The payoff is shown in Figure 5.2.

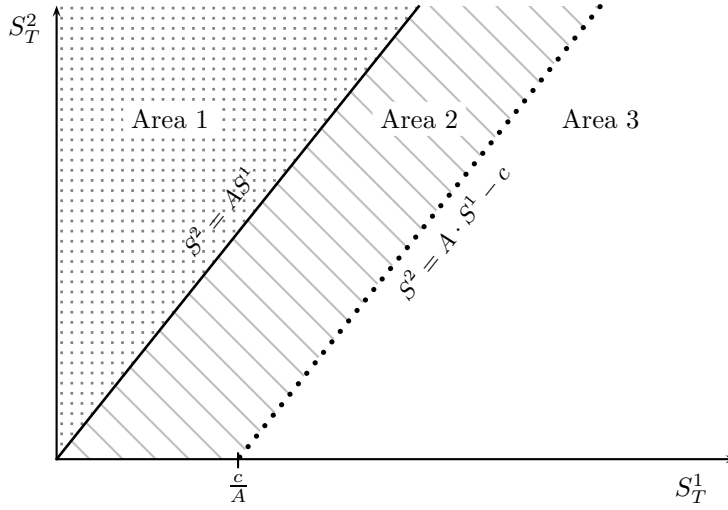


Figure 5.2: Payoff when it is possible to cancel at delivery time, as given by Equation (5.4). The fee to cancel is  $c$  and  $B = 0$ . In area 1, the payoff is positive, so it is not optimal to cancel. In area 2, the payoff is negative but better than the fee. In Area 3, the payoff is smaller than the cancellation fee, so it is optimal to cancel.

We can find the value of the cancellation option backwards. To do this, we first define auxiliary functions  $V^n(t, S)$  defined on  $[t_{n-1}, t_n] \times \mathbb{R}^K$ . Letting  $t \in [t_{n-1}, t_n)$ ,  $V^n$  is given by

$$V^n(t, S) = \mathbb{E}[V^n(t_n, S_{t_n}) | \mathcal{F}_t] . \quad (5.5)$$

For time  $t_n$ , with  $n < N$  the value of  $V^n$  is given by

$$V^n(t_n, S_{t_n}) = \max(V^{n+1}(t_n, S_{t_n}), -c_n) . \quad (5.6)$$

If the contract does not give the right to cancel at time  $T$ , then the final payoff is given by (5.3). So

$$V^{N+1}(T, S_T) = G_T(S_T) - (AS_T^1 + B) ,$$

where the  $(N + 1)$ -st interval is  $[t_N, T]$  and corresponds to the period after the last cancellation date. If the contract gives the right to cancel at  $T$ , the final payoff would be given by (5.4). Thus, we would have

$$V^N(T, S_T) = \max(G_T(S_T) - (AS_T^1 + B), -c_N) .$$

By means of such construction, we are able to find the price for every  $t \in [0, T]$ , where we have

$$V(t, S) = V^n(t, S) \text{ for } t \in [t_{n-1}, t_n) .$$



We now study some properties of such contracts. Several aspects of the contract should be considered, like monotonicity in  $A$  and  $B$ . Another natural question is a characterization of redundant fees and when a new cancellation date actually increases the flexibility of the contract. The following theorem summarizes some properties of the cancellation contracts.

**Theorem 5.2.1** *For a cancellation contract, we have the following properties:*

1. *The contract value is nonincreasing in  $A$ ;*
2. *The contract value is nonincreasing in  $B$ ; and*
3. *If for some  $j < i$ , we have that  $c_j < c_i e^{-r(t_i - t_j)}$ , then removing the cancellation date  $t_j$  does not affect the contract value.*

**Proof:** For  $t = T$ , properties (1) and (2) are a consequence of  $S_T \geq 0$ , and the payoff formula (5.3) or (5.4), so  $V(T, S_T; A, B)$  is nondecreasing in  $A$  and  $B$ . For  $t \in [0, T)$ , the result follows from the construction of  $V$  and the fact that given  $X \leq Y$ , with  $X$  and  $Y$   $\mathcal{F}_s$ -adapted, then for  $t < s$  we have  $\mathbb{E}[X|\mathcal{F}_t] < \mathbb{E}[Y|\mathcal{F}_t]$ , and  $\max(X, c) \leq \max(Y, c)$ .

To prove (3), suppose that we have  $c_j, c_i$  with  $j < i$  and  $c_j \geq c_i e^{-r(t_i - t_j)}$ . Saving  $c_j$  at  $t_j$  and investing at risk free rate, at  $t_i$  we pay  $c_i \leq c_j e^{r(t_i - t_j)}$  at  $t_i$ , so the cancellation at  $t_j$  can be ignored. ■

The results (1) and (2) of Theorem 5.2.1 show that increasing the delivery price for LNG decreases the price of the contract. Result (3) of of Theorem 5.2.1 establishes conditions on the cancellation fee, so we can remove dates that are never optimal for cancellation.

We can also study the value of the cancellation optionality. In this case, we must define the value of the contract without any cancellation possibility. The contract without cancellation possibility is simply a forward given by

$$F^V(t, S_t) = \mathbb{E} [G_T - (AS_T^1 + B) | \mathcal{F}_t] . \quad (5.7)$$

Using (5.7), we can define the optionality value as

$$O(t, S_t) = V(t, S_t) - F^V(t, S_t). \quad (5.8)$$

Some properties of the optionality value are given in the next theorem.

**Corollary 5.2.2** *The optionality value has several properties:*

1. The optionality value is always positive;
2. The optionality value is nondecreasing in  $A$ ;
3. The optionality value is nondecreasing in  $B$ ; and
4. If for some  $j < i$ , we have that  $c_j < c_i e^{-r(t_i - t_j)}$ , then removing the cancellation date  $t_j$  does not affect the optionality value.

**Proof:** For  $t = T$ , property (1) follows from the definition  $V$  and  $F^V$ . For  $t$  in general, it follows from the fact that given  $X \leq Y$ , where  $X$  and  $Y$  are  $\mathcal{F}_s$ -adapted, then for  $t < s$  we have  $\mathbb{E}[X|\mathcal{F}_t] < \mathbb{E}[Y|\mathcal{F}_t]$ , and  $\max(X, c) \leq \max(Y, c)$ , as property (1) of Theorem 5.2.1.

To prove property (2), notice that for a given  $A > \tilde{A}$  we have  $F_A^V(t, S_t) - F_{\tilde{A}}^V(t, S_t) = (A - \tilde{A})\mathbb{E}[S_T^1|\mathcal{F}_t] > 0$ . Suppose that  $O_A(t, S_t) < O_{\tilde{A}}(t, S_t)$ , so buying  $V_A$ ,  $F_{\tilde{A}}$ , and selling  $V_{\tilde{A}}$  and  $F_A$ , you receive  $V_A + F_{\tilde{A}} - V_{\tilde{A}} - F_A > 0$  at  $t$ . Then two possibilities should be considered:

- If the owner of  $V_{\tilde{A}}$  cancels the contract, we cancel it too. We receive the fee for the contract  $\tilde{A}$  and pay the same fee for cancelling the contract  $A$ , so the payoff at cancellation date is zero, and at  $T$  is  $(A - \tilde{A})S_T^1 > 0$ .
- If the owner does not cancel, we do not cancel it either. The payoff at  $T$  is zero.

This is an arbitrage opportunity, so we must have  $O_A(t, S_t) \geq O_{\tilde{A}}(t, S_t)$ . The proof of property (3) is similar to that of (2).

The value of the future does not depend on the cancellations dates, so property (4) follows from property (4) of Theorem 5.2.1. ■

The result above has an intuitive explanation. Property (1) follows from the fact that the cancellation contract is an option over a forward, so its value is always above the forward value. Properties (1) and (2) of Theorem 5.2.1 show that the price of the contract drops with  $A$  and  $B$ , so the probability of a negative payoff increases, and therefore the value of the cancellation right is higher. This explains (2) and (3) of Corollary 5.2.2.

The final result of this section gives a restriction on parameters  $A$  and  $B$ .

**Proposition 5.2.3** *If  $A \leq 1$  and  $B \leq \min_{k=1, \dots, K}(-f_k)$ , it is never optimal to cancel.*

**Proof:** At  $T$ , the owner of the contract can receive a LNG cargo, paying  $AS_T^1 + B < G_T(S)$ . ■

The result above shows a case where the optionality has null value. When we have  $A$  and  $B$  as in Proposition 5.2.3, it is never optimal to cancel, so the value of the optionality is zero.

The results mentioned above are useful not only for theoretical reasons, but also because they can be used to test and validate numerical implementation.

### 5.3 Least-Squares Monte Carlo

Pricing the contracts of the previous section requires the use of numerical techniques. Numerical methods for high dimensional problems have received a lot of attention and recently several Monte Carlo methods have been proposed. They turn out to be very efficient for those problems [Gla04].

In this section, we describe the method used to solve numerically the model. The method we chose was the regression-based Monte Carlo proposed by [LS01].

The convergence of the method, under fairly general conditions, was proved by [CLP02]. For example, considering only Markovian processes  $S_t \in \mathbb{R}^k$  such that  $S_t \in L^2(\Omega, d\mathbb{P})$ ,  $\forall t \in [0, T]$ , then convergence of least-squares Monte Carlo method for cancellation options follows from [CLP02].

The main idea of the method is to use the fact that

$$\mathbb{E}[V(t_{n+1}, S(t_{n+1})) | \mathcal{F}_{t_n}]$$

is  $\mathcal{F}_{t_n}$ -measurable, so that it may be represented as

$$\mathbb{E}[e^{-r(t_{n+1}-t_n)} V(t_{n+1}, S(t_{n+1})) | S(t_n) = x] = \sum_{r=1}^{\infty} \beta_r \gamma_r(x), \quad (5.9)$$

for some base  $\{\gamma_r\}$  of  $L^2(\mathbb{R}^k)$ . We can approximate (5.9) by

$$V(t_n, S(t_n)) \approx \sum_{r=1}^R \beta_r \gamma_r(S(t_n)). \quad (5.10)$$

To compute  $\beta$ , we solve the following problem by least-squares

$$\begin{bmatrix} \gamma_1(S^1(t_n)) & \cdots & \gamma_R(S^1(t_n)) \\ \vdots & \ddots & \vdots \\ \gamma_1(S^J(t_n)) & \cdots & \gamma_R(S^J(t_n)) \end{bmatrix} \begin{bmatrix} \beta_1 \\ \vdots \\ \beta_R \end{bmatrix} = e^{-r(t_{n+1}-t_n)} \begin{bmatrix} V(t_{n+1}, S^1(t_{n+1})) \\ \vdots \\ V(t_{n+1}, S^J(t_{n+1})) \end{bmatrix} \quad (5.11)$$

Using equation (5.6), we have

$$V(t_n, S(t_n)) \approx \max \left( \sum_{r=1}^R \beta_r \gamma_r(S(t_n)), -c_n \right). \quad (5.12)$$

### 5.3.1 An Example

The goal of this section is to present some numerical results obtained by least-squares Monte Carlo. The model we choose for the price dynamics is the mean reverting process, which is very popular for commodities. See [BCSS95] and [Sch97] for studies in the mean reverting nature of commodity prices. The price dynamic in this model is given by

$$\begin{aligned} S_t^i &= e^{X_t^i} \\ dX_t^i &= \kappa_i (\theta_i - X_t^i) dt + \sum_j A_{i,j} dW_j(t). \end{aligned} \quad (5.13)$$

The solutions is then

$$X_i(t) = e^{-\kappa_i(t-s)} X_i(s) + \theta_i (1 - e^{-\kappa_i(t-s)}) + \int_s^t e^{-\kappa_i(t-u)} \sum_j A_{i,j} dW_j(u). \quad (5.14)$$

It is easy to see that

$$\begin{aligned} \mathbb{E}[X_i] &= \mu_i = e^{-\kappa_i(t-s)} X_i(s) + \theta_i (1 - e^{-\kappa_i(t-s)}) \\ \text{Cov}[X_i(t), X_j(t) | \mathcal{F}_s] &= \frac{1}{(\kappa_i + \kappa_j)} (1 - e^{-(\kappa_i + \kappa_j)(t-s)}) (AA^t)_{(i,j)}. \end{aligned} \quad (5.15)$$

Taking  $t \rightarrow \infty$  in the covariance, we obtain the ergodic covariance.

We will now study the sensibility of the model and the numerical method. Unless not otherwise specified, the following parameters will be used:

- The base is the polynomial base;
- Maximum degree of the basis is 5;
- Number of simulations:  $3 \times 10^4$ ;
- $A = 1.0$ ,  $B = 2.0$ ,  $r = 0$ ;
- fee=(1, 1.25);
- Cancellation dates (0.5, 1.0) and  $T = 1.5$ ;

- $\kappa = (3, 3)$ ;
- $X_0 = (3, 3)$ ;
- $\theta = (3, 1.5)$ ; and
- Ergodic covariance  $\begin{bmatrix} 1 & 0.1 \\ 0.1 & 1 \end{bmatrix}$ .

We measure the computational time to evaluate the option price. The results are expressed in Figure 5.3. Solving the least-squares problem (5.11) takes  $\mathcal{O}(JR^2 + R^3/3)$ , where  $J$  is the number of simulations and  $R$  is the elements in the base, as confirmed by results in Figure 5.3. The examples indicate a linear increase of the computational time with the number of simulations. Concerning the dependence on the basis degree, the number of elements in the base is  $R = (K + 1)^P$ , where  $P$  is the maximum degree of the basis. The numerical results confirms this exponential increase of the computational time with the maximum degree of the base.

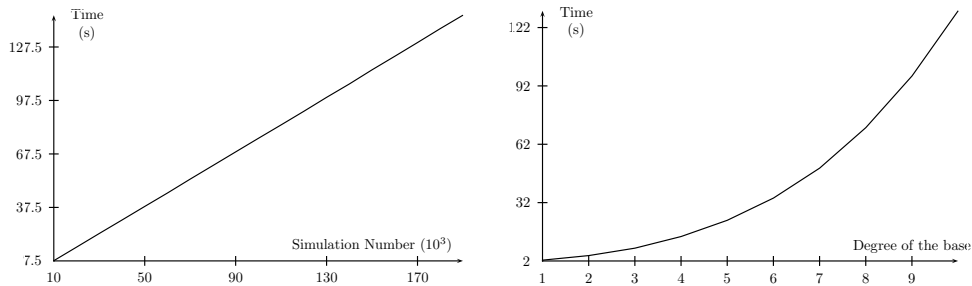


Figure 5.3: Computational time of least-squares Monte Carlo for different number of simulations and different base sizes.

In Theorem 5.2.1, we proved some monotonicity results that are confirmed in Figure 5.4. A natural result is that, for large value of  $A$  and  $B$ , the option value is negative and the value converges to the cancellation fee.

The convergence of the algorithm is proved by [CLP02]. In Figure 5.5 we present some numerical results about this convergence. The option value is calculated with a total of  $1 \times 10^4$  to  $2 \times 10^5$  simulations and has a difference of no bigger than 5.12%. If we only consider the results for more than  $5 \times 10^4$

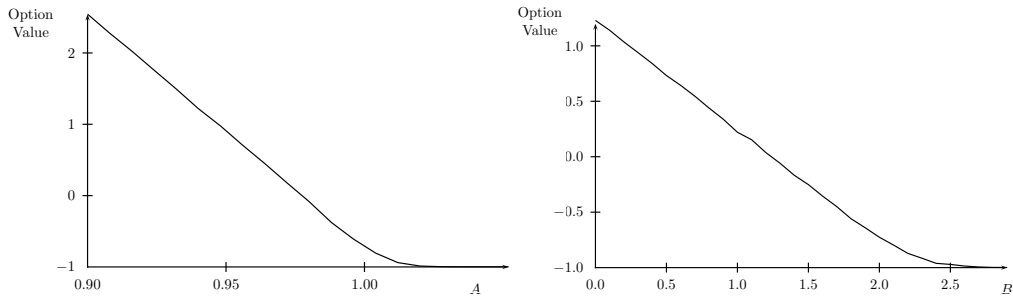


Figure 5.4: Monotonicity. The option value is monotone in A and B.

simulations, the difference was no more than 1.5%. We also measured the numerical standard error of the estimator. To calculate this, a total of 20 samples of the algorithm are used and the standard error is computed with the usual estimator. As expected, the standard error of the estimator decays with the number of simulations.

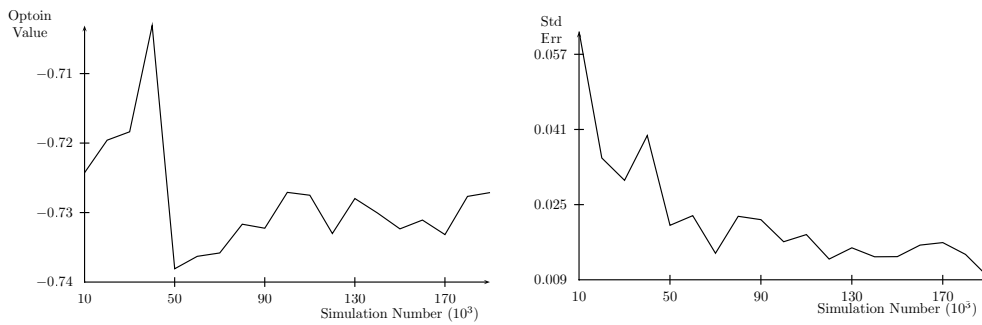


Figure 5.5: Number of simulations. The option value and numerical standard error of the estimator for different number of simulations.

In our final results, we present results for different size of bases. In Figure 5.6 we show the results. The difference in prices for different bases appears to be robust. The increase in standard error is expected, since we keep the number of simulations constant.

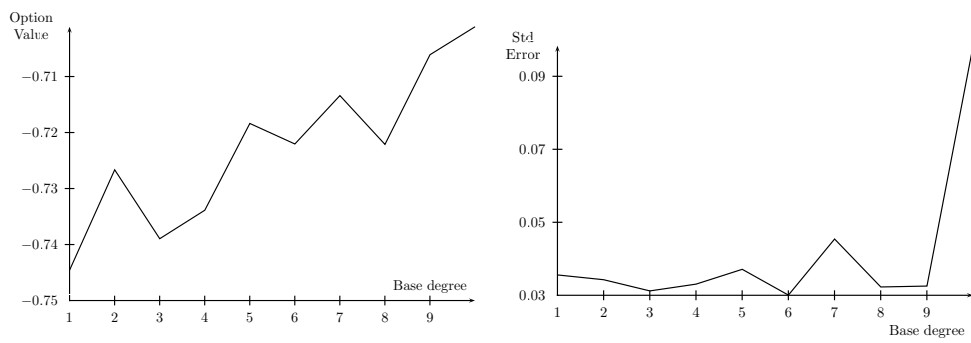


Figure 5.6: Base size. The option value and numerical standard error of the estimator for different sizes of the base.

# Chapter 6

## Interest Rates

In many countries, a monetary authority decides the short rate target. It uses open market operations to execute this policy. In the United States, the short rate role is performed by the federal funds and the target decision is chosen by the Federal Open Market Committee (FOMC). In Brazil, the monetary authority instrument is the Special System for Settlement and Custody (SELIC), and the decision of the short rate target is made by the Monetary Policy Committee (COPOM). Furthermore, there is an important short-term rate, the Interbank Deposit (DI), that follows very closely the SELIC rate.

The Chicago Board of Trade (CBOT) has future contracts on US federal funds among other derivatives. The Brazilian Securities, Commodities and Futures Exchange (BM&FBOVESPA) has one-day interbank deposit future contracts, and options on average one-day interbank deposit rate index contract. Those derivatives over short rates have received a lot of attention recently due to the increase in their liquidity.

In this chapter we propose a model for short-term rates taking into consideration monetary authority. We use such model to recover expectation about future decisions by the monetary authority, from derivative contracts. To do so, we were led to use regularization techniques to deal with the ill-posedness nature of the problem.

Some work has been done to incorporate monetary decisions to interest rate models as pure jump process [Pia05]. In a different direction, market data can be used to recover the probability of each possible monetary policy decision [CCM05]. The idea of recovering probabilities from derivatives data goes back to [BL78]. More recent work has been done by [JR96]. The literature on regularization and inverse problems is quite extense. See [Zub05] for general references and [Ave99], [EE05], [EHH06] for applications in quantitative finance.



## 6.1 Model and Notation

In this section, we present a model for the short rate. This model is based on the central bank target rate and the spread between the target and the realized rate. This chapter focus on the Brazilian market, and we will give now a brief review of the two relevant short rates for this chapter. For a complete review see [For08].

- Special System for Settlement and Custody (SELIC) - It is the average one day operation guaranteed by the Brazilian federal government securities. The model is based on the SELIC target ( $r_S$ ) decided by the COPOM. So the  $r_S$ , if expressed as an annual compounded tax, is a multiple of 25 basis points (bp) annually compounded, where a bp is 1/100th of a percentage point.
- Interbank Deposit (DI) - It is the average one day operation guaranteed by private securities ( $r_{DI}$ ).

Before we describe our model, we will give a brief overview of the Vasicek interest rate model [Vas77]. This model will be later used for modeling the spread between DI and SELIC. For a complete review of interest rate models see [JW01]. In the Vasicek model, the interest rate process is given by an Ornstein-Uhlenbeck process on the filtered complete probability space  $(\Omega_1, \mathcal{F}^1, \mathbb{F}_1, \mathbb{P}_1)$ . The dynamics for the short rate  $x(t)$ ,  $t > 0$ , is given by

$$dx(t) = k(\theta - x(t))dt + \sigma dW(t). \quad (6.1)$$

The solution of the stochastic differential equation (6.1) for  $s < t$  is given by

$$x(t) = x(s)e^{-k(t-s)} + \theta(1 - e^{-k(t-s)}) + \sigma \int_s^t e^{-k(t-u)} dW(u). \quad (6.2)$$

To model the SELIC target rate, note that this process is constant between the COPOM's meeting, we assume that the monetary authority only changes the rate at scheduled meetings. We define  $\tau_j$  for the time of the  $j$ th meeting after a starting time  $t$ . We define  $r_S$  on  $(\Omega_2, \mathcal{F}^2, \mathbb{F}_2, \mathbb{P}_2)$  as

$$r_S(t) := H_0 \mathcal{X}_{[t_0, \tau_1]}(t) + \sum_{j=1}^N H_j \mathcal{X}_{(\tau_j, \tau_{j+1}]}(t), \quad (6.3)$$

where  $H_j$  is the target rate decided at the  $j$ th meeting. Since  $\mathcal{F}_{\tau_j}^2$  correspond to the information up to the  $j$ th meeting we must have  $H_j \in \mathcal{F}_{\tau_j}^2$ . The COPOM meeting only changes the rate on 25 bp, so

$$\frac{\ln(H_j(\omega)) - 1}{2.5 \cdot 10^{-3}} \in \mathbb{N} \quad \forall j \in \mathbb{N}, \omega \in \Omega_2 \quad (6.4)$$

We assume  $\Omega_2$  finite.

To model the  $DI$  rate, we consider the direct product and the product measure both denoted by  $\otimes$  and given by  $(\Omega_1 \otimes \Omega_2, \mathcal{F}^1 \otimes \mathcal{F}^2, \mathbb{F}_1 \otimes \mathbb{F}_2, \mathbb{P}_1 \otimes \mathbb{P}_2)$ , and the  $DI$  rate is given by

$$r_{DI}(t) = \bar{x}(t) + \bar{r}_S(t) , \quad (6.5)$$

where, to define  $x$  and  $r_S$  in this probability space, we use the projection  $\bar{r}_S(\omega_1, \omega_2) := r_S(\omega_2)$ , and  $\bar{x}(\omega_1, \omega_2) := x(\omega_1)$ , but from now on, we make no distinction between  $\bar{x}$  and  $x$ , and  $\bar{r}_S$  and  $r_S$ .

So far, we have focused on the real measure  $\mathbb{P}_1 \otimes \mathbb{P}_2$ , but it is well known in the literature of interest rate the existence of risk premium in bond markets [FB87]. Recent studies have shown the presence of risk premium in federal fund derivatives [PS08]. So we need to study a risk neutral measure, which is denoted as  $\mathbb{Q} := \mathbb{Q}_1 \otimes \mathbb{Q}_2$ .

We assume a constant market price of risk process,  $\lambda$ , for the risk-neutral measure. It will be denoted by  $\lambda$ , so

$$\begin{aligned} dx(t) &= k(\theta^{\mathbb{P}} - x(t))dt + \sigma dW(\mathbb{P}) \\ dx(t) &= k(\theta^{\mathbb{Q}} - x(t))dt + \sigma dW(\mathbb{Q}) , \end{aligned}$$

where

$$\theta^{\mathbb{P}} = \frac{\lambda}{\sigma} + \theta^{\mathbb{Q}} .$$

For the SELIC target we study only the risk neutral,  $\mathbb{Q}_2$ , which is the important probability to study derivative pricing. We can also suppose no risk premium for the SELIC rate, as in the expectations hypothesis [Pia03].

### 6.1.1 One-Day Interbank Deposit Futures Contract

The BM&FBOVESPA has future contracts over  $DI$ . The basis of each such contract is the unit price defined as 100.000 discounted by  $DI$ . This derivative is quoted as the annual percentage rate compounded daily based on a 252-day year, to two decimal places, that we denote here as  $cot$ . So, we have

$$PU = \left(1 + \frac{cot}{100}\right)^{\frac{T-t}{252}} .$$

The daily cash flow of the owner of the contract is

$$PU \left( \left(1 + \frac{cot}{100}\right)^{\frac{1}{252}} - e^{\frac{1}{252}r_{DI}} \right) .$$

In the next theorem we present a pricing formula for this contract.

**Theorem 6.1.1** *The price of the future contract is given by*

$$F_{DI}(t, T, r_{DI}(t)) = P_V(t, T, x(t)) \sum_{\omega \in \Omega_2} e^{(-\int_t^T r_S(u, \omega) du)} \mathbb{Q}_2(\omega), \quad (6.6)$$

where

$$\begin{aligned} P_V(t, T) &= A(t, T) e^{-B(t, T)x(t)} \\ B(t, T) &= \frac{1}{k} (1 - e^{-k(T-t)}) \\ A(t, T) &= e^{(\theta - \frac{\sigma^2}{2k^2})(B(t, T) - T + t) - \frac{\sigma^2}{4k} B(t, T)^2}. \end{aligned}$$

**Proof:** The future price is given by

$$F_{DI}(t, T, r_{DI}(t)) = \mathbb{E} \left[ e^{-\int_t^T r_{DI}(s) ds} \middle| \mathcal{F}_t \right].$$

From the definition of  $r_{DI}$  and Equation (6.2), we have

$$r_{DI}(t) = r_S(t) + x(t)e^{-k(t-s)} + \theta(1 - e^{-k(t-s)}) + \sigma \int_s^t e^{-k(t-u)} dW(u). \quad (6.7)$$

To compute the integral in (6.7), note that

$$\begin{aligned} \int_t^T x(t) e^{-k(u-t)} du &= x(t) \frac{1}{k} (1 - e^{-k(T-t)}) = x(t) B(t, T) \\ \int_t^T \theta(1 - e^{-k(u-t)}) du &= \theta \left( T - t - \frac{1}{k} (1 - e^{-k(T-t)}) \right) \\ &= \theta (T - t - B(t, T)) \\ \int_t^T \int_t^u e^{-k(u-s)} dW(s) du &= \frac{1}{k} \int_t^T (1 - e^{-k(T-s)}) dW(s). \end{aligned} \quad (6.8)$$

Then, we have

$$\mathbb{E} \left[ e^{-\int_t^T x(s) ds} \middle| \mathcal{F}_t \right] = e^{-\theta(T-t-B(t, T)) - x(t)B(t, T)} \mathbb{E} \left[ e^{-\sigma \int_t^T B(T, s) dW(s)} \right].$$

The term associated with the expectation integral above, can be computed as

$$\begin{aligned} \mathbb{E} \left[ e^{\sigma \int_t^T B(T, s) dW(s)} \right] &= e^{\frac{\sigma^2}{2} \int_t^T B(T, s)^2 ds} \mathbb{E} \left[ e^{-\frac{\sigma^2}{2} \int_t^T B(T, s)^2 ds - \sigma \int_t^T B(T, s) dW(s)} \right] \\ &= e^{\frac{\sigma^2}{2} \int_t^T B(T, s)^2 ds}. \end{aligned}$$

The last remaining integral is given by

$$\begin{aligned}\int_t^T B(T, s)^2 ds &= \frac{1}{k^2} \left( T - t - \frac{2}{k} (1 - e^{-k(T-t)}) + \frac{1}{2k} (1 - e^{-2k(T-t)}) \right) \\ &= \frac{1}{k^2} \left( T - t - B(t, T) - \frac{k}{2} B(t, T)^2 \right).\end{aligned}$$

The result now follows from

$$\begin{aligned}\mathbb{E} \left[ e^{\int_t^T (x(s) + r_S(s)) ds} \right] &= \mathbb{E} \left[ e^{\int_t^T x(s) ds} \right] \mathbb{E} \left[ e^{\int_t^T r_S(s) ds} \right] \\ &= \mathbb{E} \left[ e^{\int_t^T x(s) ds} \right] \sum e^{(-\int_t^T \bar{r}_S(u, \omega) du)} \mathbb{Q}_2(\omega).\end{aligned}\quad \blacksquare$$

We remark that the future price can be written as

$$\begin{aligned}F_{DI}(t, T, \omega) &= P_V(t, T) e^{(-\int_t^T y(u, \omega) du)} \\ F_{DI}(t, T) &= \sum F_{DI}(t, T, \omega) \mathbb{Q}_2(\omega).\end{aligned}\tag{6.9}$$

### 6.1.2 Options on Average One-Day Interbank Deposit Rate Index

The Interbank Deposit Rate Index (IDI) is an index that the BM&FBOVESPA created. It is defined as

$$IDI_t = 10^5 e^{\int_{t_0}^t r_{DI}(s) ds},$$

where  $t_0$  was chosen as 2003-01-02.

The IDI option is a plain vanilla derivative over the IDI index. To find its arbitrage free value, the following result is needed.

**Lemma 6.1.2 ([BM01])** *Let  $\log(X)$  be a log-normal random variable with mean  $(\mu)$  and variance  $(\sigma^2)$ . Then*

$$\mathbb{E} \left[ \left( \widehat{K} - X \right)^+ \right] = -e^{(\mu + \frac{1}{2}\sigma^2)} N \left( \frac{-\mu + \log(\widehat{K}) - \sigma^2}{\sigma} \right) + \widehat{K} N \left( \frac{-\mu + \log(\widehat{K})}{\sigma} \right).$$

where  $N$  is the cumulative standard normal distribution

$$N(y) = \frac{1}{\sqrt{2\pi}} \int_{-\infty}^y e^{-z^2/2} dz.$$

Using Lemma 6.1.2 we can prove a pricing formula for the IDI options, which is given in the next theorem.

**Theorem 6.1.3** *The IDI call options price is given by*

$$C_{IDI}(t, T, K, x(t), \omega) = IDI_t N(d_1(\omega)) - KF_{DI}(t, T, \omega) N(d_2(\omega)) ,$$

where

$$\begin{aligned} d_1(\omega) &= \frac{-\bar{\mu} + \ln(V(\omega))}{\bar{\sigma}} , \\ d_2(\omega) &= \frac{-\bar{\mu} + \ln(V(\omega)) - \bar{\sigma}^2}{\bar{\sigma}} , \\ V(\omega) &= \frac{1}{K} \left( IDI_t e^{\int_t^T y(s, \omega) ds} \right) , \\ \bar{\mu} &= -x(t)B(t, T) - \theta(T - t - B(t, T)) , \\ \bar{\sigma}^2 &= \frac{\sigma^2}{k^2} \left( T - t - B(t, T) - \frac{k}{2} B(t, T)^2 \right) . \end{aligned}$$

**Proof:** The price of a call option is given by

$$\begin{aligned} C_{IDI}(t, T, x(t), \omega) &= \mathbb{E} \left[ e^{-\int_t^T r_{DI}(s) ds} \left( 10^5 e^{\int_0^T r_{DI}(s) ds} - K \right)^+ \middle| \mathcal{F}_t \right] \\ &= K e^{-\int_t^T r_S(s, \omega) ds} \mathbb{E} \left[ \left( V(\omega) - e^{-\int_t^T x(s) ds} \right)^+ \middle| \mathcal{F}_t \right] , \end{aligned}$$

where

$$\begin{aligned} V(\omega) &= \frac{10^5}{K} e^{(\int_0^t r(s) ds + \int_t^T r_S(s, \omega) ds)} \\ &= \frac{1}{K} \left( IDI_t e^{\int_t^T r_S(s, \omega) ds} \right) . \end{aligned}$$

Defining  $\bar{\mu}$  and  $\bar{\sigma}$  for the mean and variance of the process

$$- \int_t^T x(s) ds ,$$

respectively. Using (6.8), it follows that

$$\begin{aligned} \bar{\mu} &= -x(t)B(t, T) - \theta(T - t - B(t, T)) \\ \bar{\sigma}^2 &= \frac{\sigma^2}{k^2} \left( T - t - B(t, T) - \frac{k}{2} B(t, T)^2 \right) . \end{aligned}$$

Then,

$$C_{IDI}(t, T, K, x(t), \omega) = IDI_t N(d_1(\omega)) - KF_{DI}(t, T, \omega) N(d_2(\omega)) , \quad (6.10)$$

where

$$d_1(\omega) = \frac{-\bar{\mu} + \ln(V(\omega))}{\bar{\sigma}},$$

$$d_2(\omega) = \frac{-\bar{\mu} + \ln(V(\omega)) - \bar{\sigma}^2}{\bar{\sigma}}. \quad \blacksquare$$

Since the space  $\Omega_2$  is taken to be discrete, the price of the Call option can be written as

$$C_{IDI}(t, T, x(t)) = \sum_{\omega \in \Omega_2} C_{IDI}(t, T, x(t), \omega) \mathbb{Q}_2(\omega). \quad (6.11)$$

The same arguments can be used to find the price of the put option

$$P_{IDI}(t, T, K, x(t), \omega) = KF_{DI}(t, T, \omega)N(-d_2(\omega)) - IDI_t N(-d_1(\omega)). \quad (6.12)$$

## 6.2 Recovering Probabilities

The main target of this chapter is to use the model presented in Section 6.1 to recover the probabilities associated to the paths of the short rate target,  $r_S$ . First, the spread is studied, then the problem of recovering the target rate path's probability is addressed.

For the real probability of the spread model,  $\mathbb{P}_1$ , we use daily quotes for DI, and SELIC. The maximum likelihood [BM01] is applied to calibrate the real measure. For risk neutral probability, future contracts where there was no uncertainty about the SELIC rate, are used. Those contracts are the ones that have no COPOM meeting before the maturity, so  $r_S$  is deterministic until maturity. The result is shown in Table 6.1.

Parameter	Value
$k$	128.18
$\theta$	$-2.89e^{-4}$
$\theta^{\mathbb{Q}}$	$-6.89e^{-4}$
$\sigma^2$	$1.82e^{-5}$

Table 6.1: Parameter estimation for the real and risk neutral dynamic of  $r_{DI}$ .

We assume that  $\Omega_2$  is finite and has only paths with positive probability, that is  $\omega \in \Omega_2 \Rightarrow \mathbb{Q}_2(\omega) > 0$ . This reduces the problem of recovering the probability  $\mathbb{Q}_2$  to that of finding  $p = (\mathbb{Q}_2(\omega_1), \dots, \mathbb{Q}_2(\omega_U))^t$ .

Suppose there are future contract quotes,  $\{\widehat{F}_i\}_{i=1}^f$ , with expiration,  $\{T_i^F\}_{i=1}^f$ , and call options quotes,  $\{\widehat{C}_j\}_{j=1}^c$ , with the associated pair of strikes and maturity,  $\{K_j, T_j^C\}_{j=1}^c$ . Using (6.9) and (6.11), we can try to recover  $\mathbb{Q}_2$  solving

$$\begin{aligned}\widehat{F}_{DI}(t, T_i) &= \sum F_{DI}(t, T_i, \omega) \mathbb{Q}_2(\omega) \quad i = 1, \dots, f \\ \widehat{C}_{IDI}(t, T_j, K_j) &= \sum C_{IDI}(t, T_j, K_j, \omega) \mathbb{Q}_2(\omega) \quad j = 1, \dots, c\end{aligned}\tag{6.13}$$

This problem is linear although its dimension is quite high. We use the following notation

$$E_{k,u} = \begin{cases} \widehat{F}_{DI}(t, T_k) - F_{DI}(t, T_k, \omega_u) & \text{if } 0 < k \leq f \\ \widehat{C}_{IDI}(t, T_j, K_j) - C_{IDI}(t, T_j, K_j, \omega_u) & 0 < j = k - f + 1 \leq c \end{cases}.\tag{6.14}$$

Using the notation in Equation (6.14), the problem (6.13) is simply  $Ep = 0$ , so finding a risk neutral probability is equivalent to finding a positive solution of a linear system. The next theorem gives a very simple condition for non arbitrage of market prices.

**Theorem 6.2.1** *A set of prices,  $\{\widehat{F}_i\}_{i=1}^f$ ,  $\{\widehat{C}_j\}_{j=1}^c$  is arbitrage free, if and only if, there is  $p \in \mathbb{R}_{++}^n$  such that  $Ep = 0$ , where  $\mathbb{R}_{++}$  denotes the set of strictly positive real numbers.*

**Proof:** The result follows from the Fundamental Theorem of asset pricing (Theorem 1.3.1) and by noticing that, by assumption,  $\mathbb{Q}_2(\omega) > 0$  for  $\omega \in \Omega_2$ . ■

The next theorem gives some characterization of the set of arbitrage free prices.

**Theorem 6.2.2** ([Rom08]) *Let  $S$  be the row space of  $E$ , then*

- $S \cap \mathbb{R}_+^n = \emptyset \Leftrightarrow S^\perp \cap \mathbb{R}_{++}^n \neq \emptyset$  ; and
- $S \cap \mathbb{R}_{++}^n = \emptyset \Leftrightarrow S^\perp \cap \mathbb{R}_+^n \neq \emptyset$ .

The problem of solving  $Ep = 0$  is ill-posed. In this chapter, we propose some regularization for this problem. The main idea of regularization is find a family  $(R_\gamma)_{\gamma>0}$ , such that

$$\lim_{\gamma \downarrow 0} R_\gamma Ep = p \quad \forall p \in \mathbb{R}^n .$$

Where the solutions of the regularized problem

$$\begin{aligned}
R_\gamma p &= 0, \\
\text{s.t. } p &\in \mathbb{R}_{++}^n \\
\sum_{j=1}^n p_j &= 1
\end{aligned} \tag{6.15}$$

is well-posed. In our case, instead of solving  $Ep = 0$  for some  $p \in \mathbb{R}_{++}^n$ , we solve

$$\begin{aligned}
\min_p & \|DEp\|^2 + g_\gamma(p, p^*) \\
\text{s.t. } & \sum_{j=1}^n p_j = 1 \\
& p_j \geq 0 \quad j = 1, \dots, n
\end{aligned}$$

Where  $p^*$  is a *prior* probability. In this sections we present a choice for  $D$ , several choices for the family  $(g_\gamma)_{\gamma>0}$  and different priors.

For market data, the condition number of  $E$  is usually very high, sometimes above  $10^{14}$ . One of the reasons for this problem is the different magnitudes of the assets treated. To mitigate it, we use a preconditioner matrix  $D$ , defined as

$$D = \text{Diag}(\|E_{1,1:U}\|^{-1}, \dots, \|E_{f+c,1:U}\|^{-1}), \tag{6.16}$$

where  $E_{j,1:U}$  is the  $j$ th row of the matrix  $E$ .

From now on,  $\hat{E}$  denotes the preconditioned  $\hat{E} = DE$ .

As in many Inverse Problems and in Approximation Theory, one has to consider different notions of distance. In particular we shall use the followings:

- $d_J(r_1, r_2) = \|r_1' - r_2'\|_2^2 = \sum_n ((r_1(\bar{t}_n^+) - r_1(\bar{t}_n^-)) - (r_2(\bar{t}_n^+) - r_2(\bar{t}_n^-)))^2$ . This distance represents the geometric Euclidean distance of jumps size, it is related to the quadratic variation of the paths' differences. The distance  $d_J$  focus on the idea that the distance of the paths are based on the change of interest rate on each COPOM meeting.
- $d_A(r_1, r_2) = \|r_1 - r_2\|_1 = \int_t^T |r_1(s) - r_2(s)| ds$ . This distance represents the difference of accumulated interest rates. The distance  $d_A$  focuses on the difference of interest rate applied in the economy during a certain period of time.



Regularization techniques are heavily dependent on the existence of *priors*. We shall denote this prior as  $p^*$ . Some options for  $p^*$  considered here are:

- $p^* = p_{n-1}$ , that is, the result for  $t_{n-1}$  is used as a prior for the problem in  $t_n$ .
- $p_i^* = d(r_S(\omega_i), r^*)$ , where

$$r^*(t) := r_0 \mathcal{X}_{[t_0, \tau_1]}(t) + \sum_{j=1}^N r_j \mathcal{X}_{(\tau_j, \tau_{j+1}]}(t),$$

where  $r_j \in \mathbb{R} \forall j$  is the deterministic path that better fits the future prices. It is the deterministic version of (6.3) with no restriction about possible values of the target. In case of more than one solution, the one with lower  $d_J(r, r)$  is used.

- $p_i^* = \sum_{k=1}^{c+f} (E_{k,i})^2$ , that is, the sum of the error for every contract.

## Tikhonov

A popular way of regularization is the so-called Tikhonov regularization [BL05]. For our purposes, we choose a prior  $p^*$  and solve the following regularized version of the problem

$$\begin{aligned} \min_{p_n} \frac{1}{2} p_n^t (E^t E) p_n + \gamma \|p_n - p^*\|^2 \\ \sum p_n^i = 1 \\ p_n^i \geq 0. \end{aligned} \tag{6.17}$$

## Smoothness

In [JR96] a regularization was proposed, which was based on finding the smoothest distribution. They minimized the discretization of the second order differential operator. There is no natural order in  $\Omega_2$ , the notion of smoothness is based on a distance between paths.

Given a distance  $d$ , the matrix of distances  $S$  will be defined as follows

$$S_{i,j} = d(\omega_i, \omega_j).$$

The regularized problem is

$$\begin{aligned} \min_{p_n} \frac{1}{2} p_n^t (E^t E + \beta S) p_n + \gamma p_n p^* \\ \sum p_n^i = 1 \\ p_n^i \geq 0. \end{aligned} \tag{6.18}$$

## Entropy

The last proposed regularization is entropy, which is given by

$$\begin{aligned} \min_p \frac{1}{2} p^t (E^t E) p + \sum \frac{p_i}{p_i^*} \log \frac{p_i}{p_i^*} \\ \sum p_i = 1 \\ p_i \geq 0. \end{aligned} \tag{6.19}$$

We notice that we must have  $\sum p_i^* = e^{-1}$  as prior. Indeed

$$x^* = \arg \min_x \frac{x}{ex^*} \ln \frac{x}{ex^*}. \tag{6.20}$$

## 6.3 Numerical Results

In this section, we present a back-test of the model's capacity of forecast on future decisions of the monetary authority. To do so, we consider quotes for futures over DI, and options over IDI ranging from 2007-12-18 to 2008-03-05. The COPOM had a meeting on this day, when they have chosen 11.25 as the SELIC rate. In order to construct the back-test, we present the model's probability addressed to the rate of 11.25 in every day of the time window of the data set.

Our first result concerns prior probability choice. If we focus on Figure 6.1, where the Tikhonov regularization (6.17) is used, it is clear the crucial role played by the prior. In any case, the model shows good forecast ability.

The right choice of the parameters is a central issue in regularization of ill-posed problems. In Figures 6.2 and 6.3, we show the results based on the smoothness regularization, (6.18), for different parameters. The wrong choice of the parameters, like  $\beta = 1$ , in Figure 6.2, can produce bad results, but in general we obtain good results for a large range of parameters.

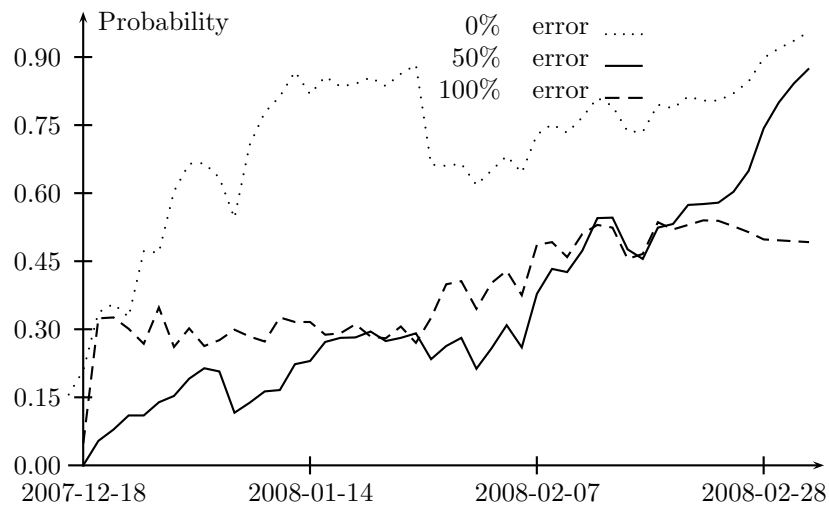


Figure 6.1: Probability of having interest rate of 11.25% at the meeting of 2008-03-05. The probability is based on the solution of (6.17), using a mixed probability, error as prior, and  $\gamma = 10^{-1}$ .

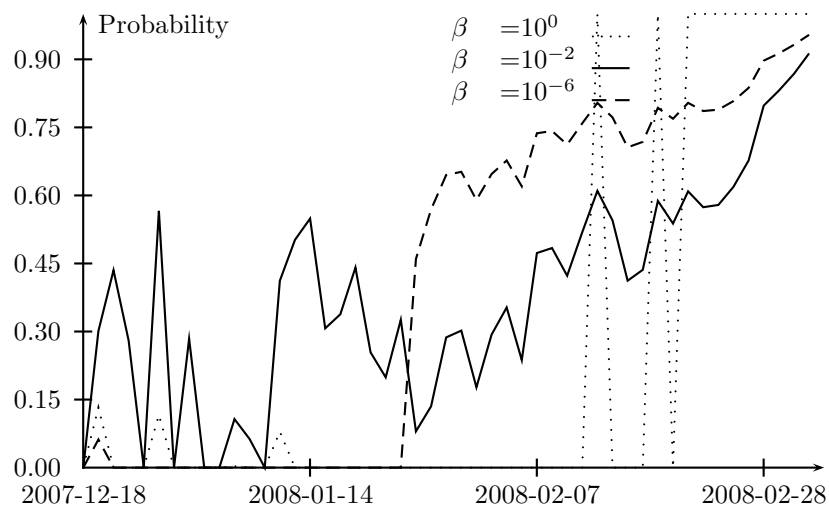


Figure 6.2: Probability of having interest rate of 11.25% at the meeting of 2008-03-05. The probability is based on the solution of (6.18) for  $\gamma = 10^{-5}$ , using  $p_{n-1}$  as prior.

Our final result presents the forecast based on the entropy regularization (6.19), and can be seen in Figure 6.4.

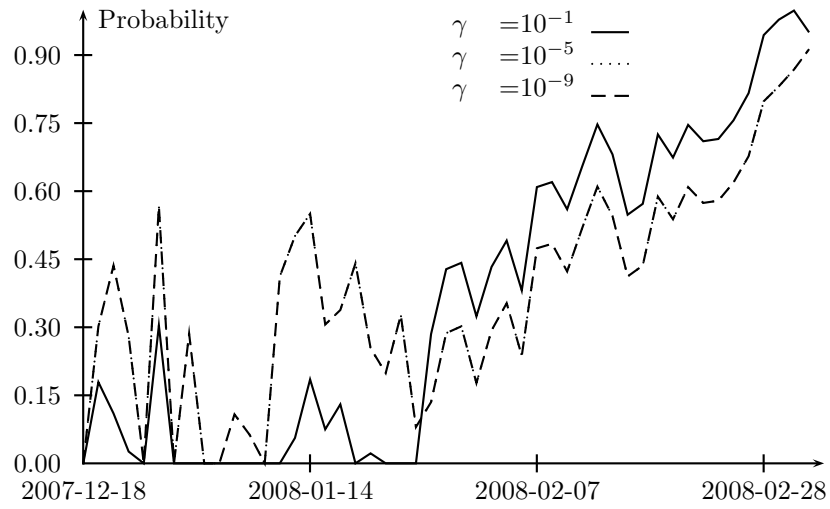


Figure 6.3: Probability of having interest rate of 11.25% at the meeting of 2008-03-05. The probability is based on the solution of (6.18) for  $\beta = 10^{-2}$ , using the vector based on the distances as prior.

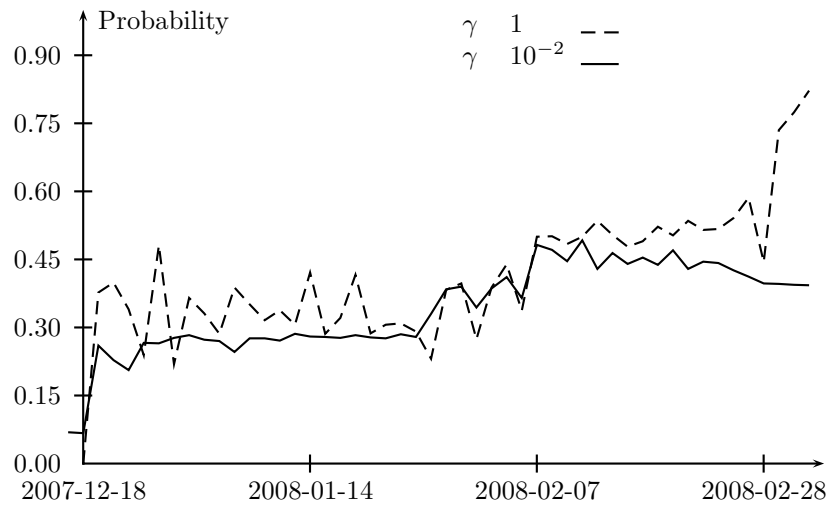


Figure 6.4: Probability of having interest rate of 11.25% at the meeting of 2008-03-05. The probability is based on the solution of (6.19), using error as prior.

## 6.4 Conclusion

The objective of this chapter was to recover the monetary authority decision probabilities, using market data on derivatives over interest rates. The results of this section show that our goal was achieved. The model, when combined with the proper regularization techniques can recover with good accuracy market expectation from data.

The choice of the right regularization technique plays a central role in recovering the probabilities due to the ill-posed nature of the problem. Some regularization techniques did not present good results for this problem, such as the entropy (6.19), while others such as smoothness (6.18) and Tikhonov (6.17) presented good results. The Tikhonov method achieved even better results, as seen in Figure 6.1, and it is interesting to notice the effect of the right prior in the quality of the results.

# Chapter 7

## Final Considerations and Future Work

Quantitative finance is the source of a number of mathematical problems in a wide range of areas with immediate impact to market applications. In this thesis, we addressed three different problems in quantitative finance and while studying them, we worked on the development of new mathematical techniques and new applications of well known mathematical methods to relevant problems in finance.

In this final chapter, we draw some final comments on the results presented in this thesis and also point out some directions towards future work.

In Chapters 2, 3, and 4 we focused our attention on Fourier methods and its use in finance. In Chapter 2, we presented a pricing formula for several derivatives. It is valid for a broad range of stochastic processes models, including Heston, Merton, and Kou models. Some numerical results were shown in Section 4.3 based on quadrature techniques presented in Chapter 3.

One of the applications of the results of this part of the thesis is that putting together the pricing formula of Chapter 2, the bounds for Fourier transform in Chapter 3, and the algorithm of Chapter 4, it is possible to find a grid that achieves a desired accuracy in pricing a portfolio of derivatives, even when this portfolio has different maturities.

The bounds developed in Chapter 3 have Black-Scholes model as a natural example, but to find the proper bounds for different models proved to be a difficult task. We are now working on bounds based on the Faà di Bruno's formula [Har06].

It is interesting to notice that, even using the same bounds we used for the Black-Scholes case, the non-uniform quadrature proved itself to be very accurate for several models. In Figure 7.1, we show some results for the Heston model, whose characteristic is given by Equation 1.23. We also

present some preliminary results for the Merton model, given in Figure 7.2, and Kou model, given in Figure 7.3. The characteristic function for those last two processes are given in Table 1.1.

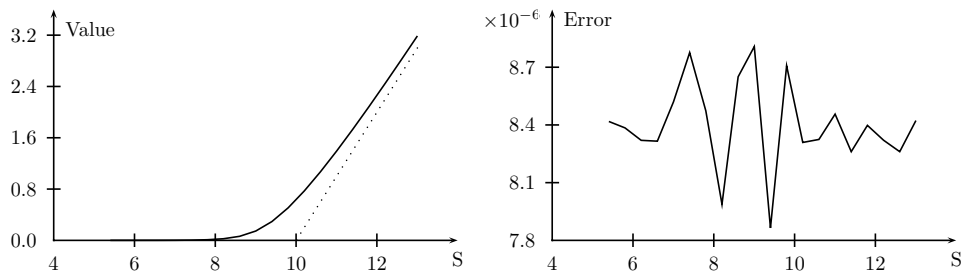


Figure 7.1: The error in the price computation of a call option in the Heston model, using the bounds of Chapter 3. The parameters used were  $v = 0.02$ ,  $\bar{v} = 0.03$ ,  $\nu = 0.4$ ,  $\rho = -0.7$ ,  $\lambda = 1.3$ ,  $k = \log(10)$ ,  $S_k = 5 + 0.4 \cdot j$  for  $j = 1, \dots, 20$ , precision  $\epsilon = 10^{-2}$ ,  $r = 0$ , and  $t = 1$ . We used 472 mesh points.

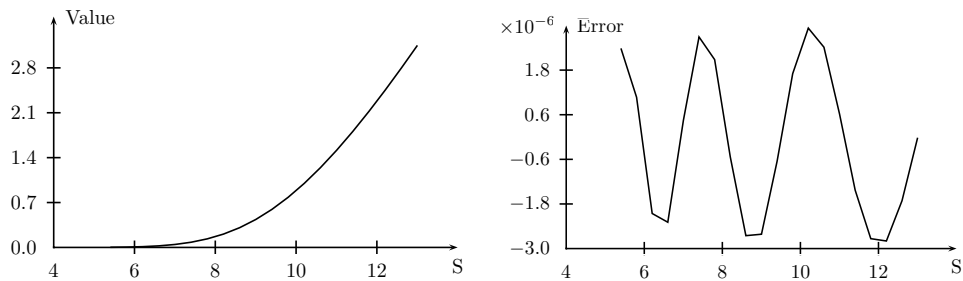


Figure 7.2: The error in the price computation of a call option in the Merton model, using the bounds of Chapter 3. The parameters used were  $\mu = 0$ ,  $\lambda = 1.3$ ,  $\sigma = 0.2$ ,  $\delta = 0.1$ ,  $k = \log(10)$ ,  $S_k = 5 + 0.4 \cdot j$  for  $j = 1, \dots, 20$ , precision  $\epsilon = 10^{-4}$ ,  $r = 0$ , and  $t = 1$ . We used 184 mesh points.

In another direction, we are also working on different quadrature schemes to evaluate the pricing formula of Theorem 2.2.2, but again bounds for the derivatives of the characteristic functions must be estimated.

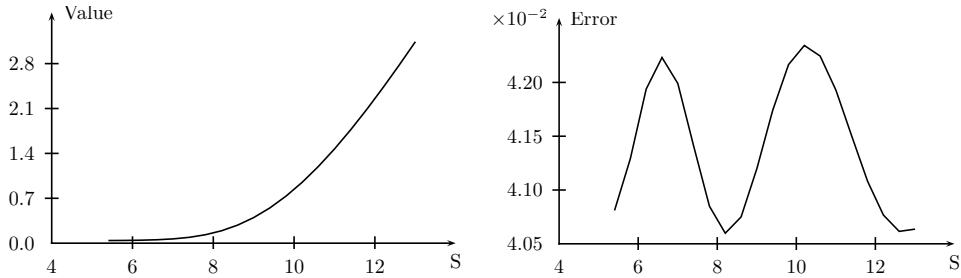


Figure 7.3: The error in the price computation of a call option in the Kou model, using the bounds of Chapter 3. The parameter used were  $\lambda = 1$ ,  $\nu_1 = 0.4$ ,  $\nu_2 = 0.6$ ,  $p = 0.4$ ,  $\sigma = 0.2$ ,  $k = \log(10)$ ,  $S_k = 5 + 0.4 \cdot j$  for  $j = 1, \dots, 20$ , precision  $\epsilon = 10^{-2}$ ,  $r = 0$ , and  $t = 1$ . We used 124 mesh points.

The quadrature bounds presented in Chapter 3 have several applications. Among them, it is possible to extend the numerical solution of the inhomogeneous heat equation in free space, used in [LG07], to more general initial conditions. Even within the same class of initial conditions, the bounds developed here represent some improvement over [LG07], see Figure 3.2. A numerical study of such application is a possible follow up of Chapter 3 and an important extension of the numerical results presented in Section 4.3.

The bounds obtained in Chapter 3 include bounds for

$$\int h(s)e^{ixs} ds, \quad \int \frac{h(s)e^{ixs}}{is} ds, \quad \text{and} \quad \int \frac{h(s)e^{ixs}}{c + is} ds.$$

We are currently working on estimates for

$$\int \frac{h(s)e^{ixs}}{(c + is)^n} ds,$$

following the lines of the previous bounds. The difficulty here lies in the factor  $n$ , which implies a polynomial growth of the derivative, and makes it difficult to find a sharp estimate.

In Chapter 5, we presented a model for LNG prices, and several derivatives over the spot price. The model reflects several stylized facts about this market. We are now working on the calibration of the model for real data. We are also working on extending the bound of Chapter 3 to the multidimensional case, so it would be possible to attack the numerical solution of the model developed in Chapter 5 with the same techniques used in Chapters 2 and 3.

Finally, in Chapter 6 we presented a model for interest rates taking into account the monetary policy. Using inverse problem techniques we were able



to recover market expectation about the monetary authority decision. The applications of these techniques in financial planning are self-evident. In Section 6.3, we presented some numerical results obtained by the model as well as some back-test examples.

During the development of this thesis options on One-Day Interbank Deposit Futures Contract became liquid. Thus, we will incorporate those contracts to the model in a future work. We are currently developing an algorithm based on the convex hull [BDH96] in order to find the set of arbitrage free prices. We intend to apply the ideas of Chapter 6 for general discrete frameworks, and one possible application of such result would be the set of arbitrage free prices for several digital options.

# Bibliography

- [AD96] C. Anderson and M.D. Dahleh. Rapid computation of the discrete Fourier transform. *SIAM Journal on Scientific Computing*, 17:913, 1996.
- [AS65] M. Abramowitz and I.A. Stegun. *Handbook of mathematical functions with formulas, graphs, and mathematical table*. Courier Dover Publications, 1965.
- [Ave99] Marco Avellaneda. An introduction to option pricing and the mathematical theory of risk [ MR1678312 (2000e:91029)]. In *Introduction to mathematical finance (San Diego, CA, 1997)*, volume 57 of *Proc. Sympos. Appl. Math.*, pages 25–48, Providence, RI, 1999. Amer. Math. Soc.
- [Bac00] L. Bachelier. *Theorie de la speculation*. Gauthier-Villars Paris, 1900.
- [BCSS95] H. Bessembinder, J.F. Coughenour, P.J. Seguin, and M.M. Smoller. Mean reversion in equilibrium asset prices: evidence from the futures term structure. *Journal of Finance*, pages 361–375, 1995.
- [BDH96] C.B. Barber, D.P. Dobkin, and H. Huhdanpaa. The quickhull algorithm for convex hulls. *ACM Transactions on Mathematical Software (TOMS)*, 22(4):469–483, 1996.
- [BL78] D.T. Breeden and R.H. Litzenberger. Prices of State-Contingent Claims Implicit in Option Prices. *Journal of Business*, 51(4):621, 1978.
- [BL05] J. Baumeister and A. Leitao. Topics in inverse problems. *Publicacoes Matematicas do IMPA.[IMPA Mathematical Publications]*. Instituto Nacional de Matematica Pura e Aplicada (IMPA), Rio de Janeiro, 25, 2005.
- [Bla76] F. Black. The pricing of commodity contracts. *Journal of Financial Economics*, 3:167–179, 1976.

- [BM01] D. Brigo and F. Mercurio. *Interest Rate Models: Theory and Practice*. Springer, 2001.
- [BS73] Fischer Black and Myron Scholes. The pricing of options and corporate liabilities. *Journal of Political Economy*, 81(3):637–654, 1973.
- [CCM05] J.B. Carlson, B.E.N.R. Craig, and W.R. Melick. Recovering market expectations of fomc rate changes with options on federal funds futures. *The Journal of Futures Markets*, 25(12):1203–1242, 2005.
- [Chu01] K.L. Chung. *A course in probability theory*. Academic press, 2001.
- [CLP02] E. Clément, D. Lamberton, and P. Protter. An analysis of a least squares regression method for American option pricing. *Finance and Stochastics*, 6(4):449–471, 2002.
- [CM99] P. Carr and D. Madan. Option valuation using the fast Fourier transform. *Journal of Computational Finance*, 2(4):61–73, 1999.
- [CT65] J.W. Cooley and J.W. Tukey. An algorithm for the machine calculation of complex Fourier series. *Mathematics of computation*, pages 297–301, 1965.
- [CT04] R. Cont and P. Tankov. *Financial modelling with jump processes*. Chapman & Hall/CRC, 2004.
- [CW90] Kai Lai Chung and Ruth J. Williams. *Introduction to Stochastic Integral*. Birkhauser, 1990.
- [DL92] A. Deaton and G. Laroque. On the Behaviour of Commodity Prices. *Review of Economic Studies*, 59(1):1–23, 1992.
- [DPS00] D. Duffie, J. Pan, and K. Singleton. Transform analysis and asset pricing for affine jump-diffusions. *Econometrica*, pages 1343–1376, 2000.
- [DR75] P.J. Davis and P. Rabinowitz. *Methods of Numerical Integration*. New York, 1975.
- [DR93] A. Dutt and V. Rokhlin. Fast Fourier transforms for nonequispaced data. *SIAM Journal on Scientific computing*, 14:1368, 1993.
- [DR95] A. Dutt and V. Rokhlin. Fast Fourier transforms for nonequispaced data, II. *Applied and Computational Harmonic Analysis*, 2(1):85–100, 1995.

- [DS94] F. Delbaen and W. Schachermayer. A general version of the fundamental theorem of asset pricing. *Mathematische Annalen*, 300(1):463–520, 1994.
- [DS98] F. Delbaen and W. Schachermayer. The fundamental theorem of asset pricing for unbounded stochastic processes. *Mathematische Annalen*, 312(2):215–250, 1998.
- [EE05] Herbert Egger and Heinz W. Engl. Tikhonov regularization applied to the inverse problem of option pricing: convergence analysis and rates. *Inverse Problems*, 21(3):1027–1045, 2005.
- [EHH06] Herbert Egger, Torsten Hein, and Bernd Hofmann. On decoupling of volatility smile and term structure in inverse option pricing. *Inverse Problems*, 22(4):1247–1259, 2006.
- [FB87] Eugene F. Fama and Robert R. Bliss. The information in long-maturity forward rates. *American Economic Review*, 77:68092, 1987.
- [Fel66] W. Feller. An introduction to probability theory and its applications. Vol II. *New York*, 1, 1966.
- [For08] E. Fortuna. *Mercado financeiro produtos e serviços*. Qualitymark, 2008.
- [FPS00] J.P. Fouque, G. Papanicolaou, and K.R. Sircar. *Derivatives in financial markets with stochastic volatility*. Cambridge University Press, 2000.
- [FS06] W.H. Fleming and H.M. Soner. *Controlled Markov processes and viscosity solutions*. Springer, 2006.
- [Gat06] J. Gatheral. *The volatility surface: a practitioner’s guide*. Wiley, 2006.
- [GKP89] R.L. Graham, D.E. Knuth, and O. Patashnik. *Concrete mathematics: a foundation for computer science*. Addison-Wesley Longman Publishing Co., Inc. Boston, MA, USA, 1989.
- [GL00] L. Greengard and P. Lin. Spectral Approximation of the Free-Space Heat Kernel. *Applied and Computational Harmonic Analysis*, 9(1):83–97, 2000.
- [Gla04] P. Glasserman. *Monte Carlo methods in financial engineering*. Springer, 2004.

- [Har06] M. Hardy. Combinatorics of partial derivatives. *the electronic journal of combinatorics*, 13(R1):1, 2006.
- [Hes93] S.L. Heston. A closed-form solution for options with stochastic volatility with applications to bond and currency options. *Review of Financial Studies*, 6(2):327–343, 1993.
- [HJB85] M.T. Heideman, D.H. Johnson, and C.S. Burrus. Gauss and the history of the fast Fourier transform. *Archive for History of Exact Sciences*, 34(3):265–277, 1985.
- [HP81] J.M. Harrison and S.R. Pliska. Martingales and stochastic integrals in the theory of continuous trading. *Stochastic processes and their applications*, 11:215–260, 1981.
- [Hul08] J. Hull. *Options, futures, and other derivatives*. Pearson Prentice Hall, 2008.
- [Jen03] J.T. Jensen. The LNG revolution. *Energy Journal*, 24(2):1–46, 2003.
- [JJSB] K.R. Jackson, S. Jaimungal, V. Surkov, and S.F. Building. Fourier space time-stepping for option pricing with levy models.
- [JR96] J.C. Jackwerth and M. Rubinstein. Recovering Probability Distributions from Option Prices. *Journal of Finance*, 51(5):1611–1631, 1996.
- [JSB] S. Jaimungal, V. Surkov, and S.F. Building. A Levy Based Framework for Commodity Derivative Valuation via FFT.
- [JW01] J. James and N. Webber. *Interest rate modelling*. Wiley Chichester, United Kingdom, 2001.
- [Kou02] SG Kou. A Jump-Diffusion Model for Option Pricing. *Management Science*, 48(8):1086, 2002.
- [Lee04] R.W. Lee. Option pricing by transform methods: extensions, unification and error control. *Journal of Computational Finance*, 7(3):51–86, 2004.
- [Lew00] A.L. Lewis. A Simple Option Formula for General Jump-Diffusion and Other Exponential Levy Processes. 2000.

- [LFBO07] R. Lord, F. Fang, F. Bervoets, and K. Oosterlee. A fast and accurate FFT-based method for pricing early-exercise options under Lévy processes. *Center for Mathematics and Computer Science (CWI)*, 2007.
- [LG07] J.R. Li and L. Greengard. On the numerical solution of the heat equation I: Fast solvers in free space. *Journal of Computational Physics*, 226(2):1891–1901, 2007.
- [LS01] FA Longstaff and ES Schwartz. Valuing American options by simulation: a simple least-squares approach. *Review of Financial Studies*, 14(1):113–147, 2001.
- [Mer73] R.C. Merton. Theory of rational option pricing. *The Bell Journal of Economics and Management Science*, pages 141–183, 1973.
- [Mer75] R.C. Merton. Option pricing when underlying stock returns are discontinuous. 1975.
- [MR05] M. Musiela and M. Rutkowski. *Martingale methods in financial modelling*. Springer, 2005.
- [Oks05] Bernt Oksendal. *Stochastic Differential Equation*. Springer, 2005.
- [Pia03] M. Piazzesi. Affine term structure models. *Handbook of Financial Econometrics*, 2003.
- [Pia05] Monika Piazzesi. Bond yields and the federal reserve. *Journal of Political Economy*, 113(2):311–344, 2005.
- [Pro04] P.E. Protter. *Stochastic integration and differential equations*. Springer, 2004.
- [PS08] Monika Piazzesi and Eric Swanson. Futures prices as risk-adjusted forecasts of monetary policy. *Journal of Monetary Economics*, 2008.
- [PST98] D. Potts, G. Steidl, and M. Tasche. Fast Fourier transforms for nonequispaced data: A tutorial. *Modern Sampling Theory: Mathematics and Applications*, pages 249–274, 1998.
- [Rom08] S. Roman. *Advanced linear algebra*. Springer, 2008.
- [RR04] Michael Renardy and Robert C. Rogers. *An Introduction to Partial Differential Equations*. Springer, 2004.

- [RS75] M. Reed and B. Simon. Methods of modern mathematical physics. II: Fourier analysis, self-adjointness. 1975.
- [Sat99] K.I. Sato. *Lévy processes and infinitely divisible distributions*. Cambridge University Press, 1999.
- [Sch97] E.S. Schwartz. The stochastic behavior of commodity prices: Implications for valuation and hedging. *Journal of finance*, pages 923–973, 1997.
- [Sha08] LF Shampine. Vectorized adaptive quadrature in MATLAB. *Journal of Computational and Applied Mathematics*, 211(2):131–140, 2008.
- [Shr04] S.E. Shreve. *Stochastic Calculus for Finance II: Continuous Time Models*. Springer New York, 2004.
- [SLNv05] B. Siliverstovs, G. L’Hégaret, A. Neumann, and C. von Hirschhausen. International market integration for natural gas? A cointegration analysis of prices in Europe, North America and Japan. *Energy Economics*, 27(4):603–615, 2005.
- [Ste98] G. Steidl. A note on fast Fourier transforms for nonequispaced grids. *Advances in computational mathematics*, 9(3):337–352, 1998.
- [SZ07] M.O. Souza and J.P. Zubelli. On the Asymptotics of Fast Mean-Reversion Stochastic Volatility Models. *International Journal of Theoretical and Applied Finance*, 10(5):817, 2007.
- [Sza51] O. Szasz. On the relative extrema of the Hermite orthogonal functions. *J. Indian Math. Soc.*, 25:129–134, 1951.
- [Van92] C. Van Loan. *Computational frameworks for the fast Fourier transform*. Society for Industrial Mathematics, 1992.
- [Vas77] Oldrich Vasicek. An equilibrium characterization of the term structure. *Journal of financial Economics*, 5:177–188, 1977.
- [VJ06] J.A. Villar and F.L. Joutz. The relationship between crude oil and natural gas prices. *EIA manuscript, October*, 2006.
- [Yan98] J.A. Yan. A new look at the fundamental theorem of asset pricing. *J. Korean Math. Soc.*, 35(3):659–673, 1998.
- [Zub05] Jorge Zubelli. Inverse problems in finance: A short survey on calibration techniques. *Proceedings of the Second Brazilian Conference on Statistical Modelling in Insurance and Finance*, pages 64–76, 2005.